



Virginia Commonwealth University  
VCU Scholars Compass

---

Theses and Dissertations

Graduate School


---

2014

## Development of Bivalent Ligands Targeting the Putative CCR5-MOR Heterodimer

Thomas Raborg  
*Virginia Commonwealth University*

Follow this and additional works at: <https://scholarscompass.vcu.edu/etd>

 Part of the [Medicinal and Pharmaceutical Chemistry Commons](#)

© The Author

---

Downloaded from

<https://scholarscompass.vcu.edu/etd/3553>

This Thesis is brought to you for free and open access by the Graduate School at VCU Scholars Compass. It has been accepted for inclusion in Theses and Dissertations by an authorized administrator of VCU Scholars Compass. For more information, please contact [libcompass@vcu.edu](mailto:libcompass@vcu.edu).

Development of Bivalent Ligands Targeting the  
Putative CCR5-MOR Heterodimer

A dissertation submitted in partial fulfillment of the requirements for the degree of master of  
science at Virginia Commonwealth University.

By

Thomas Raborg  
University of Kansas, B.S. Cellular Biology

Director: Dr. Yan Zhang,  
Assistant Professor, Medicinal Chemistry

Virginia Commonwealth University  
Richmond, VA  
July 28, 2014

### Acknowledgement

I could not have acquired a master's degree in medicinal chemistry without the constant help and support of family members and friends since childhood. Growing up my mother, Marija Raborg, always used to make me read the works of classical authors, and she would tutor me every day after arriving home from work. While I did not realize it at the time, she sacrificed a lot to make sure that I took education and hard-work seriously. I can only imagine the effort on her part, given that on top of an eight-hour workday she would commute to New York City and back from a home in another state. She instilled in me a love of literature and writing, and I still read (and prefer) the works of pre-20<sup>th</sup> century authors because of her tutelage. I also have to thank my father, Joseph Helvetio Raborg, for instilling in me the moral fiber and discipline that were required to succeed in school and at life. I still fondly recall how he would read us letters and addresses from famous former statesmen and philosophers, particularly those associated with the nascent United States. Finally, I have to thank my brother, Joseph Anthony Raborg, and my sister, Katherine Mary Raborg, as they both provided me with a fun and memorable childhood, one that I still like recalling to this day.

Within the Department of Medicinal Chemistry and Virginia Commonwealth University, I first have to thank my advisor, Dr. Yan Zhang. It was because of his encouragement, advice and commitment to my success as a graduate student that I can now graduate with an advanced degree in an applied science. He made sure that I had all the help that I needed to complete my studies and research goals while attending graduate school. Along with him, I have to also thank members of Dr. Zhang's laboratory group – with special mentions to Drs. Yunyun Yuan, Christopher Kent Arnatt and Saheem Zaidi – for their help in furthering the completion of my

research. I could not have succeeded without their help and constant attention to my progress both as a student and as a researcher in the Dr. Zhang laboratory.

I am very grateful for my time at the Department of Medicinal Chemistry at Virginia Commonwealth University, as I was able to learn and research about a subject that I have grown to love and admire. Finally, I have to thank Drs. MaryPeace McRae and Rong Huang for agreeing to be part of my committee. They have been invaluable in helping me reach my goal of acquiring a master's degree.

## Table of Contents

|  |      |
|--|------|
| Acknowledgements.....  | ii   |
| Table of Contents.....   | iv   |
| List of Tables.....  | vii  |
| List of Figures.....   | viii |
| List of Schemes.....   | ix   |
| List of Abbreviations.....   | x    |
| Abstract.....  | xi   |
| 1. Introduction.....   | 1    |
| 1.1 Chemokine Receptor CCR5.....   | 1    |
| 1.1.1 Function of Chemokines and Chemokine Receptors.....                    | 1    |
| 1.1.2 Chemokine Receptor Type CCR5 and GPCRs.....                            | 1    |
| 1.1.3 CCR5 Downstream Effects and Regulation.....                            | 3    |
| 1.1.4 GPCRs as Drug Targets and CCR5 in HIV-Associated Diseases.....         | 5    |
| 1.1.5 CCR5's Association with HIV/AIDS.....                                  | 6    |
| 1.1.6 Small molecules targeting CCR5.....                                    | 7    |
| 1.2 The Mu Opioid Receptor.....  | 9    |
| 1.2.1 Opioid Receptors.....  | 9    |
| 1.2.2 Mu Opioid Receptor Structure and Downstream Signaling.....             | 10   |
| 1.2.3 Opioid Addiction and Its Effects on HIV/AIDS Infected Individuals..... | 11   |
| 1.2.4 Addiction in NeuroAIDS.....  | 12   |

|   |    |
|---|----|
| 1.2.5 Mu Opioid Receptor Ligands: Agonists and Antagonists.....   | 12 |
| 1.3 GPCR Dimerization.....  | 16 |
| 1.3.1 Mu Opioid Receptor Dimerization.....  | 17 |
| 1.3.2 Bivalent Ligands Targeting GPCR Heterodimers.....   | 18 |
| 2. Bivalent Ligands Targeting the Putative CCR5-MOR Heterodimer.....                                    | 21 |
| 2.1 Project Design.....   | 21 |
| 2.2 6 $\beta$ -Naltrexamine Synthesis.....  | 28 |
| 2.3 Synthesis of the monovalent $\mu$ -Opioid control compounds.....                                    | 31 |
| 2.3.1 Monoprotection of diamines.....   | 32 |
| 2.3.2 Monoprotected Diamines Reacting with Dglycolic Anhydride.....                                     | 36 |
| 2.3.3 Monoprotected Intermediates Undergo Amide-Coupling Reaction with 6 $\beta$ -<br>naltrexamine..... | 38 |
| 2.3.4 Deprotection.....   | 39 |
| 2.3.5 Final Product Synthesis.....  | 40 |
| 3. In Vitro Studies.....  | 41 |
| 3.1 Results from Calcium Mobilization Assays with Initial 21-Atom Bivalent<br>Compound.....             | 41 |
| 3.2 MOR-Radiobinding Assay.....   | 45 |
| 3.3 CCR5-MOLT4 Calcium Mobilization Assay.....  | 46 |
| 3.4 hMOR-CHO Calcium Mobilization Assay.....  | 48 |
| 3.5 Conclusions from In Vitro Studies.....  | 49 |
| 4. In Silico Studies.....   | 49 |

|   |    |
|---|----|
| 4.1 Introduction to Conformational Analysis.....            | 50 |
| 4.2 Choosing a Conformational Analysis Software.....        | 51 |
| 4.3 Molecular Building.....                                 | 52 |
| 4.4 Global Minimization Conformational Analysis.....        | 52 |
| 4.5 DIVERSESET Conformational Analysis.....                 | 55 |
| 5. Experimental.....  | 60 |
| 5.1 Chemistry Intermediates.....                            | 60 |
| 5.2 Biology Methods.....                                    | 69 |
| 5.2.1 hMOR Competitive Radioligand Binding Assay.....       | 69 |
| 5.2.2 Calcium Mobilization Assays.....                      | 70 |
| 5.2.2.1 hMOR-CHO Cells.....                                 | 70 |
| 5.2.2.2 CCR5-MOLT-4 Cells.....                              | 71 |
| 5.3 Computational Methods.....                              | 71 |
| 5.3.1 Small Molecule Construction.....                      | 71 |
| 5.3.2 Global Minimization Conformational Analysis.....      | 72 |
| 5.3.3 Diverse Conformer Subset Conformational Analysis..... | 72 |
| References.....   | 74 |
| Vita.....   | 89 |

**List of Tables**

|  |    |
|--|----|
| <b>Table 1.</b> Small molecule CCR5 antagonists.....                                       | 8  |
| <b>Table 2.</b> Three MOR agonists.....  | 13 |
| <b>Table 3.</b> Six MOR antagonists.....   | 14 |
| <b>Table 4.</b> Selective bivalent compounds targeting MOR and another receptor.....       | 19 |
| <b>Table 5.</b> MOR-radiobinding assay.....  | 46 |
| <b>Table 6.</b> Antagonism of calcium mobilization in RANTES-stimulated MOLT-4 cells.....  | 47 |
| <b>Table 7.</b> Antagonism of calcium mobilization in DAMGO-stimulated hMOR-CHO cells..... | 49 |



## List of Figures

|  |    |
|--|----|
| <b>Figure 1.</b> A canonical representation of a GPCR.....   | 2  |
| <b>Figure 2.</b> The CCR5 signaling cascade leads to multiple downstream effects.....                                  | 4  |
| <b>Figure 3.</b> CCR5 and CXCR4 act as co-receptors in helping facilitate viral entry into host cells..                | 7  |
| <b>Figure 4.</b> $\beta$ -FNA ( <b>10</b> ) illustrates the message-address concept for opioid receptor selectivity... | 16 |
| <b>Figure 5.</b> Positive and negative cooperativity in GPCR dimerization.....   | 17 |
| <b>Figure 6.</b> The first reported bivalent compound targeting the CCR5-MOR heterodimer.....                          | 23 |
| <b>Figure 7.</b> Strategy for designing a bivalent compound to target the CCR5-MOR heterodimer...                      | 24 |
| <b>Figure 8.</b> Maraviroc bound to a homology model of receptor CCR5.....   | 25 |
| <b>Figure 9.</b> Comparison of the abilities of <b>18</b> and <b>19</b> to target MOR and CCR5.....                    | 26 |
| <b>Figure 10.</b> Compounds synthesized to target CCR5, MOR and the CCR5-MOR heterodimer...                            | 28 |
| <b>Figure 11.</b> Original 21-atom bivalent compound ( <b>18</b> ) with controls.....                                  | 42 |
| <b>Figure 12.</b> Schematic representation of a calcium mobilization assay.....  | 43 |
| <b>Figure 13.</b> Two bivalent compounds of varying spacer length and their controls.....                              | 45 |
| <b>Figure 14.</b> Crystal structure of maraviroc bound to CCR5.....  | 48 |
| <b>Figure 15.</b> Global minimum of the 19-atom spacer.....  | 53 |
| <b>Figure 16.</b> Global minimum of the 21-atom spacer.....  | 54 |
| <b>Figure 17.</b> Global minimum of the 23-atom spacer.....  | 55 |
| <b>Figure 18.</b> Diverse set conformational ensemble of the 19-atom spacer.....                                       | 57 |
| <b>Figure 19.</b> Diverse set conformational ensemble of the 21-atom spacer.....                                       | 58 |
| <b>Figure 20.</b> Diverse set conformational ensemble of the 23-atom spacer.....                                       | 59 |

**List of Schemes**

|   |    |
|---|----|
| <b>Scheme 1.</b> 6 $\beta$ -naltrexamine ( <b>2</b> ) synthesis.....                                      | 29 |
| <b>Scheme 2.</b> Monoprotection of diamines.....  | 32 |
| <b>Scheme 3.</b> Cbz-protected diamines reacting with diglycolic anhydride.....                           | 37 |
| <b>Scheme 4.</b> Amide-coupling reaction involving the protected diamine and 6 $\beta$ -naltrexamine..... | 39 |
| <b>Scheme 5.</b> Deprotection of monoprotected intermediate.....  | 40 |
| <b>Scheme 6.</b> Amide-coupling reaction of intermediate and acidic cap.....                              | 41 |

## Abbreviations

|                  |  |
|------------------|--|
| AIDS             | acquired immunodeficiency syndrome           |
| ATP              | adenosine triphosphate                       |
| $\beta$ -FNA     | $\beta$ -funaltrexamine                      |
| BRET             | bioluminescence resonance energy transfer    |
| cAMP             | cyclic adenosine triphosphate                |
| CCK <sub>2</sub> | type 2 cholecystokine                        |
| CCR5             | chemokine receptor CCR5                      |
| CNS              | central nervous system                       |
| CXCR4            | chemokine CXC receptor 4                     |
| DAG              | diacyl glycerol                              |
| DCM              | dichloromethane                              |
| DMF              | dimethylformamide                            |
| DOR              | delta opioid receptor                        |
| EL               | extracellular loop                           |
| Env              | envelope protein                             |
| ER               | endoplasmic reticulum                        |
| ERK1/2           | extracellular signal-regulated kinases 1 / 2 |
| FRET             | fluorescence resonance energy transfer       |
| GDP              | guanosine diphosphate                        |
| gp               | glycoprotein                                 |
| GPCR             | g protein-coupled receptor                   |
| GRKs             | G protein-coupled receptor kinases           |
| GTP              | guanosine triphosphate                       |
| HAND             | HIV-associated neurocognitive disorders      |
| IL               | intracellular loop                           |
| IP <sub>3</sub>  | inositol triphosphate                        |
| KOR              | kappa opioid receptor                        |
| MAPK             | mitogen-activated protein kinases            |
| MOR              | mu opioid receptor                           |
| NMR              | nuclear magnetic resonance                   |
| NOR              | nociception/orphanin receptor                |
| Pd/C             | palladium on carbon                          |
| PIP <sub>2</sub> | phosphatidylinositol 4,5-bisphosphate        |
| PKC              | protein kinase C                             |
| PLC              | phospholipase C                              |
| PNS              | peripheral nervous system                    |
| RANTES           | regulated upon activation normally T-cell    |
| expressed        | and secreted                                 |
| SAR              | structure-activity-relationship              |
| TM               | transmembrane helix                          |
| YFP              | yellow fluorescent protein                   |

## Abstract

### DEVELOPMENT OF BIVALENT LIGANDS TARGETING THE PUTATIVE CCR5-MOR HETERODIMER

By Thomas John Raborg, B.S. Cellular Biology

A dissertation submitted in partial fulfillment of the requirements for the degree of master of science at Virginia Commonwealth University.

Virginia Commonwealth University, 2014

Major Director: Yan Zhang  
Associate Professor, Department of Medicinal Chemistry

Chemokine receptor CCR5 and the mu opioid receptor (MOR) undergo receptor dimerization in the membranes of neuronal cells. CCR5 is a co-receptor for the human immunodeficiency virus's (HIV) entry into host cells and is therefore a potential target of small molecule antagonists for therapeutic purposes. Activation of MOR is believed to both increase CCR5 expression levels and increase HIV viral entry into neuronal cells by dimerizing with CCR5. It is therefore of interest to develop chemical probes that target the CCR5-MOR interaction.

A bivalent ligand containing both CCR5 and MOR pharmacophores was previously designed and synthesized to study the CCR-MOR heterodimer and its relevance to NeuroAIDS. In this work, two more bivalent ligands with structural modifications in spacer length were

designed and synthesized along with a number of control compounds. The structure-activity relationships of these compounds were studied in radio-ligand binding assays and cell-based functional assays. Furthermore, the original bivalent ligand and the two new ligands were subjected to conformational analysis.

In conclusion, bivalent ligands were synthesized to target the putative CCR5-MOR heterodimer, and these molecules were subjected to *in vitro* and *in silico* studies. The two new bivalent molecules bound to the MOR with an activity similar to that of naltrexone, an MOR antagonist, while they bound to CCR5 with lower affinity compared to maraviroc, a CCR5 antagonist, indicating that further structural modification to the CCR5 portion of the bivalent ligand is necessary. Also, further work is underway to verify that the two novel bivalent compounds can indeed recognize to the CCR5-MOR heterodimer with reasonable potency.

## 1. Introduction

### 1.1 Chemokine Receptor CCR5

#### 1.1.1 Function of Chemokines and Chemokine Receptors

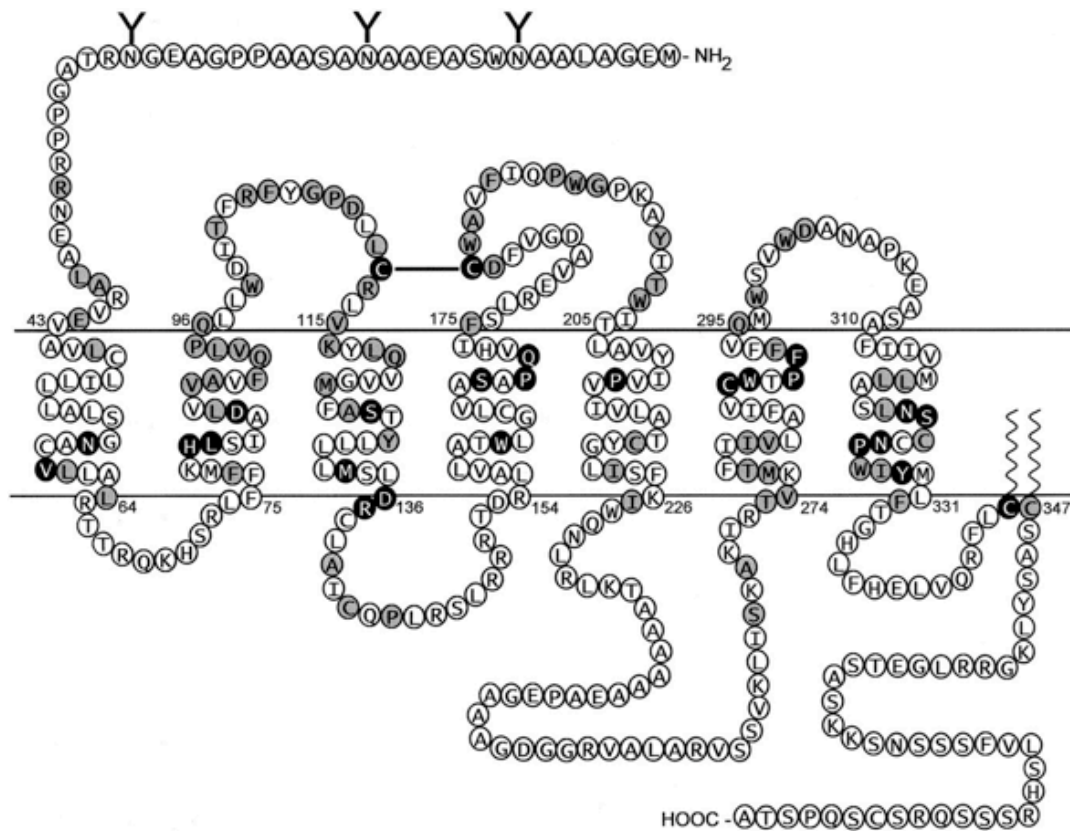
Chemokines, or chemotactic cytokines, are a small group of signal proteins that act as mediators in the process of inflammation.<sup>1-6</sup> When inflammation is induced in living tissue, mediators are released into the blood-stream; these mediators (i.e., cytokines) then bind to proteins on the membranes of leukocytes, or white blood cells, which are recruited to the site of inflammation in order to protect the body from unwanted bacteria.<sup>1-3</sup> Chemokine receptors are among several proteins on the surface of leukocyte cell membranes that interact with the mediators of inflammation.<sup>3</sup>

There are about 50 known and classified chemokines.<sup>3,6</sup> Four families of chemokines exist and they are grouped based on the conserved cysteine residues found at the N-terminal of the peptides: CC chemokine, C chemokine, CXC chemokine and CX<sub>3</sub>C chemokine.<sup>3</sup> In the CC family, the cysteine residues are adjacent to each other.<sup>3</sup> In the C family, on the other hand, one of the cysteine residues is missing.<sup>3</sup> For the CXC and CX<sub>3</sub>C families, the two cysteines are separated by one and three variable residues, respectively.<sup>3</sup> Most of the known chemokines fall into the CC and CXC families and to date there are only 18 known chemokine receptors.<sup>3</sup>

#### 1.1.2 Chemokine Receptor Type CCR5 and GPCRs

Chemokine receptors fall into a superfamily of membranous proteins called G protein-coupled receptors (GPCR).<sup>3-6</sup> These proteins are characterized by their canonical seven transmembrane (TM) helices which bind to heterotrimeric G proteins to mediate responses from outside signal molecules. The GPCR superfamily of proteins includes 791 genes encoding for six different receptor subtypes,

most of which belong to the rhodopsin-like receptor subtype, or the class A subtype.<sup>3</sup> Chemokine receptors are all within the class A GPCR subtype.<sup>3</sup> Chemokine receptors are classified based upon which chemokines bind to them; thus there are CC, CXC, XC and CX<sub>3</sub>C receptors.<sup>3</sup> Also, many of the chemokine receptors are promiscuous and bind to different chemokines within a chemokine family.<sup>1-5</sup> For example, a CC receptor can bind to many different CC chemokines. This allows for redundancy of response, given that many different chemokines within a family can elicit the same response at the same receptor.



**Figure 1.** A canonical representation of a GPCR.<sup>7</sup>

When a chemokine binds to a chemokine receptor, it starts an activation cycle that is characteristic for all GPCRs.<sup>3</sup> That is, when a resting chemokine receptor is activated by an agonist, the bound inactive heterotrimeric G protein, which is composed of guanosine diphosphate (GDP) bound

G $\alpha$  and G $\beta\gamma$  subunits, is converted to an active G protein.<sup>8-14</sup> This protein becomes active by exchanging GDP for guanosine triphosphate (GTP), whereupon the G $\alpha$  and G $\beta\gamma$  subunits dissociate from each other.<sup>11, 12, 14</sup> These subunits then go on to activate or inhibit different downstream signaling pathways through the recruitment of various second-messenger proteins such as adenylyl cyclase and phospholipase-C.<sup>11, 12</sup> These subunits remain active until the GTP is hydrolyzed back to GDP, whereupon the G $\alpha$  and G $\beta\gamma$  subunits re-associate with each other and travel back to the resting-state GPCR.<sup>11, 12, 14</sup>

Looking at agonist-bound crystal structures of GPCRs, several structural changes between activated and unactivated GPCRs are noteworthy.<sup>9, 10, 15</sup> For instance, there are several changes in the transmembrane helices upon agonist binding.<sup>9, 10</sup> These include an outward movement of TM6 and a rearrangement between TM5 and TM7.<sup>9, 10</sup> For particular amino acid residues, there is a disruption of a conserved ionic lock between aspartate/glutamate and arginine of the DRY sequence and the movement of tryptophan<sup>6.48</sup> from TM7 to TM5, both of which allow for the facilitation of the receptor to a more active state.<sup>10</sup> However, it should be noted that these structural changes have not been observed in every GPCR to date.

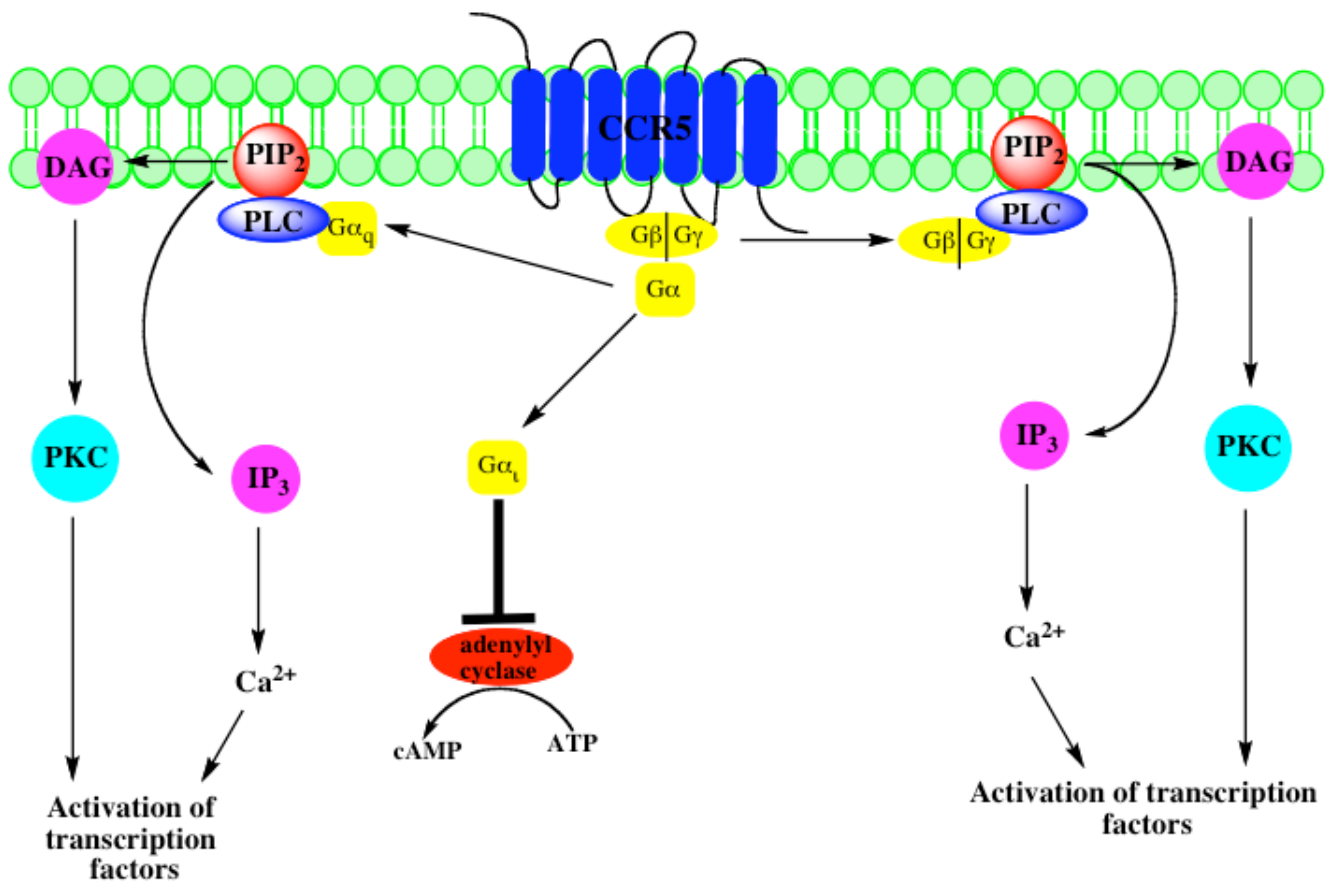
Chemokine receptor type CCR5 (CCR5) is a chemokine receptor that undergoes such conformational changes when it binds to chemokines.<sup>8, 16, 17</sup> CCR5 is expressed on leukocytes and is activated by several chemokines, including, but not limited to, macrophage inflammatory protein-1 $\alpha$  (MIP-1 $\alpha$ ), MIP-1 $\beta$  and regulated upon activation normally T-cell expressed and secreted (RANTES).<sup>8</sup> Activation of CCR5 by these chemokines leads to several signaling cascades that are characteristic of many GPCRs.

### 1.1.3 CCR5 Downstream Effects and Regulation

CCR5 induces several downstream effects upon agonist binding.<sup>16-18</sup> These include intracellular



Ca<sup>2+</sup> release from the endoplasmic reticulum (ER), activating MAP kinases and inhibiting adenylyl cyclase.<sup>16</sup> CCR5 is also promiscuous for the types of Gα subunits it activates, as it activates both Gα<sub>i</sub> and Gα<sub>q</sub>.<sup>17</sup> Because CCR5 couples to two different G proteins, it allows CCR5 to activate more than one signaling pathway.<sup>17</sup> For the pathway involving Gα<sub>i</sub>, the Gα subunit inhibits adenylyl cyclase.<sup>17</sup> This reduces the production of cAMP from ATP. For the pathway involving Gα<sub>q</sub>, phospholipase C (PLC) becomes activate and produces diacyl glycerol (DAG) and inositol triphosphate (IP<sub>3</sub>) by hydrolyzing phosphatidylinositol 4,5-biphosphate (PIP<sub>2</sub>).<sup>17</sup> DAG goes on to activate protein kinase C (PKC), whereas IP<sub>3</sub> activates calcium channels on the ER and causes the amount of intracellular calcium to increase.<sup>17</sup> The Gβγ subunit also plays a roll in downstream signaling by activating PLC, which, as already mentioned, increases the production of intracellular calcium.<sup>17</sup>



**Figure 2.** The CCR5 signaling cascade leads to multiple downstream effects.

GPCRs such as CCR5 are regulated by a variety of mechanisms; these include desensitization of the receptor, internalization of the receptor and recycling/degradation of the receptor.<sup>19, 20</sup> Desensitization of the receptor reduces its response to external stimuli, whereas internalization and recycling/degradation of the receptor reduce the amount of receptors present on the cell's membrane.<sup>19, 20</sup> Repeated activation of the receptor by agonists leads to desensitization through the phosphorylation of the GPCR's C-terminus; the protein becomes desensitized by the phosphorylation of four serine residues – S336, S337, S342 and S349 – by G protein-coupled receptor kinases (GRKs).<sup>20</sup> For the process of internalization and recycling/degradation of the receptor, the phosphorylated serine residues increase the binding affinity of GPCRs for  $\beta$ -arrestin.<sup>20</sup> When  $\beta$ -arrestin binds to a GPCR, it blocks G proteins from binding to it, thereby eliminating the GPCR's downstream signaling pathways.<sup>20</sup>  $\beta$ -arrestin can then complex with adaptor complex 2 (AP2) and clathrin.<sup>20</sup> This complex causes the GPCR to internalize by endocytosis, whereupon it is either degraded by lysosomal proteins or recycled back to the membrane.<sup>20</sup> Also,  $\beta$ -arrestins can activate several cascades by activating mitogen-activated protein kinases (MAPKs) and non-receptor tyrosine kinases (nRTKs).<sup>19, 20</sup> Furthermore, a GPCR can be desensitized through the binding of a certain ligand which reduces the GPCR's affinity for other ligands (this ligand varies depending on the GPCR to which it binds).<sup>19</sup>

#### **1.1.4 GPCRs as Drug Targets and CCR5 in HIV-Associated Diseases**

GPCRs are among the most targeted proteins for therapeutic purposes.<sup>21</sup> In fact, more than 30% of all drugs designed in the last five years target GPCRs.<sup>22, 23</sup> One of the disease states associated with GPCRs is cancer.<sup>24, 25</sup> When a gene encoding for a GPCR has been mutated in such a way so as to produce a constitutively active protein, very often the signaling pathways downstream of that GPCR remain active.<sup>24, 25</sup> This leads to the growth and differentiation of cells in which the GPCR is expressed. CCR5 is also associated with breasts cancer, ovarian cancer and prostate cancer.<sup>25 – 30</sup>

CCR5 is also associated with the human immunodeficiency virus (HIV).<sup>31</sup> In fact, CCR5 is among the most targeted proteins in HIV therapeutics.<sup>31</sup> This is because CCR5 acts as a vital co-receptor in HIV invasion into host cells.<sup>31-33</sup> Although CCR5 is predominantly expressed on leukocytes, in particular helper-T cells, it is also expressed on microglia and astroglia, and the infection of these cells contributes to the degradation of neurons.<sup>31</sup> CCR5's association with HIV-invasion in host cells is described in more detail below this section.

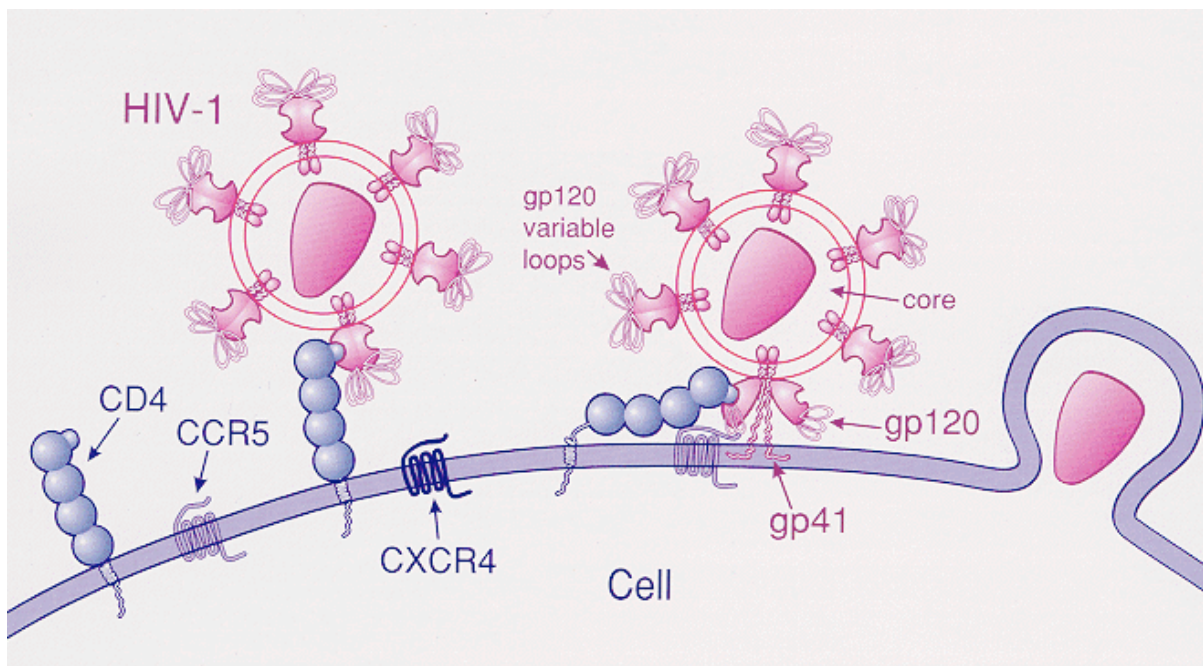
### **1.1.5 CCR5's Association with HIV/AIDS**

HIV causes the destruction of lymphocytes expressing cluster of differentiation 4 (CD4) membranous proteins.<sup>31</sup> This leads to an immunocompromised disease known as acquired immunodeficiency syndrome (AIDS).<sup>31</sup> In particular, this disease is most prevalent in developing countries in sub-Saharan Africa, and most mortalities from AIDS come from this region.<sup>27</sup> About 1.6 million people died from AIDS in 2012 according to the Center for Disease Control, and more than 2 million are infected per year on average.<sup>31</sup> The virus consists of a single strand of RNA necessary to encode viral enzymatic and structural proteins.<sup>31</sup>

The virus invades host cells by using a viral envelop protein (Env) consisting of three glycoprotein subunits that bind to and interact with CD4.<sup>31</sup> This glycoprotein consists of gp41 and gp120 subunits.<sup>31</sup> A conformational change in the gp120 subunit upon CD4 binding allows it to interact with CCR5, which acts as a co-receptor in HIV viral entry.<sup>31</sup> Once this three-protein complex is formed between CD4, gp120 and CCR5, another conformational change occurs in the Env protein that allows gp41 to insert itself into the host cell's membrane.<sup>31</sup> This further facilitates viral entry into host cells. However, although CCR5 helps the HIV virus invade host cells, receptor CD4 is the main receptor of HIV.

The importance of CCR5 in HIV infection is demonstrated by the increased resistance that

people with homozygous CCR5 recessive alleles have to HIV viral invasion.<sup>35, 36</sup> That is, if an individual has mutations in both CCR5-encoding genes, then HIV cannot use CCR5 as a co-receptor to invade host cells. Mutations to CCR5 prevent the gp120 subunit of the Env protein from binding to it and facilitating viral entry.



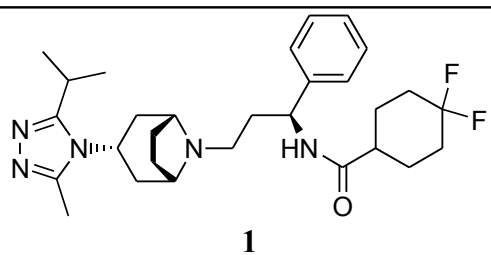
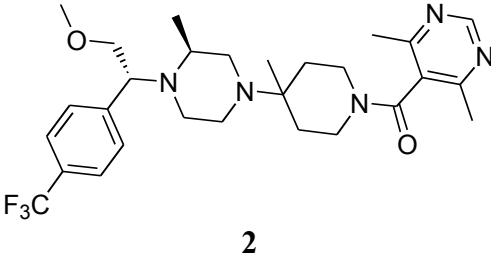
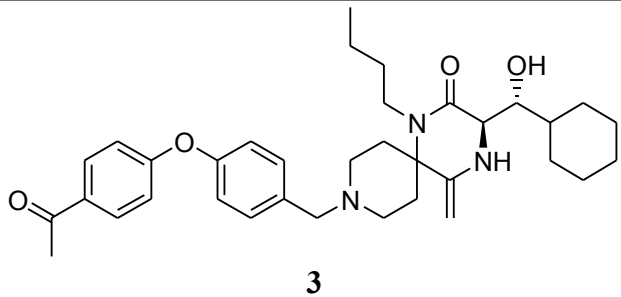
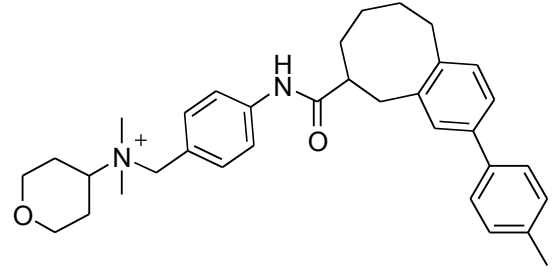
**Figure 3.** CCR5 and CXCR4 act as co-receptors in helping facilitate viral entry into host cells.<sup>37</sup>

### 1.1.6 Small molecules targeting CCR5

Pharmaceutical companies have been trying to develop small-molecule antagonists that target CCR5, mostly because of its involvement in HIV host cell invasion.<sup>39-42</sup> These efforts have led to the approval of maraviroc (**1**) by the FDA to treat retroviral infections.<sup>39-41</sup> Maraviroc was developed by Pfizer from a high-throughput screening (HTS) hit in the early 2000's.<sup>39-41</sup> The initial compound showed a high affinity for CCR5 ( $K_i = 4$  nM) but did not produce any antiretroviral activity.<sup>39, 40</sup> Therefore, the compound was modified using structure-activity relationship (SAR) techniques, and this led to a

molecule, maraviroc, that had an  $IC_{50} = 2 \text{ nM}$  for the CCR5 receptor. In fact, clinical studies indicated that two daily doses of 25 mg maraviroc were more effective at slowing the progression of HIV-1 host cell invasion than the current leading anti-HIV-1 drug at the time.<sup>41</sup>

**Table 1.** Small molecule CCR5 antagonists

| Name       | Structure  | Status                                    |
|------------|--|---|
| Maraviroc  |  <p style="text-align: center;"><b>1</b></p>   | FDA-approved                              |
| Vicriviroc |  <p style="text-align: center;"><b>2</b></p>  | Terminated                                |
| Aplaviroc  |  <p style="text-align: center;"><b>3</b></p> | Terminated                                |
| TAK-779    |  <p style="text-align: center;"><b>4</b></p> | Modified form in Phase II Clinical Trials |

Two other anti-HIV-1 drugs that showed very good antagonism for the CCR5 receptor were vicriviroc (**2**) and aplaviroc (**3**).<sup>41</sup> However, both these drugs were discontinued during Phase III clinical trials because vicriviroc had poor bioavailability and aplaviroc showed severe hepatotoxicity.<sup>41</sup> <sup>43</sup> To date, maraviroc is considered the most effective drug for inhibiting the progression of HIV through antagonism of CCR5.<sup>44</sup> However, Schering-Plough has reported the development of a second-generation CCR5 antagonist known as SCH532706.<sup>44</sup> As of right now, SCH532706 is in Phase III clinical trials, and the molecule shows both high anti-HIV-1 activity and good bioavailability.<sup>44</sup>

Before the development of maraviroc and other second-generation CCR5 antagonists, TAK-779 (**4**), the first known CCR5 antagonist, was reported by Takeda Chemicals in 1999.<sup>45</sup> The molecule was shown to inhibit HIV-1 entry with an  $IC_{50} = 3.7$  nM.<sup>45</sup> The molecule was also shown to have a very high affinity for CCR5 in a radioligand binding assay ( $K_i = 1.4$  nM).<sup>45</sup> However, the molecule's development was discontinued because of both poor oral bioavailability and toxicity issues, although modification to improve oral bioavailability led to another CCR5 antagonist which is currently in phase II clinical trials.<sup>44</sup>

## 1.2 The Mu Opioid Receptor

### 1.2.1 Opioid Receptors

Opioid receptors are the site of action for morphine and its derivatives.<sup>46</sup> The name “opioid” comes from the fact that morphine, the first known exogenous agonist of this class of receptors, was isolated from opium poppy extracts.<sup>46</sup> Opioid receptors, like chemokine receptors, are GPCRs.<sup>46</sup> To date there are four known opioid receptors that have been crystallized:  $\delta$  opioid receptor (DOR),  $\kappa$  opioid receptor (KOR),  $\mu$  opioid receptor (MOR) and nociception/orphanin opioid receptor (NOR).<sup>47–50</sup> Two of these receptors – KOR and MOR – were named according to the opiates to which they bound:

morphine and ketocyclazocine, respectively.<sup>47,49</sup> There are also small endogenous peptides that bind to opiate receptors; they include enkephalins and dynorphins.<sup>51-55</sup>

When opiates bind to their MOR, they elicit analgesic and anti-diarrheal effects.<sup>51,52</sup> This gives them a high therapeutical potential, especially in settings requiring fast-acting pain-relief. However, although opiates elicit analgesic and anti-diarrheal effects upon binding to their receptors and produce numerous therapeutic results, there are certain unwanted side-effects when taking them.<sup>56-59</sup> For instance, the molecule morphine has a high potential for abuse because of its addictive nature.<sup>56-59</sup> Much of the work that has been done modifying opiates, therefore, has focused on reducing this addictive potential.<sup>60</sup> Also, it has been discovered that while the three traditional opioid receptors – DOR, KOR and MOR – each produce analgesic effects, the neural response that each receptor controls is different.<sup>52</sup> DOR affects anxiety and depressive behaviors, KOR produces dysphoria and MOR control euphoric feelings.<sup>52</sup>

### 1.2.2 Mu Opioid Receptor Structure and Downstream Signaling

As mentioned before, opioid receptors are included in the GPCR superfamily.<sup>61</sup> Thus, the mu opioid receptor shares many structural features with other common GPCRs, most importantly the seven TM helices. Of note, MOR has a  $\beta$ -hairpin in extracellular loop (EL) 2.<sup>61</sup>

Because MOR is a GPCR, it shares many of the same signaling mechanisms as CCR5, such as the activation of a heterotrimeric G protein.<sup>61</sup> However, because it is coupled to a different G protein (i.e.,  $G\alpha_{i/o}$ ) from CCR5, it causes the activation of different downstream signaling pathways upon agonist binding.<sup>61</sup> For instance,  $G\alpha_i$  inhibits adenylyl cyclase and activates  $K^+$  channels, whereas  $G\alpha_o$  inhibits  $Ca^{2+}$  channels (and thus causes the concentration of intracellular calcium to decrease).<sup>61</sup> However, because the  $G\beta\gamma$  subunit activates PLC and thus increases the concentration of intracellular calcium, agonist binding to MOR can also cause an effect opposite from that of  $G\alpha_o$  activation. This

creates a negative feedback loop that allows for fine-tuning of downstream signaling.

As with the CCR5 receptor, MOR activity is also regulated: desensitization and protein-based trafficking also occur so as to limit the amount of receptor activity on a cell's membrane.<sup>61</sup> Phosphorylation of the serine residues located at the protein's C-terminus cause it to become desensitized to external stimuli, and this also leads to  $\beta$ -arrestin recruitment and receptor internalization.<sup>61</sup> However, it should be mentioned that morphine does not cause receptor phosphorylation at high levels.<sup>61</sup> Rather, endogenous ligands such as etorphine are responsible for such effects.<sup>55</sup>

### **1.2.3 Opioid Addiction and Its Effects on HIV/AIDS Infected Individuals**

While opiates are effective at reducing pain, they increase the risk of drug-based addiction and abuse in individual patients.<sup>56-59</sup> This abuse is particularly dangerous in patients that are infected with HIV, as it has been shown that the rate of HIV-1 progression spikes in opiate-addicted patients with AIDS.<sup>62-68</sup> This HIV-1 progression coupled with opiate addiction increases the likelihood of HIV-associated neurocognitive disorders (HANDs) and neurological complications of AIDS (neuroAIDS).<sup>62, 66</sup> Thus, the use of opiates by HIV-infected patients appears to have a complimentary effect on the rate of viral proliferation.<sup>65-67</sup>

Studies have shown that MOR is responsible for the addictive properties of morphine.<sup>58, 59</sup> In MOR-knockout mice, morphine's addictive properties were abolished.<sup>58</sup> Also, MOR-knockout mice are less prone to develop addictions to other drugs such as nicotine and alcohol, indicating the importance of the MOR in influencing general addiction.<sup>58, 59</sup> However, despite their involvement in producing and prolonging addiction, MOR agonists such as morphine are still used to treat pain. In fact, many novel drugs used to treat pain are modified analogs of morphine.<sup>60</sup> As such, most of the new drug-design projects involving opiates focus not only on improving the selectivity and potency of MOR agonists,



but also making them less addictive. Opiate addiction is still a problem in general society, however, in particular among HIV patients.<sup>62-68</sup>

#### 1.2.4 Addiction in NeuroAIDS

In HIV-infected patients, the progression of AIDS is accelerated by the use of opiates.<sup>69-71</sup> The central nervous system (CNS) in particular seems to be the most affected region of AIDS progression in opiate-addicted individuals.<sup>72, 73</sup> This is because of the fact that both CCR5 and MOR are expressed on the glial cells (astroglia and microglia) of the CNS and MOR can heterodimerize with CCR5 when activated by an opiate.<sup>69-71</sup> In fact, MOR has been shown to effect immunomodulation by acting as a chemokine and potentiating the downstream signaling pathways of chemokine receptors.<sup>74, 75</sup> Also, activation of MOR has been shown to increase the expression levels of CCR5, resulting in more co-receptors for HIV.<sup>76, 77</sup>

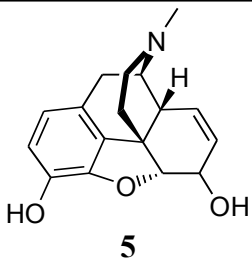
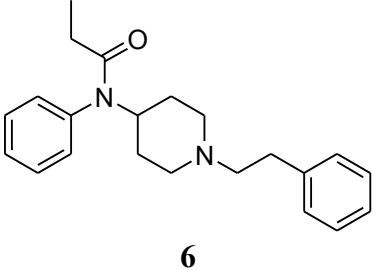
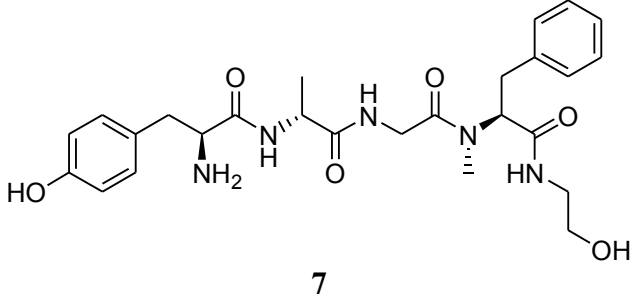
HIV does not directly degrade neurons of the CNS, but instead infects the microglia and astroglia surrounding them.<sup>73, 76</sup> This is because CCR5 is more prevalent on glial cells than on neurons.<sup>76</sup> When HIV-1 infects glial cells, it not only destroys such cells when new virions are released into the external environment; it also releases byproducts, such as viral proteins and chemokines, that result in degeneration of neuronal cells.<sup>76</sup> The proximity of glial cells to neurons result in the excreted toxins damaging neurons, which leads to inflammation.<sup>76, 77</sup> Opiates potentiate the infection of HIV in microglia through MOR dimerizing with CCR5, which makes the latter protein more susceptible to HIV-1 attachment.<sup>69-71</sup>

#### 1.2.5 Mu Opioid Receptor Ligands: Agonists and Antagonists.

There are both known exogenous and endogenous agonists that bind to MOR.<sup>78, 79</sup> While the former are small molecules derived from morphine (**5**), the latter are peptides.<sup>78</sup> Because of morphine's

unwanted side-effects, the development of new MOR agonists that have reduced addictive potentials has been explored.<sup>79</sup> The table below shows some of the peptidic and non-peptidic agonists of MOR. One of the peptidic agonists, DAMGO (7), is a synthetic peptide based off of an enkephalin, and it is highly selective for MOR over the other opioid receptors.<sup>78</sup>

**Table 2.** Three MOR agonists.

| Name     | Structure  | KOR $K_i$ (nM) | DOR $K_i$ (nM) | MOR $K_i$ (nM) |
|----------|--|----------------|----------------|----------------|
| Morphine | <br>5   | 33.7           | 111            | 2.70           |
| Fentanyl | <br>6  | 387            | 403            | 1.50           |
| DAMGO    | <br>7 | 534            | 634            | 1.23           |

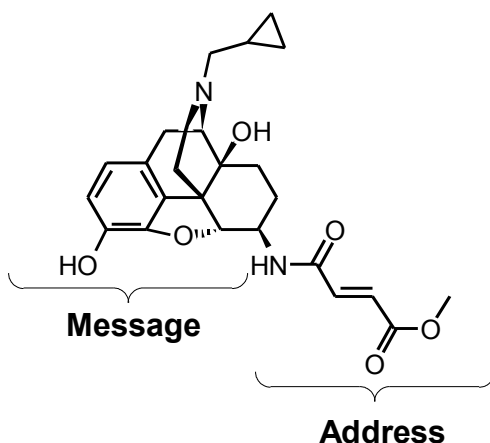
Along with the agonists, there have been several antagonists developed to treat morphine and general opiate addiction (N.B., see table below).<sup>80-83</sup> These, like the agonists, also include both small molecules and synthetic peptides.<sup>80-83</sup> Both naloxone (8) and naltrexone (9) are non-selective antagonists for all three traditional opioid receptors (i.e., DOR, KOR and MOR).<sup>80</sup>

**Table 3.** Six MOR antagonists.

| Name         | Structure     | KOR $K_i$ (nM) | DOR $K_i$ (nM) | MOR $K_i$ (nM) |
|--------------|---------------|----------------|----------------|----------------|
| Naloxone     | <br><b>8</b>  | 1.95           | 49.0           | 0.62           |
| Naltrexone   | <br><b>9</b>  | 0.28           | 6.94           | 0.11           |
| $\beta$ -FNA | <br><b>10</b> | 3.40           | 78.7           | 1.10           |
| Clocinnamox  | <br><b>11</b> | 5.70           | 1.90           | 0.70           |
| Cyprodime    | <br><b>12</b> | 2180           | 245            | 5.40           |

|      |  |      |      |      |
|------|--|------|------|------|
| CTAP | $  \begin{array}{c}  \text{D-Phe—Cys—Tyr—D} \\  \text{H}_2\text{N—Thr—Pen—ThrArg} \\  \text{Trp} \\  \mathbf{13}  \end{array}  $ | 5310 | 8450 | 2.10 |
|------|--|------|------|------|

To improve selectivity for MOR over the other two opioid receptors,  $\beta$ -FNA (**10**) was synthesized.<sup>83</sup> While  $\beta$ -FNA binds to all three receptors, it only binds to MOR irreversibly.<sup>83</sup> Notice, however, that the only difference between  $\beta$ -FNA and naltrexone is the group attached to the C-ring of the morphanin core. This fact supports the “message-address” concept proposed by Portoghese et al.<sup>84</sup> This concept is based on the premise that the morphanin scaffold has two main parts: 1) the morphanin core, or the “address” portion of the molecule, that is active at all opioid receptors and 2) the “message” portion of the molecule, which is located off of the C-ring and helps determine receptor selectivity for the molecule. In other words, selectivity for a particular receptor can be altered merely by changing the group (i.e., the “message” portion) attached to the C-ring of a morphine-derived molecule. This is why  $\beta$ -FNA is selective for MOR whereas naltrexone is not despite having similar core structures.<sup>83, 84</sup> The molecule clocinnamox (**11**) was also designed using the message-address concept in order to improve selectivity for MOR over the other two traditional opioid receptors.<sup>81</sup> Cyprodime (**12**) has the highest selectivity for MOR among the molecules presented here.<sup>80</sup> This is because removing the dihydrofuran ring from a morphanin core reduces its affinities for KOR and DOR but not MOR.<sup>80</sup> Finally, CTAP (**13**), a cyclic peptide, has the greatest affinity for the MOR receptor among the molecules listed in the table with a  $K_i$  in the low nanomolar range.<sup>82</sup>



**Figure 4.**  $\beta$ -FNA (**10**) illustrates the message-address concept for opioid receptor selectivity.

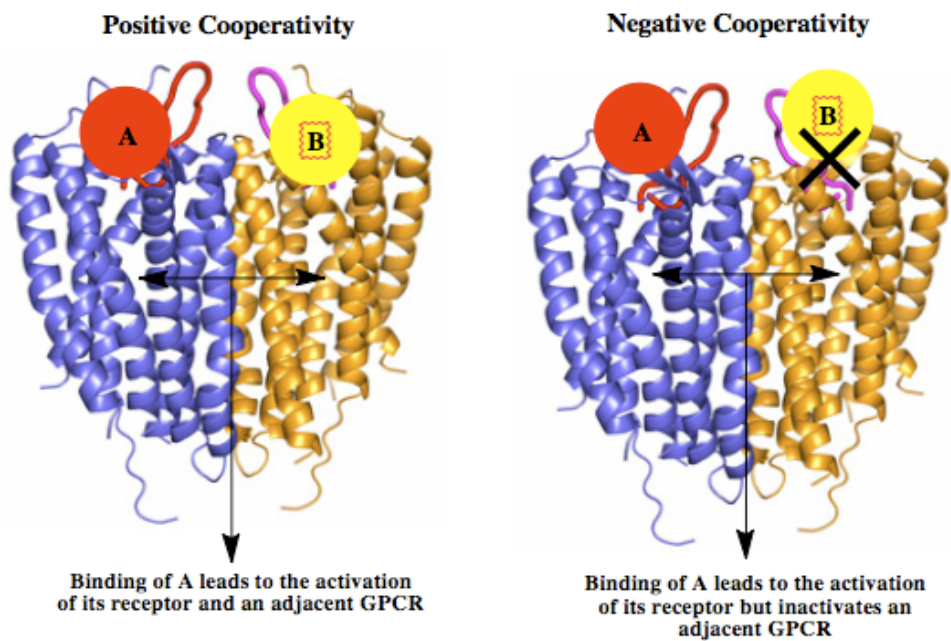
### 1.3 GPCR Dimerization

It was thought that all GPCRs acted in a monomeric fashion in which the protein's activation was dependent only upon the binding of a single ligand. However, evidence was discovered indicating that GPCRs could dimerize with one another and sometimes form oligomeric complexes.<sup>85, 86</sup> It was also discovered that the binding of one ligand to a GPCR could prevent another GPCR from interacting with its ligand.<sup>85</sup> This interaction, termed “cross-talk,” illustrates the ability of an activated GPCR to affect the activity of another GPCR for a ligand through dimerization.<sup>85, 86</sup> Furthermore, it has been demonstrated that receptor cross-talk can either enhance or decrease the activity of an adjacent, dimerized receptor for its ligand.<sup>85-89</sup>

Advanced techniques have been developed for detecting the dimerization of two GPCRs, including bioluminescence resonance energy transfer (BRET), fluorescence resonance energy transfer (FRET), and advanced crystallization techniques.<sup>91-95</sup> For FRET, two proteins are tagged with two different fluorescent proteins.<sup>91, 95</sup> If the proteins dimerize, then when one of the proteins (i.e., the donor chromophore) is stimulated by fluorescent light it will transfer energy of a particular excitation wavelength to the adjacent protein (i.e., the acceptor chromophore), causing it to also emit light of a particular wavelength.<sup>91, 95</sup> It is important to note that the acceptor chromophore will only emit light if the donor chromophore has dimerized with it. BRET also uses a similar technique, except the donor

chromophore is coupled with a bioluminescent luciferase enzyme and therefore doesn't need to be stimulated by light from an external source.<sup>91,95</sup> Either way, both techniques are ideal for detecting the presence of protein dimers using fluorescent light.<sup>91,95</sup> A more modern technique using GPCR crystallization coupled with atomic-force microscopy is also a good way of detecting GPCR dimerization.<sup>92</sup>

It is important to mention that GPCR dimerization has an important function on receptor activity and signaling. As mentioned beforehand, GPCR dimerization can either enhance the affinity of a receptor for its ligand or decrease a receptor's affinity for its ligand. The former scenario, termed positive cooperativity, leads to a receptor with greater signaling and function, whereas the latter situation, termed negative cooperativity, leads to a receptor with decreased signaling capabilities.<sup>86</sup>



**Figure 5.** Positive and negative cooperativity in GPCR dimerization.

### 1.3.1 Mu Opioid Receptor Dimerization

There have been multiple studies illustrating the ability of MOR to dimerize with another MOR

and other GPCR types.<sup>96-99</sup> MOR has been shown to dimerize with KOR, DOR, NOR, CCR5 and cannabinoid receptors.<sup>96-100</sup> Interestingly, when MOR is dimerized with another receptor, it is able to activate signaling pathways that it cannot activate on its own.<sup>99</sup> For example, when not dimerized with another opioid receptor, neither MOR nor DOR can couple with the  $G\alpha_{q/11}$  G protein.<sup>99</sup> However, when coupled together, the MOR-DOR complex activates the  $G\alpha_{q/11}$  signaling pathway quite readily.<sup>99</sup> This suggests that certain heterodimers can activate signal pathways that the monomers cannot activate themselves. Dimerization may also enhance or inhibit the rate of receptor desensitization and internalization, as evidenced by studies involving the MOR-NOR heterodimer.<sup>101</sup>

### 1.3.2 Bivalent Ligands Targeting GPCR Heterodimers.

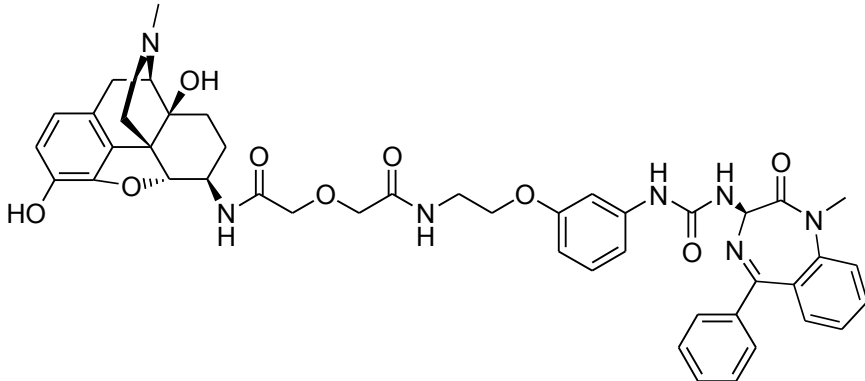

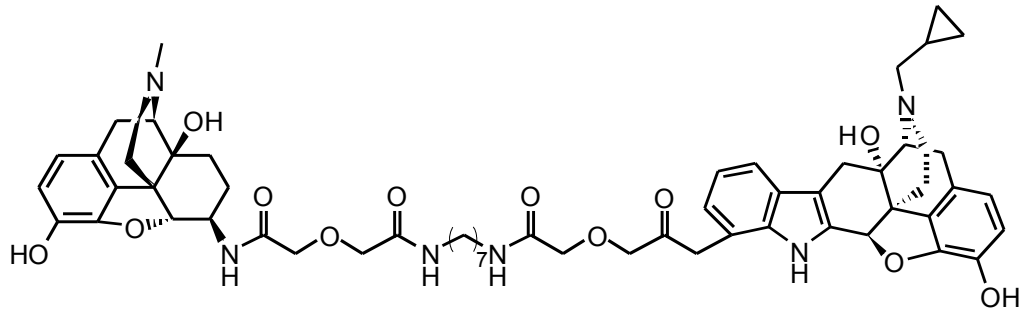
Bivalent compounds are necessary probes for studying the interaction between two distinct monomers that form a dimer.<sup>102-104</sup> Bivalent compounds are molecules that contain two distinct pharmacophores, and they can either be classified as homobivalent or heterobivalent depending on whether or not they contain the same or different pharmacophores.<sup>102</sup> In studies involving the dimerization of the same two protein types (homodimerization), a homobivalent molecule is necessary to analyze the interaction; the converse is true for studies involving the dimerization of two dissimilar protein types (heterodimerization).<sup>103</sup> By targeting a dimer of GPCRs using a bivalent compound, new pharmacological profiles can be obtained revealing information particular to that dimer.<sup>102, 104</sup> Also, bivalent compounds can lead to higher affinity and higher selectivity for the target in question.<sup>102-104</sup>

The two pharmacophores in a bivalent compound are often attached to each other – or bridged – by a linker of carbon atoms.<sup>102-104</sup> This linker both allows each pharmacophore to interact with its receptor individually and also enables both pharmacophores to bind at a similar time. Researchers have anticipated that the average distance between two GPCR dimers is anywhere from 27 Å to 32 Å. Therefore, a linker should be somewhere within that range.<sup>103</sup>

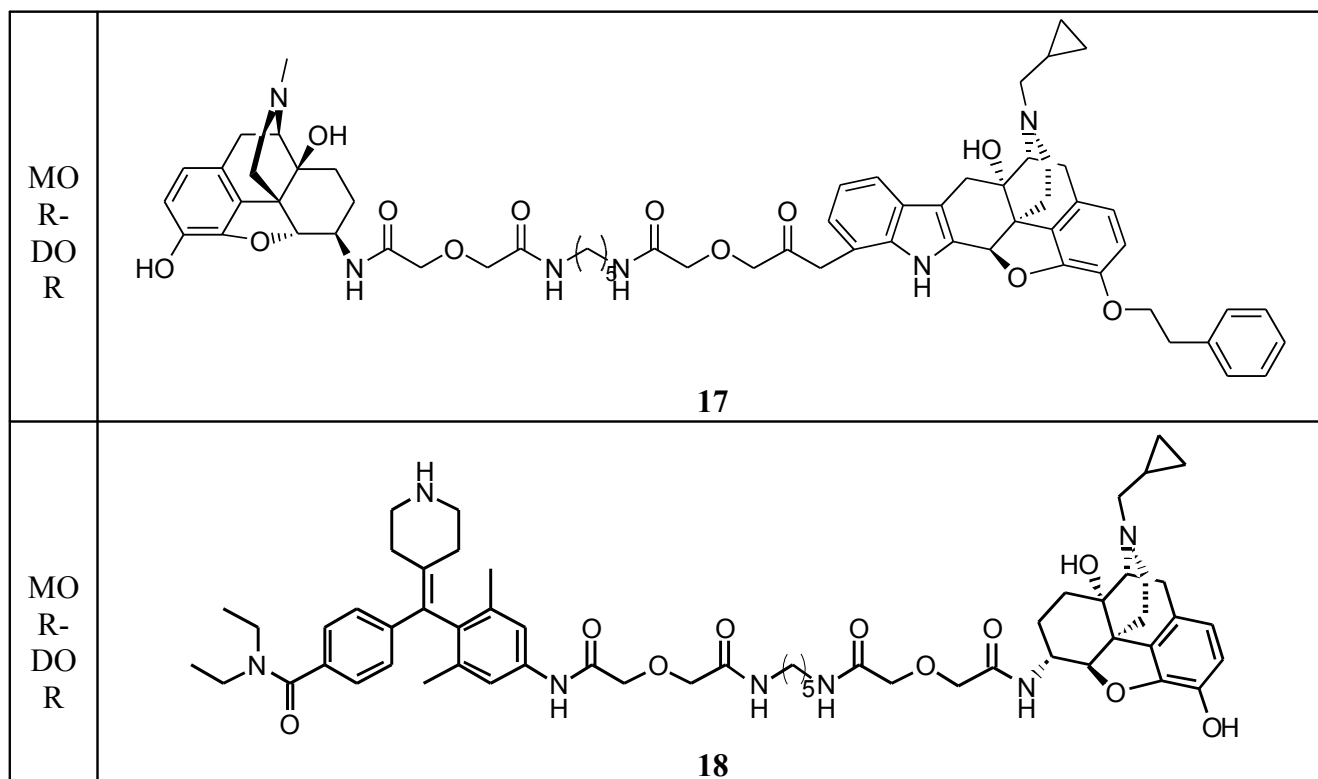
There are numerous linkers targeting MOR heterodimers that have been synthesized to date.<sup>105-</sup>

<sup>108</sup> They include an MOR agonist, oxymorphone, and a type 2 cholecystokine (CCK<sub>2</sub>) receptor antagonist being synthesized across a linker in order to determine if the MOR and CCK<sub>2</sub> associate *in vivo* (**14**).<sup>105</sup> They also include compound **15**, a MOR-KOR binding compound that contained the MOR antagonist naltrexone and the KOR antagonist 5'-GNTI.<sup>106</sup>

**Table 4.** Selective bivalent compounds targeting MOR and another receptor.

| Targets              | Structure   |
|----------------------|---|
| MOR-CCK <sub>2</sub> |  <p style="text-align: center;"><b>14</b></p>  |
| MOR-KOR              |  <p style="text-align: center;"><b>15</b></p> |
| MOR-DOR              |  <p style="text-align: center;"><b>16</b></p> |





Finally, there was a series of compounds similar to **16** that contained both pharmacophores for DOR and MOR.<sup>107</sup> This series was made to assess the functional role of the MOR-DOR heterodimer in analgesia.<sup>107</sup> Portoghesi et al. wanted to see whether or not a bivalent analgesic compound could be designed that mitigated the deleterious, addictive side-effects of morphine.<sup>107</sup> **16** was comprised of an MOR agonist, oxycodone, and a selective DOR antagonist, naltridole. The two pharmacophores were separated by a 21-atom spacer with a maximum length of 25.4 Å. It was found that this molecule was 50-fold more potent than morphine without producing tolerance or dependence side-effects, which also illustrated the importance of DOR in potentiating the activity of MOR.<sup>107</sup>

However, because molecule **16** was not selective for the MOR-DOR heterodimer over the MOR-MOR and DOR-DOR homodimers, Harvey et al. developed two finely-tuned MOR-DOR bivalent compounds – **17** and **18** – that were very selective for their intended target.<sup>108</sup> The reason they did this was because **16** could also interact with the MOR-MOR and DOR-DOR homodimers with

similar affinity to the MOR-DOR heterodimer.<sup>108</sup> In order to solve this problem and fine-tune their molecule, they constructed **17**, a molecule containing the MOR agonist oxymorphone and a low affinity DOR antagonist, ENTI, and **18**, a molecule containing the MOR antagonist naltrexone and a low affinity DOR agonist, DMSNC80. These molecules had reduced affinity for the DOR-DOR and MOR-MOR homodimers.<sup>108</sup> Of note, both compounds synergistically raised the binding affinity for the DOR pharmacophore when the binding assays were conducted using membranes composed of MOR-DOR relative to assays conducted using DOR alone membranes.<sup>108</sup> The concept of fine-tuning the ability of bivalent ligands to bind to a particular dimer using high and low affinity pharmacophores is an important aspect of drug design using bivalent compounds.

## **2. Bivalent Ligands Targeting the Putative CCR5-MOR Heterodimer**

### **2.1 Project Design**

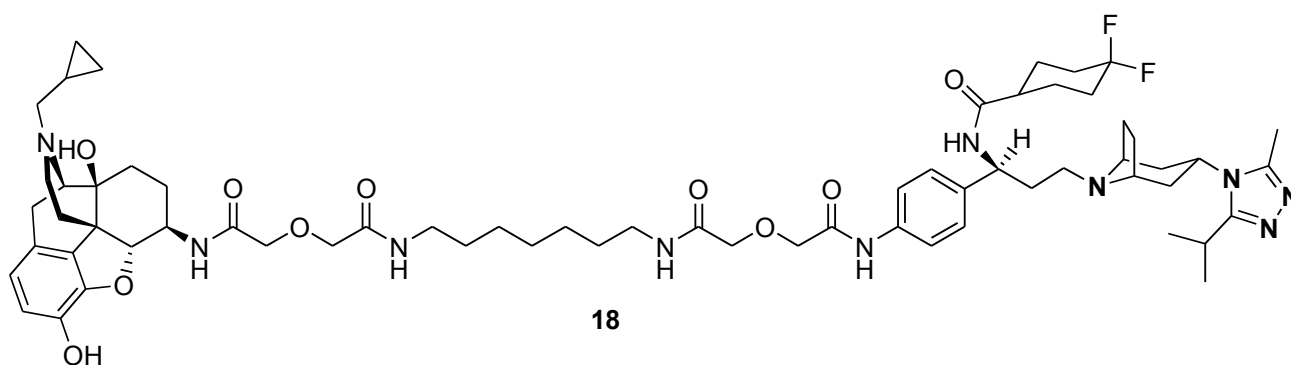
The effects of human immunodeficiency virus (HIV)-1 has been shown to be potentiated by the abuse of various drugs, including alcohol, opioids and cocaine.<sup>62, 64-67</sup> In fact, many cases of HIV infection can be attributed to the use of contaminated needles.<sup>109</sup> The abuse of certain drugs – opioids in particular – has been associated with the mu opioid receptor (MOR) due to the ability of those drugs to bind to and agonize MOR. Furthermore, the binding of opioids to MOR have been shown to change the normal response of the immune system, a condition called immunomodulation, due to the ability of MOR to regulate chemokine receptors; this condition, in turn, has been shown to produce negative immunological effects due to the inability of modulated chemokine receptors to respond to infections.<sup>62, 110</sup> Given that HIV progression is associated with the immune system and the functioning of lymphocytes, changes in the immune system can result in the potentiation of HIV.<sup>62, 68</sup>

Chemokine receptor CCR5, a G-protein coupled receptor (GPCR), is expressed on many cell types, including lymphocytes and neuronal cells.<sup>32, 33, 111, 112</sup> CCR5 has been shown to act as a co-receptor in HIV cellular invasion. It has also been demonstrated that the inhibition of CCR5 mitigates HIV viral entry into lymphatic cells and cells of the central nervous system (CNS).<sup>111-113</sup> Maraviroc, a synthetic CCR5 antagonist, was developed by Pfizer to combat the invasion of HIV into lymphatic cells in the mid 2000's.<sup>113</sup> In combination with different antiretroviral therapies, maraviroc has been shown to inhibit the progression of HIV-1 infection. However, other health complications, such as HIV-associated neurocognitive disorders (HANDS), affect half of AIDS patients and are not mitigated by maraviroc.<sup>114, 115</sup> These patients are characterized by behavioral abnormalities such as reduced cognition and motor control, health effects resulting from the invasion of HIV into cells of the CNS, in particular microglia and astrocytes.<sup>114, 115</sup> Since microglia defends primary neuronal cells from infection and astrocytes are responsible for the delivery of nutrients into the brain, complications can result from the destruction or induced inactivity of these cell types.<sup>76</sup> The immunocompromised state of these cells by HIV-1 infection results in a condition known as neuroAIDS.<sup>114, 115</sup>

The increased risk of HIV-1 infection in cells of the CNS has been linked to the stimulation of MOR by opiates.<sup>62, 64-66, 75, 77</sup> This is because, once agonized by an opioid, MOR may produce synergistic interactions with CCR5.<sup>75, 77</sup> An example of this is how activation of MOR by opioids up-regulates the expression of CCR5 in cells, which in turn promotes HIV-1 infection via the virus using CCR5 for viral entry.<sup>77</sup> Opiates can also indirectly damage primary neuronal cells by causing inflammation in microglia and astrocytes.<sup>63, 116</sup> The type and extent of neuronal injury to different neurons by HIV-1 infection has also been correlated with the amount of MOR expressed on those neuronal cell types.<sup>116, 117</sup>

Verification of the synergism between the MOR and CCR5 has been demonstrated by the ability of the receptors to heterodimerize and undergo receptor crosstalk.<sup>118, 119</sup> Since this crosstalk was discovered to take place in lymphocytes, it has been hypothesized that it also takes place in neurons and

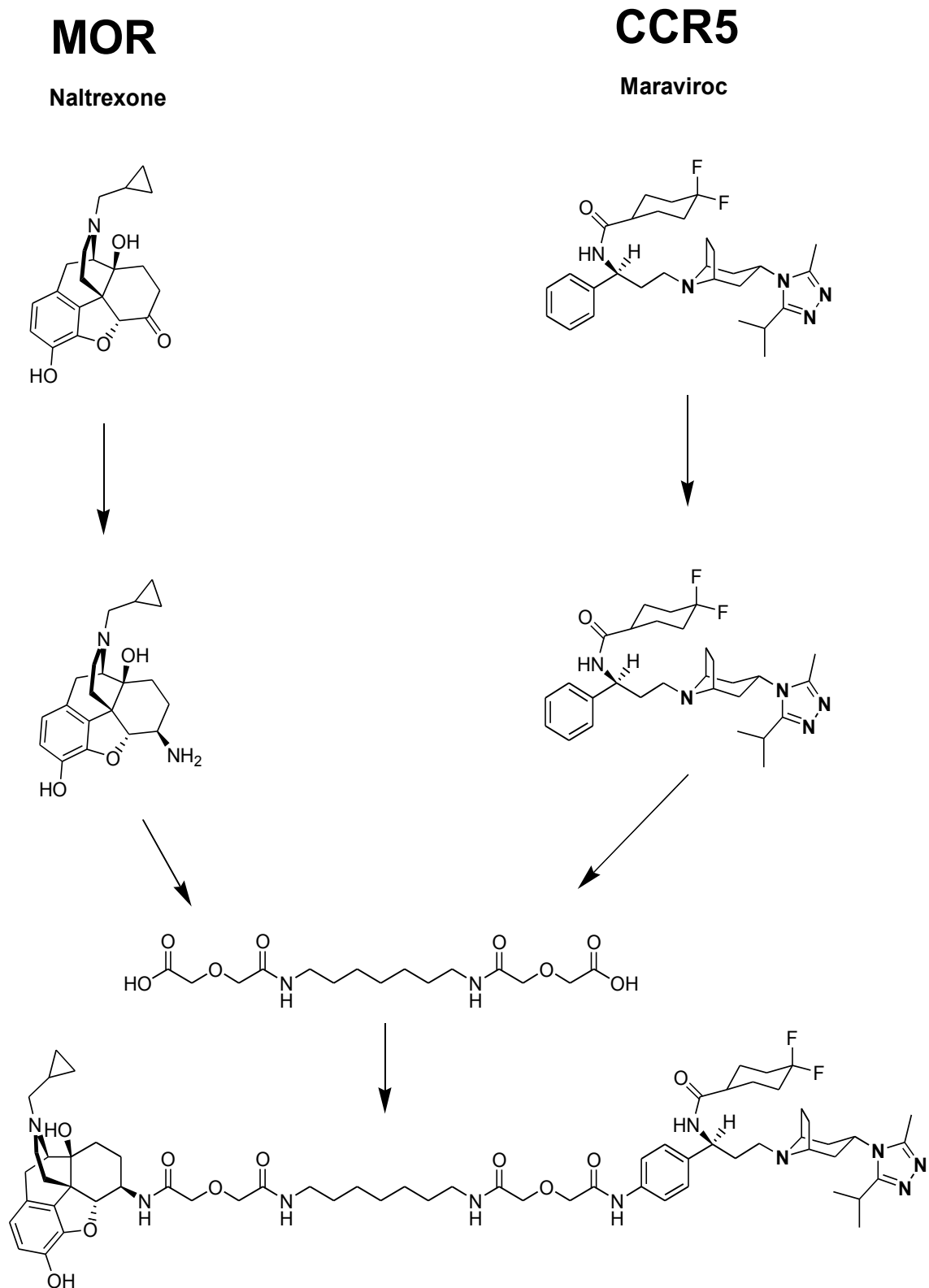
therefore may lead to the progression of neuroAIDS.<sup>118</sup> Recently, a bivalent compound (**18**) was synthesized that contained maraviroc, a CCR5 antagonist, and naltrexone (N.B., converted to 6 $\beta$ -naltrexamine), an MOR antagonist, each separated by a linker (Figure 6).<sup>120</sup> The purpose of this bivalent compound was to study the pharmacological profile of CCR5-MOR heterodimerization and its relationship with neuroAIDS.<sup>120</sup> It is worthy to note that this bivalent compound is the first compound to target the putative MOR-CCR5 heterodimer and is therefore considered a novel chemical probe in the study of neuroAIDS and HANDS.<sup>120</sup>



**Figure 6.** The first reported bivalent compound targeting the CCR5-MOR heterodimer.<sup>24</sup>

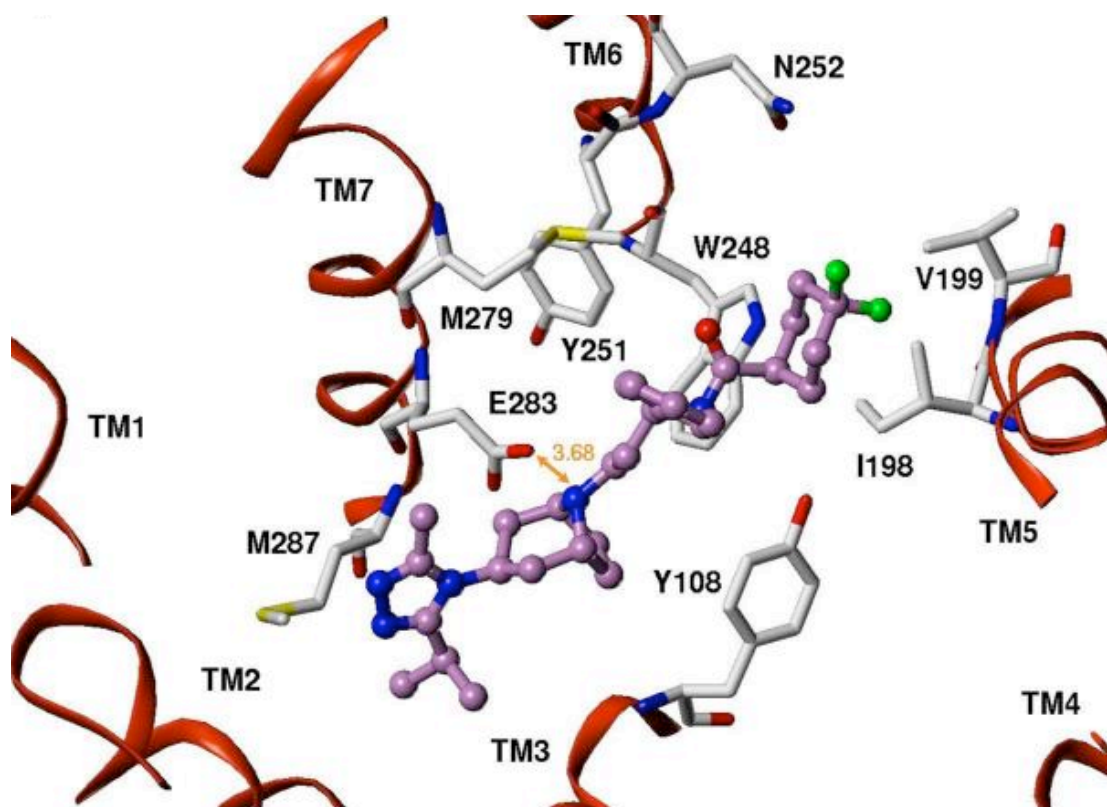
The purpose of synthesizing the bivalent compound (**18**) was to design a molecule that could antagonize both the MOR and CCR5 receptors simultaneously, as shown in Figure 7. Both maraviroc and naltrexone were selected based on their binding affinities for CCR5 and MOR (respectively) and their pharmacological profiles.<sup>120</sup> It should be noted that both molecules had to be functionalized with an amino group in order to initiate linker attachment via amide coupling.<sup>120</sup> The structure of the linker and its attachment to maraviroc and 6 $\beta$ -naltrexamine were based on the work of Daniels et al. with various opioid receptors and their antagonists.<sup>107</sup> In their research, they found that using a 21-atom spacer was optimal in studies involving opioid receptor heterodimerization, and therefore **18** was

synthesized in the study of CCR5-MOR heterodimerization carried the same spacer length.<sup>107, 120</sup>



**Figure 7.** Strategy for designing a bivalent compound to target the CCR5-MOR heterodimer.

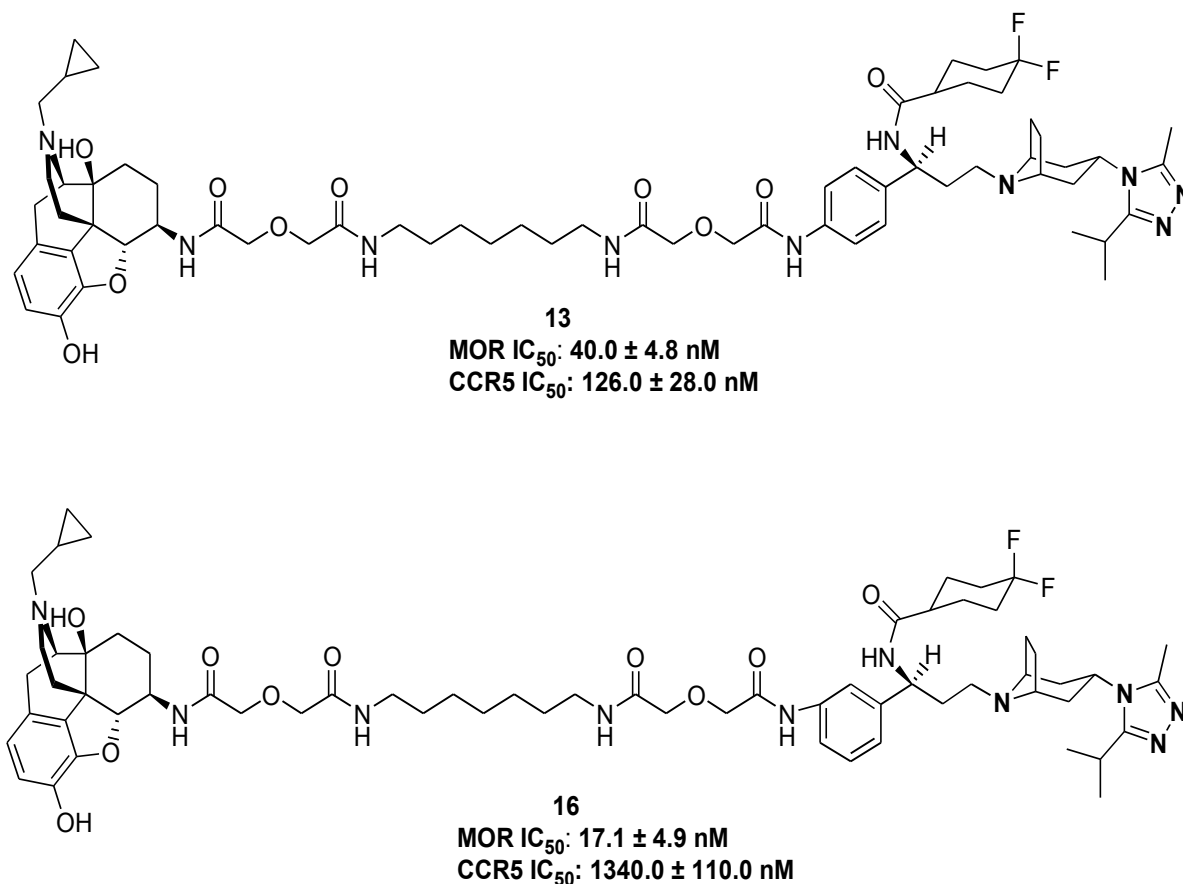
From molecular modeling studies involving the docking of maraviroc to a homology model of receptor CCR5, it was hypothesized that the phenyl ring could accommodate either a 3- or 4-position linker (Figure 8).<sup>121</sup> Therefore, testing a bivalent compound involving a 3-position linker was necessary to determine whether or not such a compound could produce better activity at the CCR5 receptor relative to the original 4-position compound (18).



**Figure 8.** Maraviroc bound to a homology model of receptor CCR5.<sup>121</sup>

After 18 was synthesized and tested in biological assays, another novel bivalent compound (19) utilizing maraviroc and 6 $\beta$ -naltrexamine pharmacophores was also synthesized and tested in biological

assays, only this time the amine group was altered from the 4-position to the 3-position of maraviroc (Figure 9). This was done to allow for fine-tuning of the bivalent compound to the CCR5-MOR heterodimer (i.e., to determine which linker attachment produced better binding).



**Figure 9.** Comparison of the abilities of **18** and **19** to target MOR and CCR5.

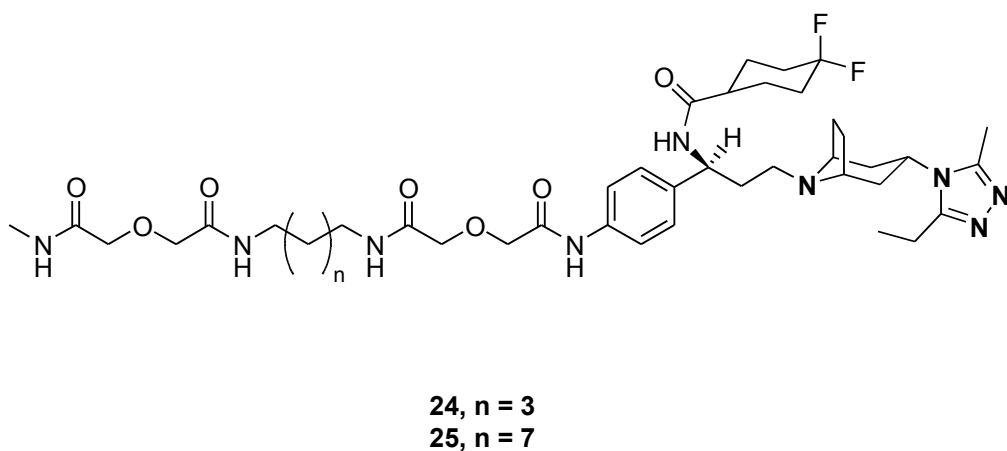
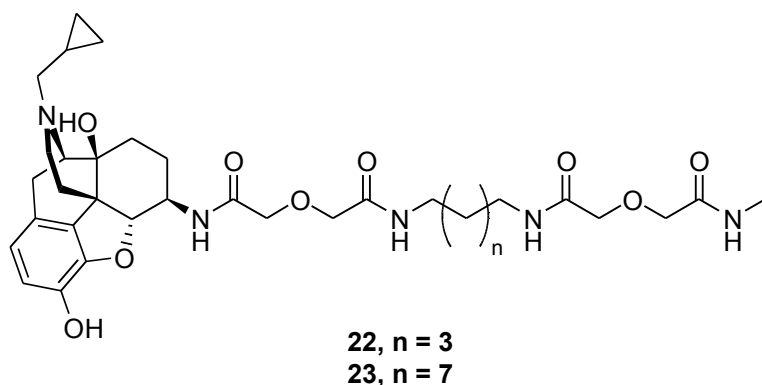
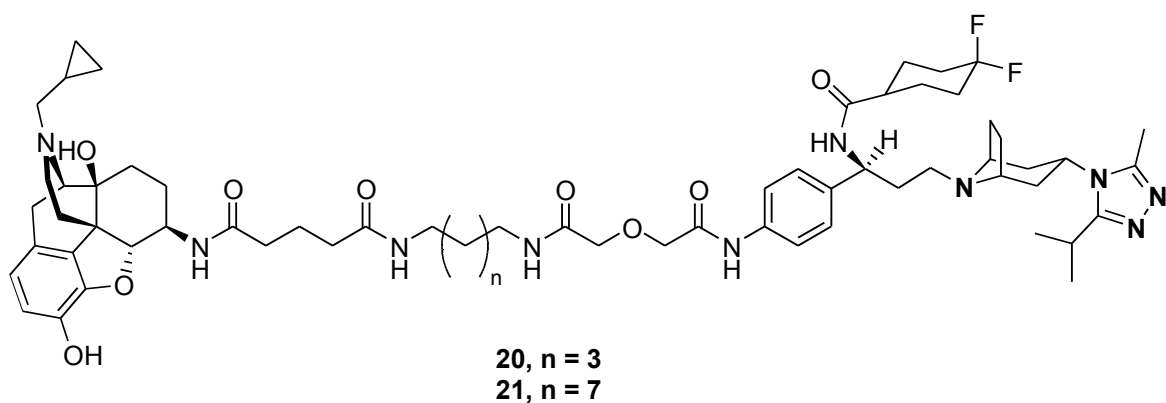
By using calcium mobilization assays to determine the functionality of each bivalent compound (**18** & **19**) to the MOR-CCR5 heterodimer, it was concluded that the modification of the amine to the 3-position produced a less potent bivalent compound. Whereas both **18** and **19** retained their antagonism toward MOR (IC<sub>50</sub>'s of 29.9 ± 2.4 and 17.4 ± 5.7, respectively), neither **18** nor **19** produced effective binding to CCR5 (IC<sub>50</sub>'s of 6240 ± 250 and 14040 ± 350, respectively). Overall, there was a 350-fold

decrease in activity for **18** but a 700-fold decrease in activity for **19**. Moreover, in CCR5 and MOR radiobinding assays, compound **19** completely lost its affinity to the CCR5 receptor.

After determining the efficacy of the 4-position over the 3-position, further fine-tuning of the bivalent compound was conducted to increase binding to the CCR5-MOR heterodimer. The 21-atom spacer in **18** was changed to a 19-atom spacer and a 23-atom spacer in **20** and **21**, respectively (Figure 10). This was done because the *in silico* research conducted by Daniels et al. was inconclusive regarding the spacer's length.<sup>107</sup>

Controls to demonstrate MOR-binding (**22** and **23**) and CCR5-binding (**24** and **25**) were also synthesized (Figure 10). Dr. Yunyun Yuan synthesized the bivalent compounds and CCR5-binding controls (**20**, **21**, **24**, **25**), whereas Thomas Raborg synthesized the MOR-binding controls (**22** and **23**). In this way we set out to test the relative potency of each novel bivalent compound to the original bivalent compound containing the 21-atom spacer (**18**).



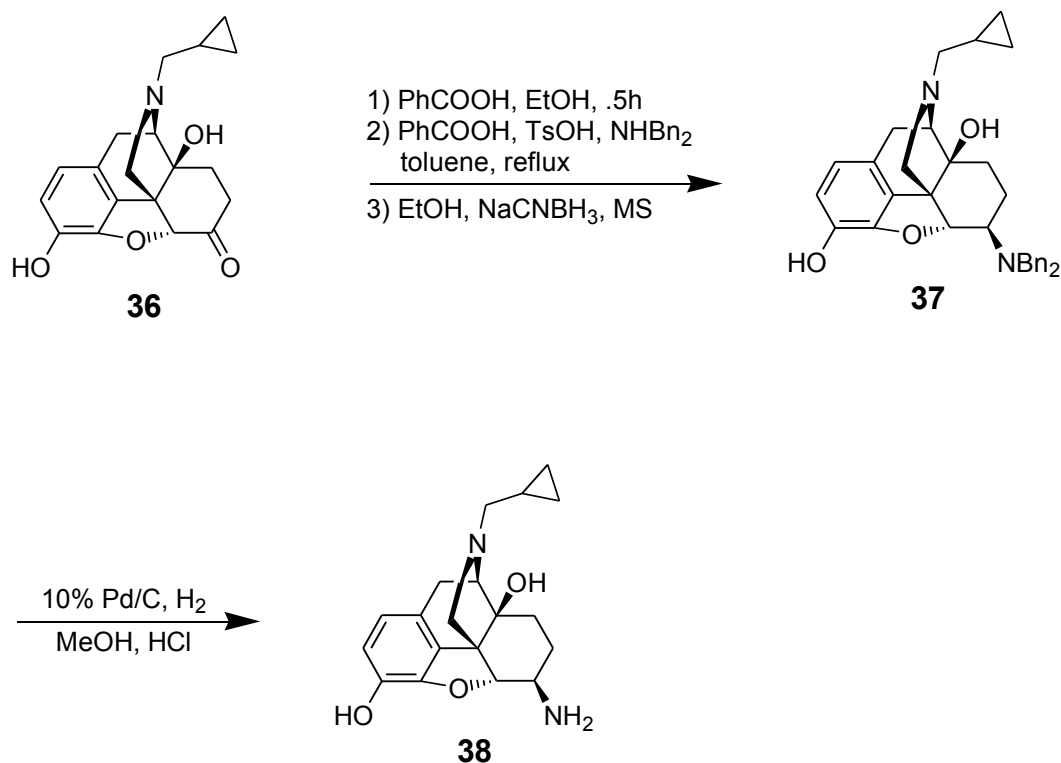


**Figure 10.** Compounds synthesized to target CCR5, MOR and the CCR5-MOR heterodimer.

## 2.2 6 $\beta$ -Naltrexamine Synthesis

In order to hook up the monoprotected 5- and 9-carbon linkers with naltrexamine through an amide coupling reaction, the opioid naltrexone, a potent  $\mu$ -opioid receptor antagonist, would have to be converted to 6 $\beta$ -naltrexamine (**38**). **38** was already synthesized according to the synthetic route

illustrated in scheme 2 by the Portuguese group.<sup>124</sup> This two-step synthetic route first converted naltrexone to a 6 $\beta$ -naltrexamine derivative containing two benzyl groups attached to a tertiary amine, replacing the keto group at the six position.<sup>124</sup> Then, this dibenzylamine derivative was reduced using Pd/C hydrogenation to form 6 $\beta$ -naltrexamine.<sup>124</sup>



**Scheme 1.** 6 $\beta$ -naltrexamine (**38**) synthesis.

The first time the reductive amination reaction was attempted, 1.00 g naltrexone (**36**) was added to 75 mL absolute EtOH and 175 mL anhydrous toluene, making a very dilute solution. The reaction was kept under anhydrous conditions and placed under a Dean-Stark trap, whereby any water formed from the reaction would be extracted from it (the solvent collected in the Dean-Stark trap was discarded). Additionally, molecular sieves were added to further prevent the presence of water from interfering with the second step of the reaction. After the dibenzylamine was added, the reaction was allowed to reflux for one night.

In the morning, the solvent mixture was found to have evaporated, leaving a burnt residue at the bottom of the flask. One hundred and fifty milliliters of toluene was added to the reaction with [1.1] equivalent  $\text{NaBH}_3\text{CN}$ , but, even after two days, **37** did not form (verified by TLC, 9:1:0.01, DCM: MeOH: $\text{NH}_4\text{OH}$ ). The reaction would have to be re-attempted, as the dibenzylamine derivative would not form.

The second time the reductive amination reaction was attempted, 0.50 g naltrexone was added to 75 ml absolute EtOH and 175 mL anhydrous toluene, making a more dilute solution than the previous attempt. The reaction was still kept under anhydrous conditions and placed under a Dean-Stark trap. [1.2] equivalent dibenzylamine was also added. However, this time, 150 mL toluene and 50 mL EtOH were added at the end of the day to ensure that the solvent mixture did not fully evaporate.

In the morning, [1.1] equivalent  $\text{NaBH}_3\text{CN}$  was added to the reaction mixture. After two days the product was confirmed to have formed by TLC (9:1:0.01, DCM: MeOH: $\text{NH}_4\text{OH}$ ). The crude product was filtered and concentrated in a flask, and then the product (**37**) was recrystallized by 9:1 MeOH: $\text{H}_2\text{O}$ . The reaction yielded 0.250 g product at 34% yield. This is approximately twice as less as the yield reported by the Portuguese group.<sup>124</sup> It was speculated that this was because of the small amount of starting material (**37**) used in the reaction (by contrast, the Portuguese group used about 2.00 g naltrexone).

The 6 $\beta$ -naltrexamine intermediate **37** was then subjected to deprotection using Pd/C hydrogenation. 0.250 g **37** was put in a  $\text{H}_2$  flask with 10% Pd/C and HCl and placed under  $\text{H}_2$  gas at 60 psi. 10% Pd/C was added two more times over the course of three days, as the product (**38**) was having trouble forming. For example, after the third 10% equivalent was added, TLC (9:1:0.01, DCM:MeOH: $\text{NH}_4\text{OH}$ ) revealed three separate spots, the starting material (**37**), an intermediate and the product (**38**). The reaction mixture was filtered a day after the third 10% Pd/C addition and recrystallization (9:1, diethyl ether:MeOH) was attempted, but no crystals formed. The precipitate was

a crude, orange, sticky product with multiple spots on the TLC. It was determined that the reductive amination reaction would have to be reattempted, this time ensuring that the product (**37**) was pure enough so that crystals of **38** would form at the end of the second reaction.

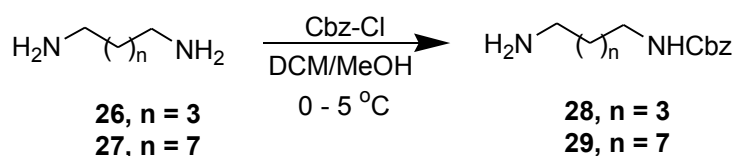
A third reductive amination reaction was attempted, this time with 0.50 g naltrexone (**36**) added to 75 mL absolute EtOH and 150 mL toluene. The reaction was again placed under a Dean-Stark trap with molecular sieves, and [1.2] equivalent dibenzylamine was added. Like in the second attempt, 150 mL toluene and 50 mL EtOH were added to the reaction mixture at the end of the day to ensure that the solvent would not totally evaporate. On the second day, [1.1] equivalent NaBH<sub>3</sub>CN was added to the reaction. When the product (**37**) formed, the reaction was filtered and concentrated to dryness. The crude product was again recrystallized in 9:1 MeOH:H<sub>2</sub>O. No product was left behind in the mother liquor, so the solid precipitate was dissolved in DCM and further purified using column chromatography (20:1:0.01, DCM:MeOH:NH<sub>4</sub>OH) to give 0.260 g **37** at a yield of 35%. This is approximately twice as less as that reported by the Portuguese group.<sup>124</sup> Reasons for this might include both the amount of SM that was used in the reaction and the dual purification process (i.e., by recrystallization and purification of the crude recrystallized product).

0.260 g **37** was then placed in a H<sub>2</sub> flask with 10% Pd/C and HCl under H<sub>2</sub> gas at 60 psi. 10% Pd/C was added two more times within a period of four days to ensure that the reaction would go to completion. The reaction was monitored by TLC (9:1:0.01, DCM:MeOH:NH<sub>4</sub>OH) until completion, and then it was filtered through celite and concentrated to dryness. The resultant crude produce was recrystallized in 9:1 diethyl ether:MeOH. However, unlike the first time recrystallization using this ratio was attempted, the product that precipitated out of the solvent was white and powdery. 0.199 g **38** was extracted at a yield of 96%.

### 2.3 Synthesis of the monovalent $\mu$ -Opioid control compounds

### 2.3.1 Monoprotection of diamines

The monovalent  $\mu$ -opioid control compound was previously synthesized using the synthetic route illustrated in scheme 1.<sup>120</sup> However, unlike the previous synthesis, which used 1,7-diaminoheptane as the starting material, the number of carbon atoms in the diamine were changed from seven to five and nine (i.e., 1,5-diaminopentane (**26**) and 1,9-diaminononane (**27**), respectively) for the current experiment. The compounds were synthesized in tandem using similar reaction conditions and reagents.



**Scheme 2.** Monoprotection of diamines.

First, diaminopentane (**26**) and diaminononane (**27**) were monoprotected using a carboxybenzyl group according to various reported methods.<sup>120, 122, 123</sup> The first time this reaction was tried, 1 g of starting material was added to 300 mL DCM and 300 mL MeOH, making a very dilute solution. The solution was further diluted by adding [1] equivalent benzyl chloroformate that was dissolved in 200 mL MeOH dropwise over the course of one week at room temperature. After the reaction was completed, TLC (9:1:0.01 DCM, MeOH,  $\text{NH}_4\text{OH}$ ) was taken to reveal that the majority spot (*UV* and iodine active) was that of the starting material. Some diprotected product formed, but very little monoprotected product formed. The difficulties of the reaction were further compounded by the fact that there were numerous byproducts in the reaction mixture that made purification difficult. Yields from this reaction under these conditions and parameters were 5-8%.

The work-up and purification of the monoprotected product is worthy of note, as many steps

were taken to ensure that the product was pure enough to initiate the next step in the reaction scheme. Special emphasis was put on purifying the product in this reaction because, as the first step in the synthetic route, an impure product would make all following reactions more difficult to initiate and purify. The difficulties of working with impure starting material were noted even as early as the second reaction (i.e., the one utilizing diglycolic anhydride in scheme 1), as, the first time it was tried, it was impossible to recrystallize the product given the impurities mixed with the starting material.

When the crude product had been concentrated to dryness, it was dissolved in DCM and put in a separation funnel. Then, H<sub>2</sub>O – which is immiscible with DCM – was put in the separation funnel and its pH was reduced to 1 using 38% HCl. The purpose of making the water acidic was to ionize the unprotected diamine and monoprotected diamine and thus make them much more polar than the diprotected byproduct. It was theorized that, because the diprotected byproduct contained no primary amines, it would be much harder to ionize than either the unprotected diamine or the monoprotected diamine, and thus it would remain in the denser, non-polar DCM layer while the other two compounds became more miscible in water. Once the DCM layer was drained from the separation funnel, the remaining water layer had its pH increased to 12 ~ 14. This was done in order to make the monoprotected product less soluble in water and more soluble in DCM. In this way the monoprotected product was separated from the more polar starting material. Results of the chemical separation were confirmed with TLC (9:1:0.01 DCM:MeOH:NH<sub>4</sub>OH).

Once the DCM containing the monoprotected compound was concentrated, it was redissolved in 1 mL DCM in preparation for column chromatography. Although the monoprotected product had been separated from its diprotected byproduct and unprotected starting material, there were still other impurities and byproducts that had formed in the reaction. Many of these had similar R<sub>f</sub> values with the monoprotected product on TLC. The column was done in gradients, starting from 50:1:0.01 DCM:MeOH:NH<sub>4</sub>OH and becoming progressively more polar. The 1,5-monoprotected diamine was

quite difficult to purify, as it didn't begin to elute from the column until the ratio was reduced to 5:1 DCM:MeOH. The 1,9-monoprotected diamine was easier to purify, as it was larger and less polar and therefore eluted from the column at the much higher ration of 10:1 DCM:MeOH. Regardless, both compounds required another round of column chromatography to separate the monoprotected product from other byproducts, as there were still impurities with the product in both cases.

The next time the reaction was tried, similar previously reported methods were utilized, but this time the amount of benzyl chloroformate was modified. Instead of adding [1] equivalent of benzyl chloroformate, [1.5] equivalent was added in the hope that it would drive the reaction to completion, thus forming more monoprotected product. This was done due to the large amount of starting material that remained unreacted the first time the reaction was tried. It was hypothesized that adding more equivalents of benzyl chloroformate would reduce the amount of starting material in favor of more monoprotected product. Even though doing so would increase the amount of diprotected byproducts as well, since there was far more starting material left over after the reaction the first time it was tried, this result was considered negligible. One gram of the starting material was diluted in 300 mL DCM and 300 mL MeOH, making a very dilute solution, and the [1.5] equivalent benzyl chloroformate was added with 200 mL MeOH dropwise over the course of one week. After the reaction was completed, TLC (9:1:0.01 DCM, MeOH, NH<sub>4</sub>OH) was taken to reveal two dark spots (*UV* and iodine active) – assumed to be the monoprotected product and diprotected byproduct – above the spot containing the starting material. As in the previous reaction, however, many byproducts were revealed to be around the monoprotected product. This made purification difficult, and the yields from this reaction under these conditions were also very low (approximately 10-15%).

From both of the previous methods, the first using [1] equivalent benzyl chloroformate and the latter using [1.5] equivalent benzyl chloroformate, two problems still persisted with the reaction: (1) the low yield of monoprotected product and (2) the formation of numerous byproducts which made

purification difficult. The methods previously detailing the reaction, however, suggested modifying the temperature under which the reaction proceeded in order to decrease the amount of byproducts formed and increase total product yield.<sup>122, 123</sup> According to the literature, decreasing the temperature of the reaction from room temperature to 5 – 10 °C would result in less diprotected byproduct and less byproducts similar in size and polarity to the monovalent product, thus making purification much less difficult and time-consuming.<sup>122, 123</sup>

The next time the reaction was proceeded by adding 1 g of starting material diluted in 300 mL DCM and 300 mL MeOH. However, instead of leaving the reaction at room temperature, the temperature was lowered to 0 – 10 °C and maintained over the course of one week as [1.5] equivalent benzyl chloroformate was added dropwise. After the reaction was completed, TLC (9:1:0.01 DCM, MeOH, NH<sub>4</sub>OH) revealed some starting material left (*UV* and iodine active), but mostly diprotected byproduct and monoprotected product. It is interesting to note, however, that some of the byproducts which had previously appeared on the TLC plate were absent. Because of the absence of these byproducts, purification was easier, but it was still quite low, at approximately 10 – 20% yield for both monoprotected products (**28 & 29**).

Despite the minor improvements in yield from the first reaction, there were still drawbacks to the reaction that persisted. It seemed that regardless of the amount of benzyl chloroformate used and regardless of the temperature, there were still going to be numerous byproducts formed, and the diprotected byproduct would always predominate over the monovalent product. Furthermore, the yield was still quite low, and it seemed like the reaction would have to be repeated numerous times in order to gather enough product to go onto the next step in the synthetic scheme. In order to improve the yield of the reaction and limit the amount of byproducts formed, it was suggested that the reaction be placed above a Dewar flask containing acetone and dry ice, cooling the temperature to -10 – 0 °C, thus making the reaction conditions even cooler than attempted previously. Furthermore, using dry ice in acetone



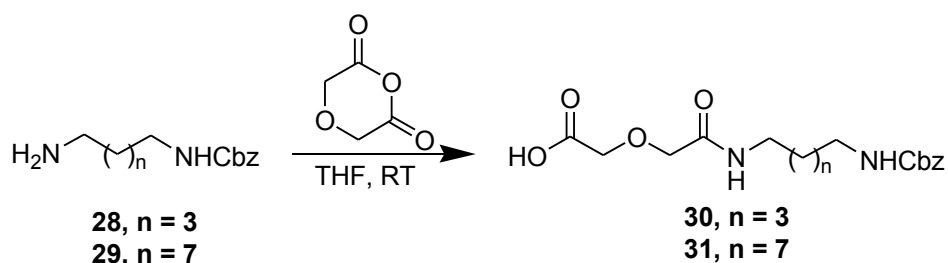
would make the reduced temperature easier to maintain. It was also suggested that the equivalent of benzyl chloroformate be modified to [.5] equivalent in order to reduce the chances of byproduct formation, in particular the diprotected byproduct. Furthermore, because of the cooler temperatures and smaller equivalent of benzyl chloroformate, less solvent would be needed to conduct the reaction. In conclusion, two conditions would be changed for the next reaction: the temperature and equivalent of benzyl chloroformate. These modified parameters would decrease the amount of solvent required for the reaction to work.

As before, 1 g of the starting material was placed in a flask. This time, however, only 250 mL DCM was used as a solvent. The reaction temperature was reduced to  $-10 - 0\text{ }^{\circ}\text{C}$  using acetone and dry ice, and [.5] equivalent benzyl chloroformate in 50 mL DCM was added dropwise over the course of one day. The temperature was monitored and dry ice and acetone were continuously added in order to maintain a constant low temperature. After the reaction was complete, TLC (9:1:0.01 DCM, MeOH,  $\text{NH}_4\text{OH}$ ) revealed little-to-no starting material, no diprotected byproduct and very little additional byproducts around the monoprotected product (*UV* and iodine active). The largest spot was the monoprotected product. The reaction was concentrated and purified using column chromatography (5:1:0.01 DCM, MeOH,  $\text{NH}_4\text{OH}$  for the monoprotected diaminopentane and 9:1:0.01 DCM, MeOH,  $\text{NH}_4\text{OH}$  for the monoprotected diaminononane). 0.770 g (**28**) was collected at a yield of 33%, by far the greatest for the reaction involving 1,5-diaminopentane starting material. 0.444 g (**29**) was collected at a yield of 24%, also the greatest for the reaction involving 1,9-diaminononane starting material. The compounds were verified by  $^1\text{H}$  NMR.

### 2.3.2 Monoprotected Diamines Reacting with Dglycolic Anhydride

The next step in the reaction scheme consisted of using **28** or **29** as the starting material and converting it to a carboxylic acid by coupling its unprotected primary amino group with diglycolic

anhydride. This reaction required an exact measurement of the amount of starting material, as reacting it with any more or less than [1] equivalent diglycolic anhydride resulted in a reaction mixture that was difficult to purify by recrystallization (N.B., the carboxylic acid product could not be separated from the reaction mixture by column chromatography, given the polarity of the compound). The first time the reaction was attempted, about 0.100 g of **28** was put inside a flask with 3 mL THF and the reaction temperature was reduced to 0 – 5 °C using an ice-water bath. Then, [1] equivalent diglycolic anhydride was added and the ice-water bath was removed, thus allowing the reaction to reach room temperature. After one day, the reaction was concentrated and recrystallization in diethyl ether:MeOH (9:0.01) was attempted. The solvent ratios were varied, but the product did not form. Given that the reported yield for this reaction was over 90%, it was assumed that the starting material was not weighed accurately, and this was why the product did not recrystallize out of the solution.



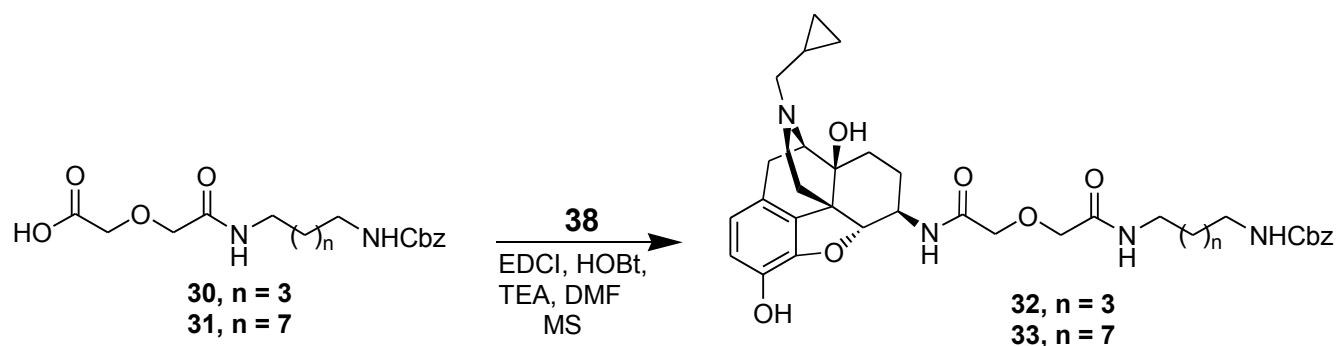
**Scheme 3.** Cbz-protected diamines reacting with diglycolic anhydride.

The second time the reaction was tried, the starting material was dried using a vacuum pump in a small 100 mL flask in order to increase the accuracy of the measured weight. After this, the starting material was put in a flask with THF and the temperature was again reduced to 0 – 5 °C using an ice-water bath. [1] equivalent diglycolic anhydride was added and the ice-water bath was removed, allowing the reaction to reach room temperature. A day later, the reaction was concentrated and recrystallization was attempted using diethyl ether:MeOH (9:0.01). This time the product was able to recrystallize out of the reaction mixture after one day of stirring in the diethyl ether:MeOH solvent

mixture. About 0.270 g **30** was obtained at a yield of 30% and 0.170 g **31** was obtained at a yield of also 30%. While adequate for conducting the remaining reactions in the synthetic scheme, these yields were much lower than yield reported in the literature.<sup>120</sup>

### 2.3.3 Monoprotected Intermediates Undergo Amide-Coupling Reaction with 6 $\beta$ -naltrexamine

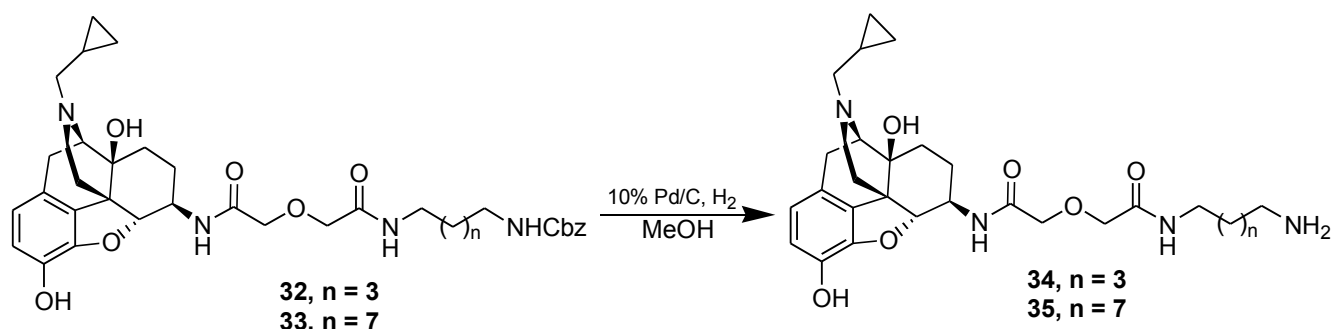
Compounds **30** and **31** were then attached to 6 $\beta$ -naltrexamine (see scheme 2 for synthetic route of 6 $\beta$ -naltrexamine) via an amide coupling reaction. The reaction consisted of putting the acid linker (**30** or **31**) in 1 mL anhydrous DMF, forming a concentrated 1 M solution. This solution was allowed to stir overnight with molecular sieves under N<sub>2</sub> gas protection in order to ensure anhydrous conditions. This stage of the reaction was critical, as water would impede the formation of the acid-EDCI intermediate, which was required for the coupling reaction to occur in a timely manner. The following day, [1.5] equivalent HOBt and [1.5] equivalent EDCI catalysts were added to the reaction according to reported methods.<sup>120</sup> Then, [1] equivalent 6 $\beta$ -naltrexamine in 1 mL anhydrous DMF was added dropwise for the coupling reaction to proceed. The reaction was given a few days to go to completion and TLC (9:1:0.01 DCM:MeOH:NH<sub>4</sub>OH) was taken to ensure that the 6 $\beta$ -naltrexamine starting material was consumed. For the formation of the 6 $\beta$ -naltrexamine with the 1,9-monoprotected acid control, an additional [.5] equivalent of EDCI was added to the reaction in order for the starting material to be consumed. Once the starting material was consumed, the reaction was filtered through celite and concentrated to dryness. The crude product was recrystallized in 20:1:0.01 DCM:MeOH:NH<sub>4</sub>OH column chromatography. 0.165 g **32** was obtained at a yield of 60%, and 0.170 g **33** was obtained at a yield of 43%. These results mimic the yield reported in the literature.<sup>120</sup>



**Scheme 4.** Amide-coupling reaction involving the protected diamine and 6 $\beta$ -naltrexamine.

### 2.3.4 Deprotection

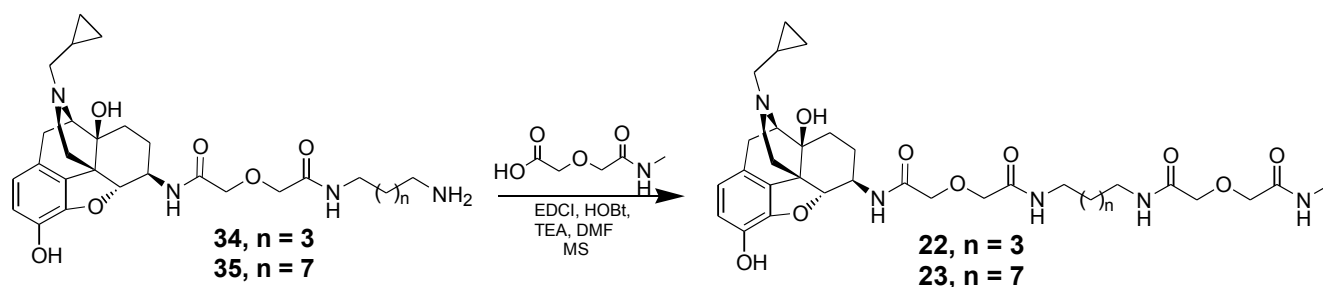
Compounds **32** and **33** were then subjected to deprotection. For this reaction, the starting material was placed inside a H<sub>2</sub> flask with MeOH and 10% Pd/C. The reaction took about three days for both starting materials. Over the course of the reaction time, multiple 10% Pd/C equivalents were added to the reaction in order to drive it to completion (N.B., the reaction was monitored by 6:1:0.01 DCM:MeOH:NH<sub>4</sub>OH). The crude product was filtered through celite and concentrated to dryness. 0.086 g **34** was obtained at a yield of 67%, which was somewhat lower than the yield reported in the literature.<sup>1</sup> 0.091 g **35** was obtained at a yield of 72%, which was also lower than previously reported yields.<sup>1</sup> It is noteworthy that both compounds were quite unstable owing to the primary amine that resulted from the deprotection reaction. In fact, the first time the reaction was attempted with **32**, the product (**34**) degraded from a rise in room temperature that took place when the laboratory's air-conditioning unit was switched off. Therefore, the second time the reaction was completed, the product was placed inside the freezer until the next step in the reaction scheme was attempted.



**Scheme 5.** Deprotection of monoprotected intermediate.

### 2.3.5 Final Product Synthesis

For the final step in the reaction scheme, compounds **34** and **35** were reacted with an acidic “cap” through an amide coupling mechanism in order to ensure their stability when performing assays at room temperature (see scheme 1 for the cap's structure). First, the cap was placed in 1 mL DMF with molecular sieves and under N<sub>2</sub> protection to ensure anhydrous conditions. Like in the previous amide coupling reaction, the presence of H<sub>2</sub>O would disrupt the formation of the acid-EDCI complex necessary for the reaction to proceed in a timely manner. After one day, [1.5] equivalent HOBt and [1.5] equivalent EDCI were added to the reaction at 0 °C and the reaction was allowed to warm up to room temperature. Then, **34** or **35** was mixed with 1 mL DMF and added dropwise to the reaction. After three days, the reaction was monitored by TLC (7:1:0.01 DCM:MeOH:NH<sub>4</sub>OH) to reveal that the amine starting material was no longer present in the reaction mixture. There was a main product spot (*UV* and iodine active) present with lots of byproducts and remaining catalyst. The reaction was filtered, concentrated to dryness and purified by column chromatography (10:1:0.01 DCM:MeOH:NH<sub>4</sub>OH). The reaction yield was quite low for both products, but this result had already been reported in the literature.<sup>1</sup> 0.030 g **22** was synthesized at a yield of 30%, and 0.030 g **23** was synthesized at a yield of 25%.



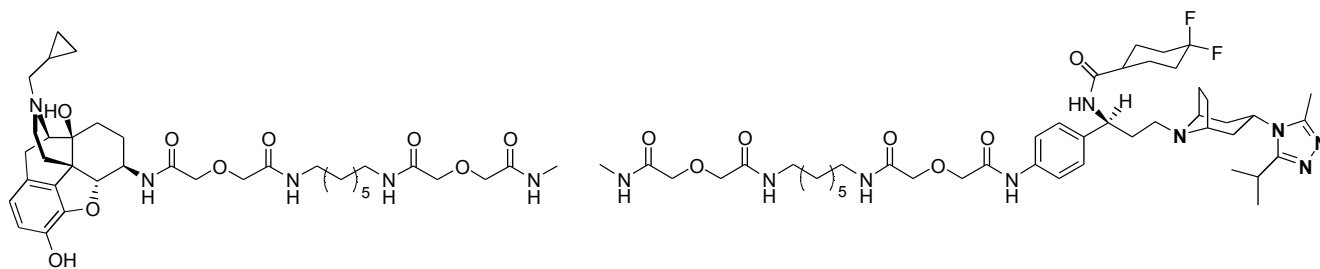
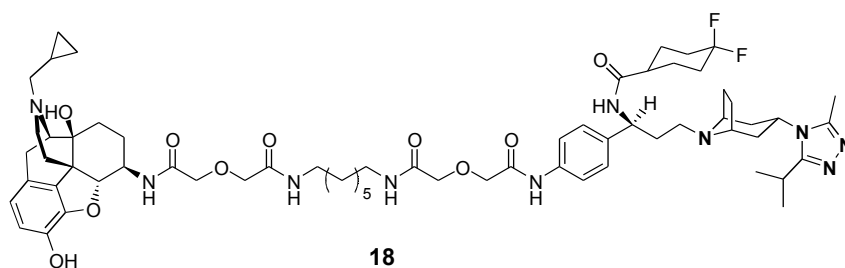
**Scheme 6.** Amide-coupling reaction of intermediate and acidic cap.

Both products were converted to hydrochloride salts and recrystallized in 9:0.1 diethyl ether:MeOH.

### 3. In Vitro Studies

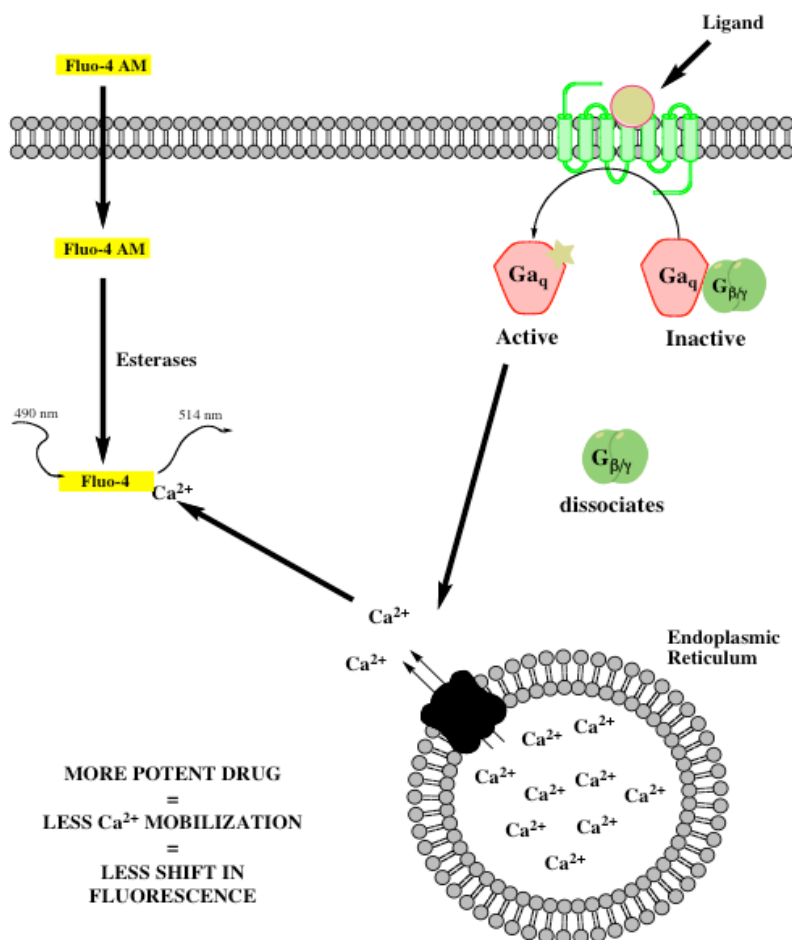
#### 3.1 Results from Calcium Mobilization Assays with Initial 21-Atom Bivalent Compound

In total, approximately 9 compounds were synthesized for the study of the CCR5-MOR heterodimer (N.B., this does not include the 3-position spacer and its maraviroc control, which were found to be less efficacious at binding to CCR5 and the CCR5-MOR heterodimer relative to the 4-position spacer and its control). Figure 11 shows the first 3 of these compounds, the 21-atom spacer and its two monovalent controls, which were synthesized by Dr. Yunyun Yuan. These compounds were tested in either CCR5- or MOR- cells and cells expressing both CCR5 and MOR.



**Figure 11.** Original 21-atom bivalent compound (**18**) with maraviroc and 6 $\beta$ -naltrexamine controls.

Calcium mobilization assays were chosen to test the functional activity of the compounds due to their simplicity.<sup>125</sup> In these assays, GPCR signaling causes the release of intracellular calcium stores.<sup>125</sup> Ideally, the IC<sub>50</sub>'s of these compounds should match both maraviroc and naltrexone, as this would indicate good inhibition at the CCR5 and MOR receptors. Figure 12 shows a schematic representation of the mechanism behind the calcium mobilization assay.



**Figure 12.** Schematic representation of a calcium mobilization assay.

The results for compound **18** in assays containing CCR5, MOR or the CCR5-MOR heterodimer are as follows. In assays utilizing human acute lymphoblastic leukemia (MOLT-4) cells transfected with CCR5, **18** had an  $IC_{50}$  of  $130 \pm 28$  nM, an approximately 60 fold-decrease in activity relative to maraviroc, which had an  $IC_{50}$  of  $2.2 \pm 0.31$  nM.<sup>120</sup> While this fold-decrease in activity is significant, it is expected given the attachment of maraviroc to a spacer and another molecule. However, the maraviroc control containing just a spacer had a much larger decrease in activity relative to maraviroc, with an  $IC_{50}$  of  $620 \pm 36$  nM (i.e., a 600 fold-decrease in activity).<sup>120</sup> More maraviroc controls and spacer molecules would have to be synthesized and tested in order to see whether or not this significant fold-decrease was consistent with attaching a spacer to the 4-position of maraviroc.

In chinese hamster ovarian (CHO) cells containing hMOR, **18** only had a slight fold-decrease in



activity relative to naltrexone. **18**'s  $IC_{50}$  was  $40 \pm 4.8$  nM, whereas naltrexone had an  $IC_{50}$  of  $8.9 \pm 0.87$  nM (a fold-decrease of 4.5).<sup>120</sup> The 6 $\beta$ -naltrexamine spacer had an  $IC_{50}$  of  $17 \pm 4.9$  nM, or a fold-decrease of 1.9, confirming that a spacer attached to the 6 position was tolerable.<sup>120</sup>

Finally, in an assay containing CHO cells transfected with both CCR5 and MOR genes, **18** was found to have an  $IC_{50}$  of  $17 \pm 5.7$  nM at the hMOR receptor, only a 3 fold-decrease from naltrexone.<sup>120</sup> This further confirms the tolerability of a spacer attached to the 6-position of naltrexone. However, at the CCR5 receptor, the compound was found to have an  $IC_{50}$  of  $6200 \pm 250$ , a 350 fold-decrease relative to maraviroc.<sup>120</sup> Thus, more compounds with modifications at the 4-position of maraviroc would have to be tested in order to verify its viability or lack thereof.

Figure **13** contains the other six compounds synthesized and tested in calcium mobilization assays. These compounds include both 19- and 23-atom bivalent compounds (**20** & **21**) along with their 6 $\beta$ -naltrexamine (**22** & **23**) and maraviroc (**24** & **25**) controls. Dr. Yunyun Yuan synthesized **20**, **21**, **24** and **25**. Thomas Raborg synthesized **22** and **23**. The maraviroc containing compounds were tested using MOLT-4 cells transfected with CCR5, whereas the 6 $\beta$ -naltrexamine compounds were tested using CHO cells transfected with hMOR.



**Figure 13.** Two bivalent compounds of varying spacer length and their controls.

### 3.2 MOR-Radiobinding Assay

Before calcium mobilization assays were performed on the compounds in Figure 13, a binding assay was run in order to verify that the 6 $\beta$ -naltrexamine-containing compounds could bind to the MOR receptor at high affinity. This assay was run by Dr. Yunyun Yuan using compounds synthesized by both Dr. Yuan and Thomas Raborg. Table 5 shows the results of the MOR-radiobinding assay for the 6 $\beta$ -naltrexamine-containing compounds. As one can observe, the bivalents (20 & 21) and their 6 $\beta$ -naltrexamine controls (22 & 23) did not have significant fold-decreases in affinity relative to

naltrexone. This indicates that all the compounds were relatively potent for the MOR receptor.

**Table 5.** MOR-radiobinding assay

| Compound   | MOR $K_i$ (nM)  | Fold-decrease in Affinity Compared to Naltrexone |
|------------|-----------------|--|
| Naltrexone | $0.7 \pm 0.1$   | -  |
| 20         | $3.8 \pm 0.55$  | 5.4  |
| 22         | $0.78 \pm 0.12$ | 1.1  |
| 21         | $1.1 \pm 0.08$  | 1.6  |
| 23         | $6.5 \pm 0.16$  | 9.3  |

A CCR5-radiobinding assay also needs to be conducted in the future to test the relative potencies of each of the maraviroc-containing compounds. This might help verify the calcium mobilization assay's result that attachments to the phenyl ring of maraviroc are not tolerated for CCR5 binding.

### 3.3 CCR5-MOLT4 Calcium Mobilization Assay

First the bivalent compounds and their maraviroc controls were tested for CCR5 agonism and antagonism in assays utilizing MOLT-4 cells transfected with CCR5. In assays testing for agonism, there was no apparent agonism of CCR5 for any of the molecules. Prior to testing for antagonism, the MOLT-4 cells were transfected with a chimeric G protein, Gq<sub>5</sub>, in order to stimulate calcium signaling. A range of concentrations was set up similar to the range of concentrations that gave accurate IC<sub>50</sub>'s of the original 21-atom bivalent spacer and its maraviroc control. Each assay well also contained a specific concentration of RANTES, a CCR5 agonist, in order to test the inhibition of calcium mobilization. All compound concentrations were run in triplicate and tested three separate times.

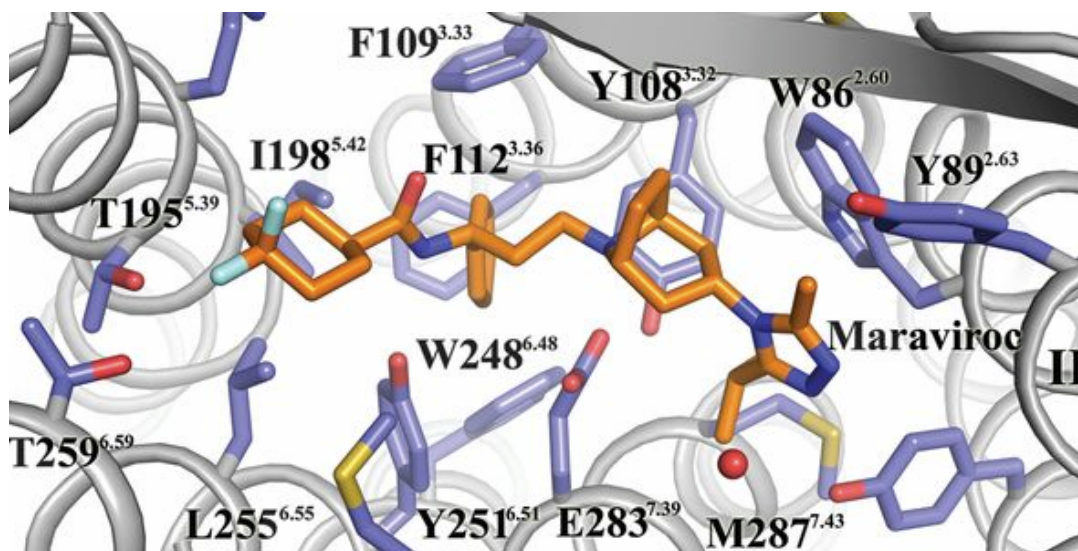
Like for the 21-atom bivalent molecule (**18**) and its maraviroc control, the 19- and 21-atom

bivalents (**20 & 21**) and their maraviroc controls (**24 & 25**) also demonstrated decreased antagonism relative to maraviroc for CCR5 (Table 5). Thus, it appears as if modifications to the phenyl ring of maraviroc are not well tolerated for CCR5-binding. Therefore, future synthetic alterations to the bivalent compound may involve changing the spacer's point-of-attachment to maraviroc.

**Table 6.** Antagonism of calcium mobilization in RANTES-stimulated MOLT-4 cells

| <b>Compound</b> | <b>CCR5 Antagonism IC<sub>50</sub> (nM)</b> | <b>Fold-decrease in Activity Compared to Maraviroc</b> |
|-----------------|---|--|
| Maraviroc       | 2.2 ± 0.3                                   | -  |
| 20              | 2400 ± 620                                  | 1100   |
| 24              | 950 ± 34                                    | 430  |
| 21              | 540 ± 79                                    | 250  |
| 25              | 390 ± 51                                    | 180  |

A recent paper published the crystal structure of maraviroc bound to CCR5. It was found that, contrary to a previously reported modeling study,<sup>121</sup> the phenyl ring of maraviroc faces inward at the maraviroc binding pocket and has many favorable hydrophobic interactions with certain amino acid R groups.<sup>126</sup> This fact demonstrates the implausibility of attaching the spacer to the phenyl ring of maraviroc, as doing so would significantly change its traditional inhibitory binding mode. While this puts a damper on the research project this laboratory has been conducting, the purported binding mode of maraviroc introduces new locations to which a future spacer may be attached.



**Figure 14.** Crystal structure of maraviroc bound to CCR5.<sup>126</sup>

### 3.4 hMOR-CHO Calcium Mobilization Assay

MOR agonism and antagonism were also tested using calcium mobilization assays. However, this time the targeted protein (i.e., hMOR) was transfected in CHO cells instead of MOLT-4 cells. Again, like in the MOLT-4 calcium assays, Gq<sub>5</sub> was transfected into the CHO cells to stimulate calcium mobilization upon agonist binding.<sup>125</sup> The compounds demonstrated no agonism. Using the MOR agonist DAMGO, the compounds were tested for their ability to inhibit calcium mobilization, and the results were tabulated in Table 6.

According to Table 6, the bivalent compounds (**20** & **21**) and their monovalent 6 $\beta$ -naltrexamine controls (**22** & **23**) did not contain significant fold-decreases in activity relative to the traditional MOR antagonist naltrexone. The compound with the greatest decrease in activity, **22**, only had a 32 fold-decrease in activity relative to naltrexone. This corresponds to a fold-decrease of only two orders of magnitude. This demonstrates that the 6-position of the naltrexone molecule can tolerate numerous structural modifications and still be able to bind to MOR. Future modifications on the bivalent compound can probably maintain the spacer at the 6-position of 6 $\beta$ -naltrexamine without worry of a

substantial decrease in activity for MOR.

**Table 7.** Antagonism of calcium mobilization in DAMGO-stimulated hMOR-CHO cells.

| <b>Compound</b> | <b>MOR Antagonism IC<sub>50</sub> (nM)</b> | <b>Fold-decrease in Activity Compared to Maraviroc</b> |
|-----------------|--|--|
| Naltrexone      | 2.9 ± 0.27                                 | -  |
| 20              | 22 ± 5.6                                   | 7.6  |
| 22              | 92 ± 020                                   | 32   |
| 21              | 22 ± 3.7                                   | 7.6  |
| 23              | 41 ± 25                                    | 14   |

### 3.5 Conclusions from In Vitro Studies

Regardless of the decrease in activity for the CCR5 receptor, the bivalent compounds still need to be tested in calcium mobilization assays involving a cell line transfected with both CCR5 and MOR. While modifications to the phenyl ring of maraviroc are not tolerated for binding to CCR5, and therefore a new spacer molecule needs to be synthesized in order to produce better binding, testing these two new bivalent compounds in a cell-line containing both receptors may indicate which spacer length is optimal for simultaneous CCR5-MOR binding. If either the 19-atom bivalent (**20**) or the 23-atom bivalent (**23**) is significantly better than the 21-atom bivalent (**18**) at inhibiting calcium mobilization in cells containing both receptors, then future modifications to the spacer's point-of-attachment to maraviroc may incorporate this change in spacer length.

## 4. In Silico Studies

#### 4.1 Introduction to Conformational Analysis

A molecule can undergo spatial rearrangements that do not alter its basic chemical structure. The study of the differences between these rearrangements – called conformations – is called conformational analysis.<sup>126–128</sup> These spatial rearrangements occur through changes in rotation around a single chemical bond that do not affect the bond's length or physical characteristics. If a particular rotation around a single chemical bond produces interactions that are not favorable within a molecule, then the resultant conformation is not considered viable.<sup>126</sup> The corollary to this is that if a rotation around a chemical bond does produce favorable interactions within a molecule, then the resultant conformation is deemed viable. Since a receptor often interacts with a ligand only when that ligand is in a specific conformation, and since the number of viable conformations a molecule can undergo is limited, it is important to identify possible binding conformations. Furthermore, since a molecule's external environment is subject to change (and it can undergo drastic changes), it is important to identify all viable conformations of a molecule independent of its external environment.<sup>126</sup>

Using conformational analysis molecular modeling software, there are two important ways to identify viable conformations of a molecule.<sup>126</sup> One way is through *energy minimization*, i.e., through rearranging the atoms of a molecule until it adopts a global minimum energy conformation.<sup>126</sup> This method is based on the assumption that a molecule will adopt a conformation either identical or similar to its lowest energy state in reality. When this method is adopted, a molecule will rearrange in a manner to produce the least torsional strain between atoms around a single chemical bond and also try to maximize intramolecular van Der Waals interactions.<sup>126</sup> When this procedure is conducted, the product is a single molecule. Given that this method may produce a conformation that is not viable for binding to a receptor, another method, termed *systematic conformational search analysis*, is sometimes required.<sup>126</sup> Using this method, a set of rotatable bonds in a molecule is identified and those rotatable bonds are altered with respect to all other bonds in a molecule.<sup>126</sup> In other words, each rotatable bond is

altered and examined as a function to all other molecular bonds. For each different conformation that is achieved as a result of a single chemical bond rotation, all internal distances are computed, and a conformation is rejected if the distance between the interacting species is greater than the sum of the van der Waals radii.<sup>126</sup> By using this method, all viable conformers within a certain energy range of the global minimum are identified. Unlike the global minimization analysis, the systematic conformational search analysis method produces a set of viable conformers that can exist in solution. This method is useful in that it produces multiple viable conformations that can exist besides the global minimum.

#### 4.2 Choosing a Conformational Analysis Software

Multiple molecular modeling programs exist for performing conformational analysis. Among them are *Systematic Conformational Search*, *Grid Search*, *Random Conformation Search*, *GA Conformational Search* and *Confort Conformational Analysis Modeling Software*.<sup>126, 127</sup> Methods such as *Systematic Conformational Search*, *Grid Search*, *Random Conformation Search* and *GA Conformational Search* rotate an individual chemical bond within a specified increment until a minimum energy is achieved.<sup>126, 127</sup> Although these methods produce a set of viable conformations, they are not exhaustive and they are poor at calculating global minima. *Confort*, on the other hand, has algorithms both for calculating global minima and producing a set of viable, diverse conformations that approximate a global minimum.<sup>126</sup> *Confort*, therefore, was used in the following conformational analysis study rather than other methods.

There were two purposes regarding the conformational analysis study on the 19-, 21- and 23-atom spacers: 1) to see if all three spacer had viable binding conformations (i.e., viable in the sense that the molecules could potentially bind to two different GPCR's simultaneously), and 2) to see if all three spacers adopted similar viable conformations. Completion of the former objective could be used to hypothesize that the molecules actually bind to their target receptors simultaneously. Completion of the



latter objective could be used to hypothesize that the 3 spacers can adopt identical binding conformations in solution and, therefore, any difference in binding between the three molecules is primarily because of spacer length (and not differences in conformation).

### 4.3 Molecular Building

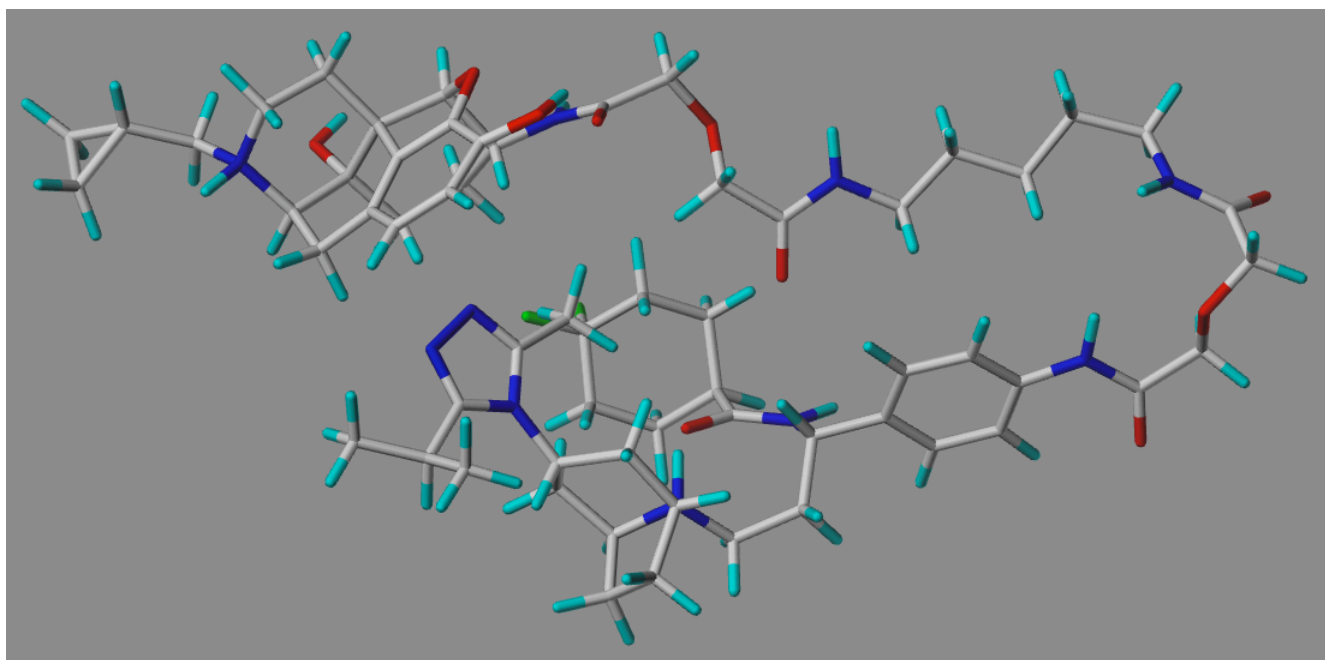
All ligands used in the conformational analysis studies were built with standard bonds and angles using the molecular modeling software SYBYL-X 2.0. The proper stereochemical arrangements were also assigned for each asymmetric carbon to ensure viability of results and uniform spatial arrangements between each spacer molecule. For the process of energy minimization (to establish a local minimum conformation for each small molecule), each small molecule was assigned Gasteiger-Huckel charges and then minimized using the Tripos Force Field.

### 4.4 Global Minimization Conformational Analysis

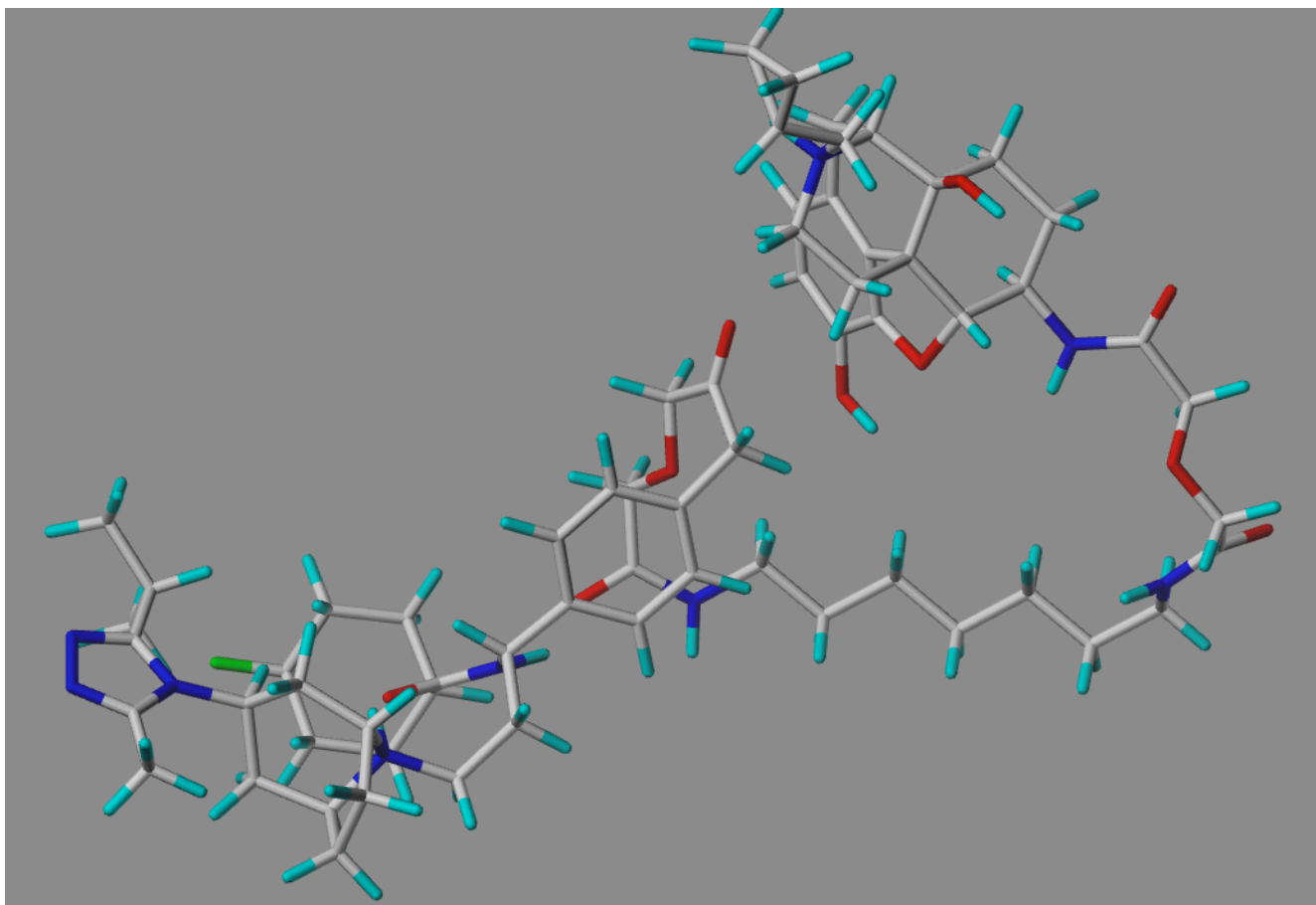
In order to identify viable conformations for the three spacer molecules, global minimization was conducted using *Confort*. Again, this technique assumes that a molecule will adopt a conformation similar to its global minimum in actuality.<sup>128</sup> However, before running the global minimum simulation, certain parameters were set in order to achieve optimal results. First, the search was set to include analyses of all rotatable bonds and a maximum number of concurrently searched rotors. Maximums of 100 acyclic bonds, 20 ring system bonds and 10 single-ring bonds were defined. Then, the precision of the results was set to .001 kcal/mol and Gasteiger-Huckel charges were applied. The output file was set to include the the global minimum with 9 lowest-energy conformers approximating the global minimum. After these parameters were set, the program was run for each spacer individually.

For the 19-, 21- and 23-atom spacers, each molecule adopted a “folded” conformation, one in which the spacer contorted to bring the maraviroc portion of the molecule in close proximity with the

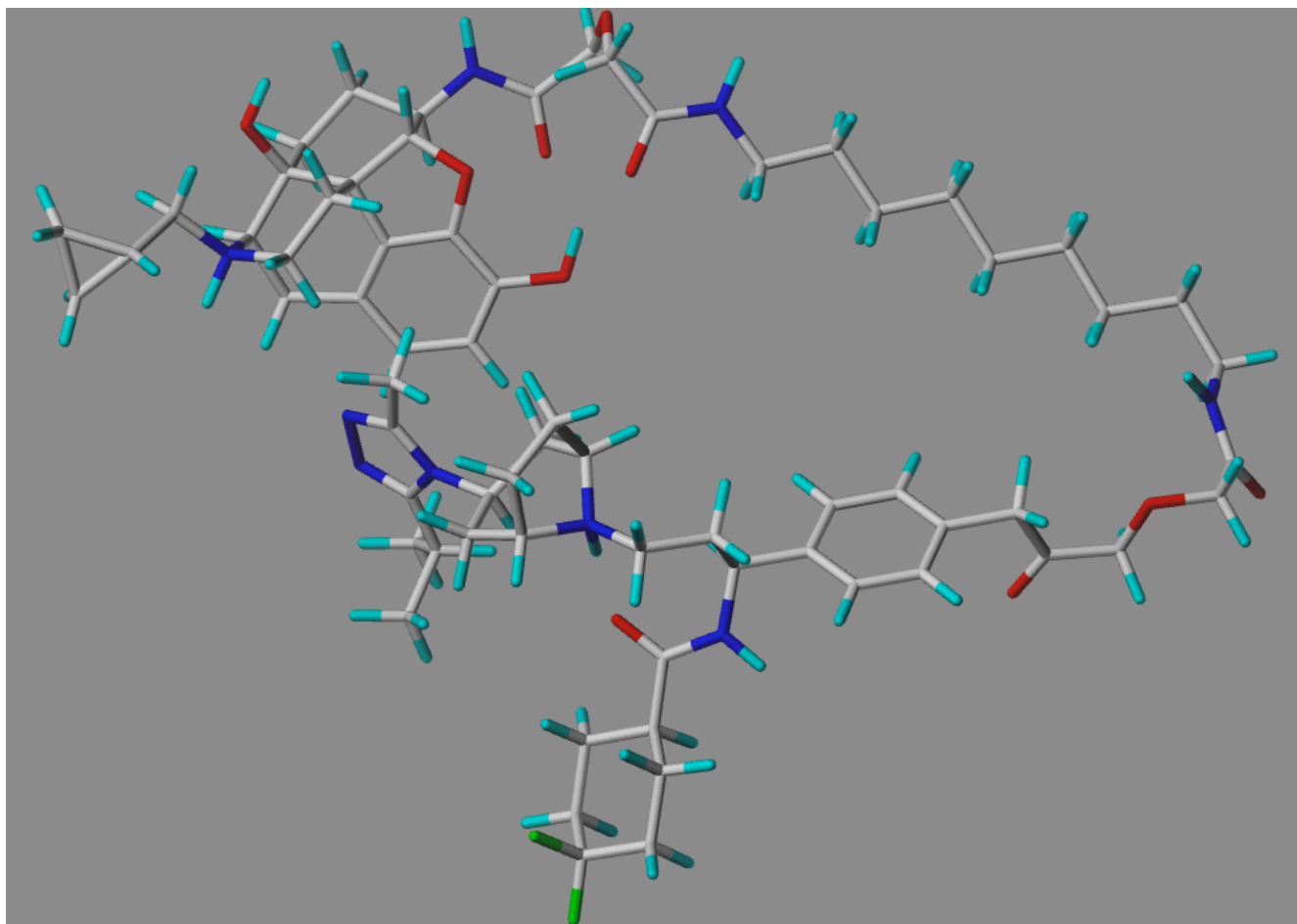
6 $\beta$ -naltrexamine portion (see Figures 14, 15, and 16). This makes sense because in order to achieve a global minimum a molecule has to contort in such a way as to allow maximum van der Waals interactions. Thus, the molecules contorted at the center of the spacer, as this allowed the molecules' two groups (i.e., maraviroc and 6 $\beta$ -naltrexamine) to best engage in van der Waals interactions. While this conformational change was similar in all three spacer molecules (thus producing similar global minimum conformations), it should be noted that this change did not produce a molecule conducive for binding to two different receptors. If the maraviroc portion interacts with the naltrexamine portion in a manner similar to that seen in the three figures, then how is the molecule going to bind to two different receptors at once? Furthermore, such a conformation would negate the importance of spacer length in binding to the two receptors. From this study, it was obvious that a set of diverse conformers for each of the three molecules was necessary to verify that the molecules adopted plausible binding conformations.



**Figure 15.** Global minimum of the 19-atom spacer.



**Figure 16.** Global minimum of the 21-atom spacer.



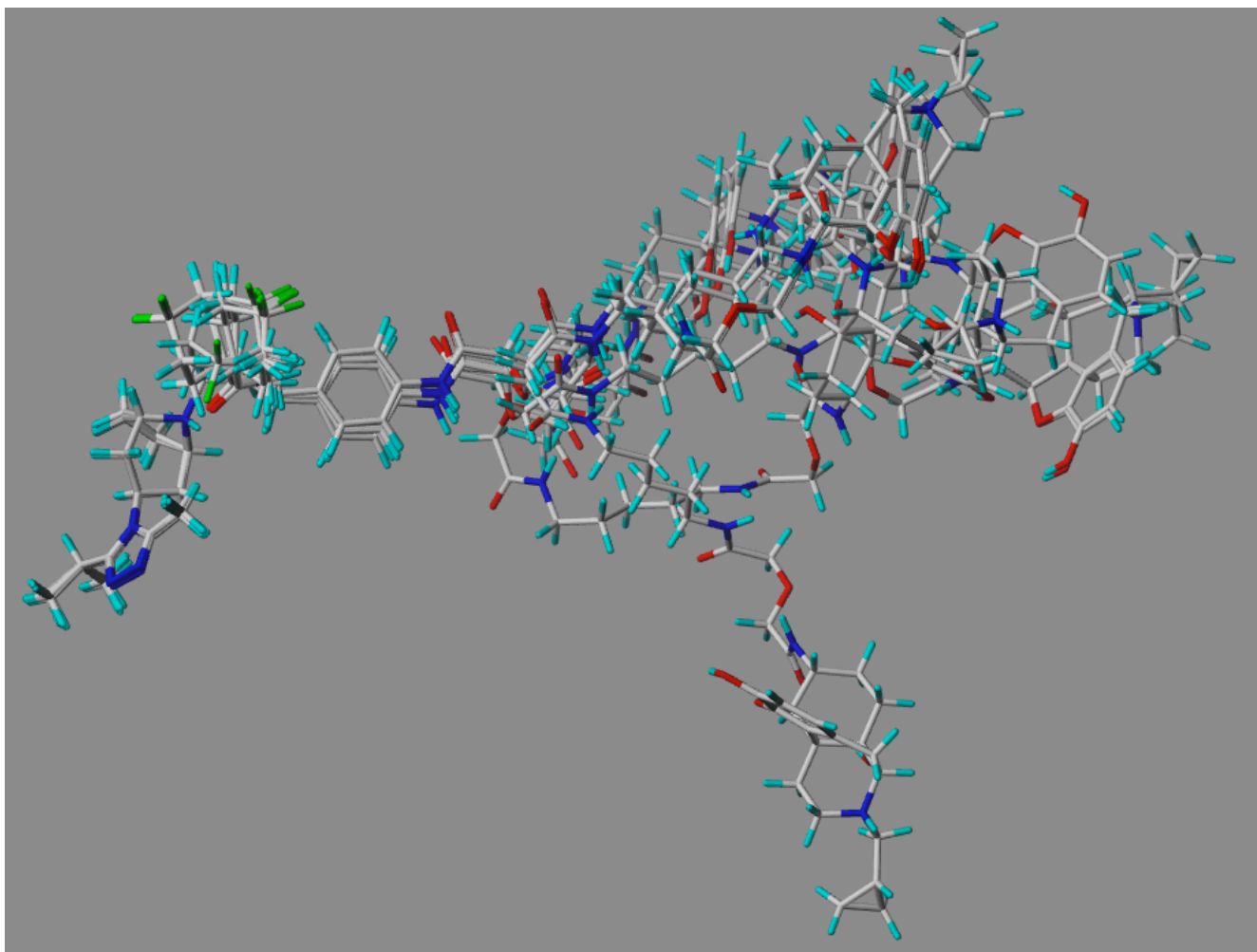
**Figure 17.** Global minimum of the 23-atom spacer.

#### 4.5 DIVERSESET Conformational Analysis

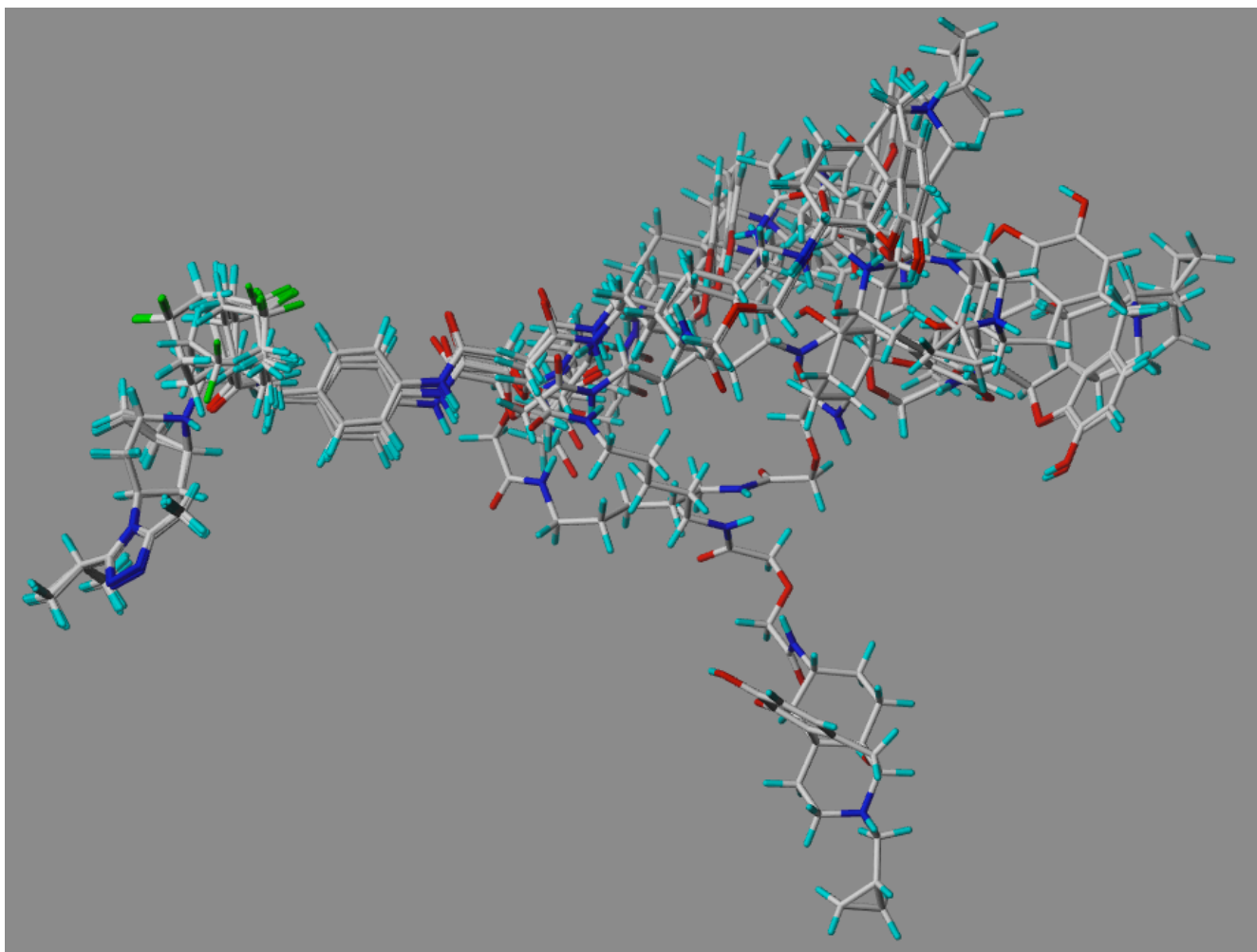
DIVERSESET, a *Confort* algorithm used to generate sets of different and diverse conformations, was implemented in order to obtain plausible and viable conformations for each molecule. When using DIVERSESET, it is still assumed that the the global minimum is the most likely conformation to exist in reality. However, DIVERSESET also produces many low-energy conformations that approximate the global minimum and are therefore also likely to exist in solution. Like in the global minimization analysis, the search options were also set to include all rotatable bonds and a maximum number of concurrently searched rotors. The precision was set to .001 kcal/mol and each molecule was assigned Gasteiger-Huckel electrostatics. This time, however, the software was set

to generate a set of molecules (500 max.). The output was further optimized by including a maximum output number of 500 diverse molecular conformations within 100 kcal/mol of the minimum. The program was then run for all three spacer molecules individually (the Figures **17**, **18**, and **19** for results).

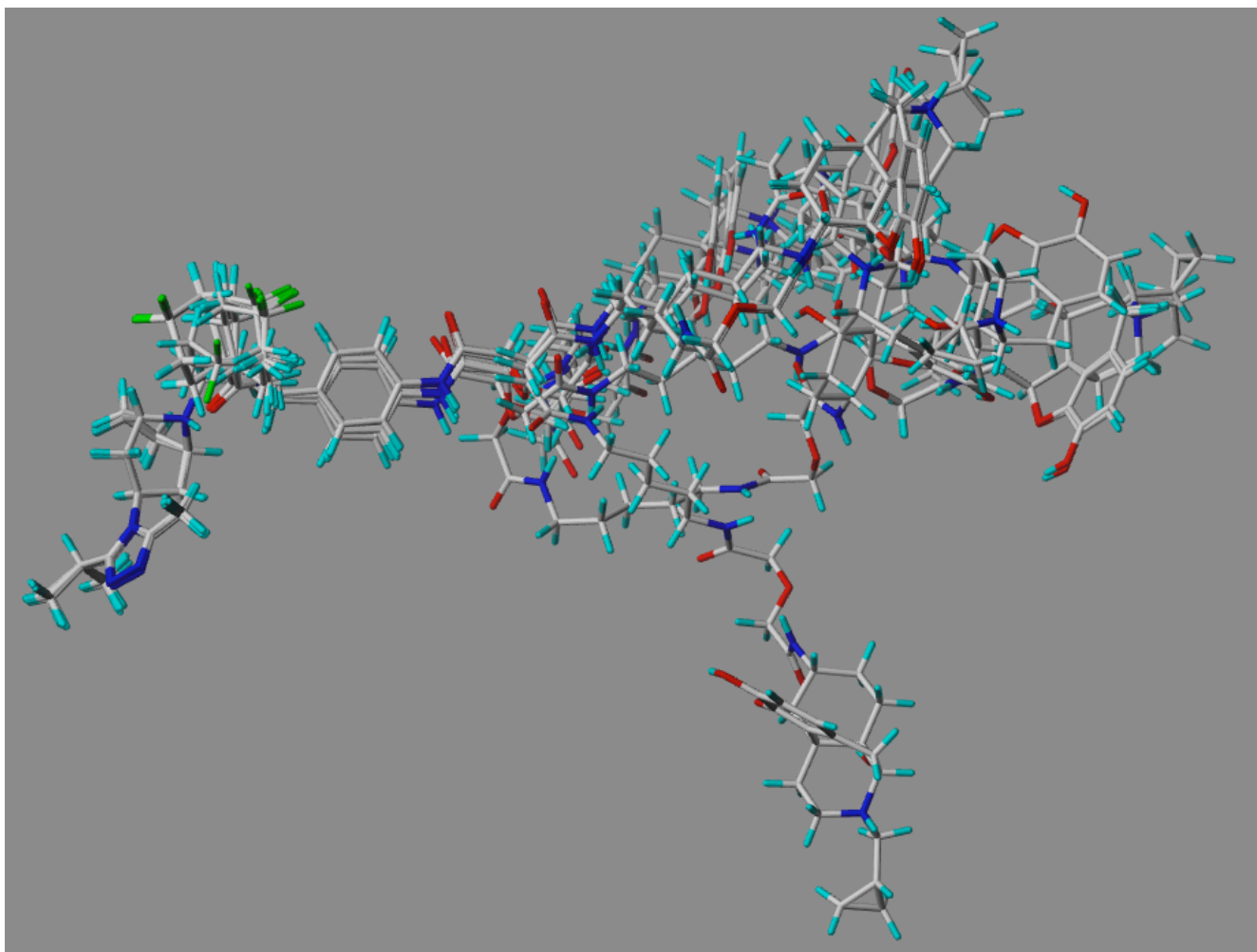
Unlike in the global minimization analysis, the DIVERSESET algorithm produced conformations for each spacer that allowed it to adopt an “elongated” spatial arrangement. That is to say, many of the low-energy conformers could theoretically bind to both the hMOR receptor and CCR5 receptor at once, unlike the 3 global minima generated from the global minimization analysis. Looking at Figures **18**, **19**, and **20**, in which 10 low-energy conformers were superimposed upon one another, we can see similar elongated conformations for all three spacers (elongated in the sense that the maraviroc and naltrexamine portions are kept separate from one another). Because of the similar conformations shared by the three spacer molecules, it can be hypothesized that any differences in binding activity are attributable to the length of the spacer and not drastic differences in conformation. Therefore, the DIVERSESET algorithm has produced results consistent with the two purposes of the conformational analysis study, i.e., to verify conformational similarity between the three spacers and to verify their viability in binding to two different receptors at once.



**Figure 18.** Diverse set conformational ensemble of the 19-atom spacer.



**Figure 19.** Diverse set conformational ensemble of the 21-atom spacer consisting.

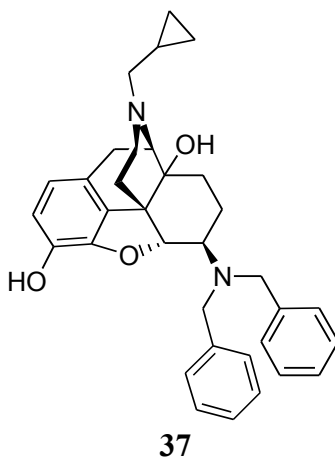


**Figure 20.** Diverse set conformational ensemble of the 23-atom spacer



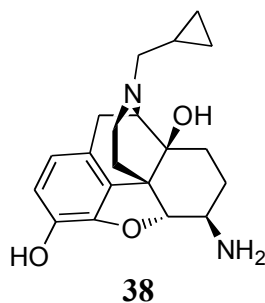
## 5. Experimental

### 5.1 Chemistry Intermediates

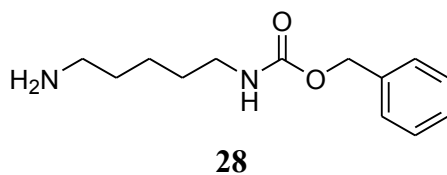


(4R, 4aS, 7R, 7aR, 12bS)-3-(cyclopropylmethyl)-7-(dibenzylamino)-2,3,4,4a,5,6,7,7a-octahydro-1H-4,12-methanobenzofuro[3,2-e]isoquinoline-4a,9-diol (**37**). Naltrexone, free base, (0.5 g, 0.001460 mol) was dissolved in 50 mL absolute EtOH. Benzoic acid (1.1 eq, 0.18 g, 0.001474 mol) was added and the mixture was allowed to stir for 30 minutes under N<sub>2</sub> protection. 150 mL toluene was added to the flask with benzoic acid (1.1 eq, 0.18 g, 0.001474 mol), dibenzylamine (1.2 eq, 0.34 mL, 0.001812 mol) and a trace amount of p-toluenesulfonic acid. The reaction was refluxed for 24 hours under N<sub>2</sub> protection with a Dean-Stark trap to remove any H<sub>2</sub>O produced from the reaction. One hundred and fifty mL of toluene was added during the course of the day. One hundred mL EtOH, molecular sieves, and NaBH<sub>3</sub>CN (1.1 eq, 0.100 g, 0.001591 mol) were added and allowed to stir under N<sub>2</sub> protection for 24 hours. The mixture was then filtered, rotovaped and re-dissolved in dichloromethane with 3% aqueous NH<sub>4</sub>OH. The chloroform was rotovaped and (**37**) was recrystallized in 9:1 MeOH/H<sub>2</sub>O to give 0.260 g at 35% yield. <sup>1</sup>H NMR (400 MHz, CDCl<sub>3</sub>) δ 0.096 (m, 2H), 0.495 (m, 2H), 0.815 (m, 1H), 1.230 (td, *J* = 10.4, 2.8 Hz, 1H), 1.409 (dd, *J* = 10.3, 2.4 Hz, 1H), 1.575 (m, 1H), 1.681 (m, 1H), 1.955-2.119 (m, 2H), 2.170-2.244 (m, 1H), 2.327 (m, 2H), 2.475 (dd, *J* = 12.6, 5.8 Hz, 1H), 2.547-2.62 (m,

2H), 2.971 (m, 1H), 3.593 (d,  $J = 14.2$  Hz, 1H), 3.874 (m, 2H), 4.693 (d,  $J = 7.8$  Hz, 1H), 6.420 (d,  $J = 8$  Hz, 1H), 6.551 (d,  $J = 8$  Hz) 7.819 (m, 2H), 7.279 (m, 5H), 4.222 (d,  $J = 7.2$ , 4H).

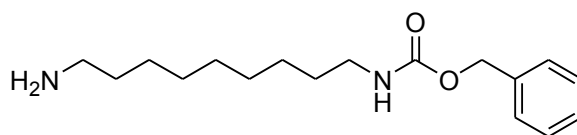


6 $\beta$ -naltrexamine (**38**). In a 250 mL hydrogenation flask, **37** (0.260 g, 0.0004990 mol) was dissolved in 5 mL MeOH. 10% Pd/C (0.026 g, 10% w/w) and concentrated HCl (2 eq, 0.06 mL, 0.002036 mol) was added. The flask was placed on a hydrogenator at 60 psi H<sub>2</sub> gas for 24 hours and monitored with TLC (10:1:0.01 DCM:MeOH:NH<sub>4</sub>OH). Once completed, the reaction mixture was filtered through celite and evaporated. **38** was recrystallized in 9:1 diethyl ether:MeOH to give a total of 0.199 g x2 hydrochloride salt, giving a yield of 96%. <sup>1</sup>H NMR (400 MHz, DMSO-d<sub>6</sub>)  $\delta$  0.41 (m, 1H), 0.51 (m, 1H), 0.59 (m, 1H), 0.67 (m, 1H), 1.06 (m, 1H), 1.32 (m, 1H), 1.46 (d,  $J = 8.8$  Hz, 1H), 1.78 (m, 1H), 1.82 (d,  $J = 14.4$  Hz, 1H), 1.99 (q,  $J = 12.5$ , Hz, 1H), 2.50 (m, 2H), 2.90 (m, 2H), 3.04 (d,  $J_1 = 6.0$  Hz,  $J_2 = 18.8$  Hz, 2H), 3.33 (m, 2H), 3.90 (d,  $J = 4.8$  Hz, 1H), 4.68 (d,  $J = 7.2$  Hz, 1H), 6.40 (brs, 1H), 6.67 (d,  $J = 8.0$  Hz, 1H), 6.80 (d,  $J = 8.0$  Hz, 1H), 8.43 (m, 2H, exchangeable), 8.91 (brs, 1H, exchangeable), 9.58 (s, 1H, exchangeable).



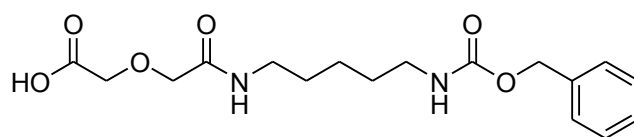
(5-Amino-pentyl)-carbamic acid benzyl ester (**28**). In a 500 mL flask, 1,5-diaminopentane (1 eq, 1 g,

0.009804 mol) was dissolved in 250 mL DCM and stirred above a Dewar container containing 2-10 dry ice cubes and acetone. Temperature was set to 0-5 °C. To the reaction mixture, Cbz-Cl (0.5 eq, 0.84 g, 0.004924 mol) in 250 mL DCM was added dropwise for 12 hours while keeping the temperature at 0-5 °C. After the addition, the reaction mixture was evaporated to dryness and concentrated with a vacuum pump. The crude product was then purified with column chromatography (5:1:0.01 DCM:MeOH:NH<sub>4</sub>OH) to give 0.770 g **28** at 33% yield. <sup>1</sup>H NMR (400 MHz, CDCl<sub>3</sub>) δ 1.345 (m, 2H), 1.500 (m, 4H), 2.706 (t, *J* = 7.06 Hz, 2H), 3.204 (q, *J* = 6.4 Hz, 2H), 4.816 (s, 1H), 5.094 (s, 2H), 7.525 (m, 5H).



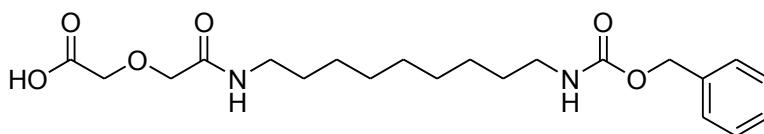
**29**

(9-Amino-nonyl)-carbamic acid benzyl ester (**29**). In a 500 mL flask, 1,9-diaminononane (1 eq, 1 g, 0.006300 mol) was dissolved in 250 mL DCM and stirred above a Dewar container containing 2-10 dry ice cubes and acetone. Temperature was set to 0-5 °C. To the reaction mixture, Cbz-Cl (0.5 eq, 0.49 g, 0.002872 mol) in 250 mL DCM was added dropwise for 12 hours while keeping the temperature at 0-5 °C. After the addition, the reaction mixture was evaporated to dryness and concentrated with a vacuum pump. The crude product was then purified with column chromatography (10:1:0.01 DCM:MeOH:NH<sub>4</sub>OH) to give 0.440 g **29** at 24% yield. <sup>1</sup>H NMR (400 MHz, CDCl<sub>3</sub>) δ 1.286 (broad s, 10H), 1.489 (brs, 4H), 2.731 (t, *J* = 7.06 Hz, 2H), 3.187 (q, *J* = 6.4 Hz, 2H), 4.740 (s, 1H), 5.094 (s, 2H), 7.348 (m, 5H).



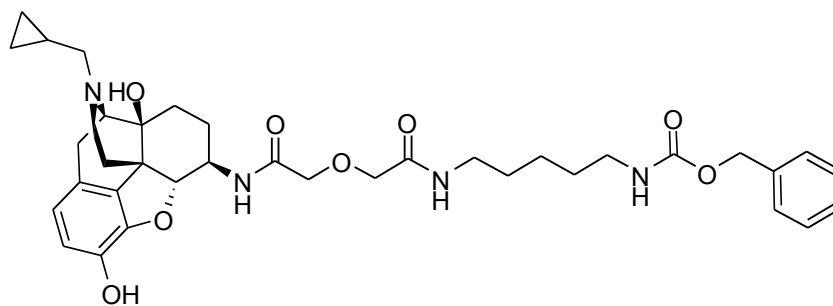
**30**

[(5-Benzyloxycarbonylamino-pentylcarbamoyl)-methoxy]-acetic acid (**30**). **28** (1 eq, 0.770 g, 0.003257 mol) was dissolved in 18 mL THF above an ice-water bath at 0 °C. Diglycolic anhydride (1 eq, 0.38 g, 0.003276 mol) was added to the mixture, the water bath was removed and the reaction was allowed to continue at room temperature. The solution was stirred overnight and then evaporated to dryness. The crude product was recrystallized in 9:1 MeOH:diethyl ether to give 0.270 g at a yield of 30%. <sup>1</sup>H NMR (400 MHz, CDCl<sub>3</sub>) δ 1.352 (m, 2H), 1.534 (m, 4H), 3.113 (t, *J* = 6.9 Hz, 2H), 3.239 (t, *J* = 6.9 Hz, 2H), 4.045 (s, 2H), 4.171 (s, 2H), 5.057 (s, 2H), 7.308 (m, 5H).



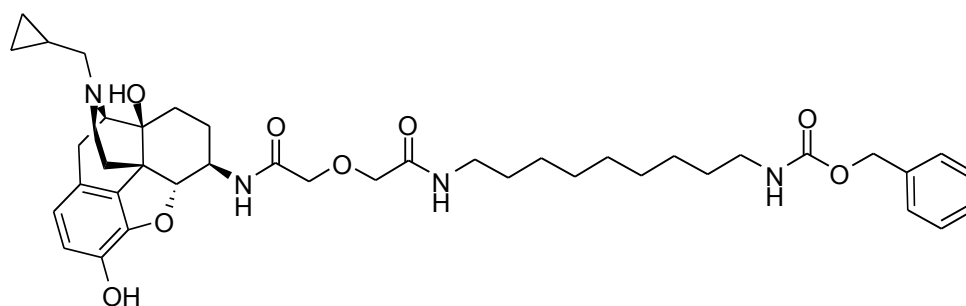
**31**

[(9-Benzyloxycarbonylamino-nonylcarbamoyl)-methoxy]-acetic acid (**31**). **29** (1 eq, 0.416 g, 0.001423 mol) was dissolved in 10 mL THF above an ice-water bath at 0 °C. Diglycolic anhydride (1.1 eq, 0.18 g, 0.001442 mol) was added to the mixture, the water bath was removed and the reaction was allowed to continue at room temperature. The solution was stirred overnight and then evaporated to dryness. The crude product was recrystallized in 9:1 MeOH:diethyl ether to give 0.170 g at a yield of 30%. <sup>1</sup>H NMR (400 MHz, CDCl<sub>3</sub>) δ 1.316 (brs, 10H), 1.512 (m, 4H), 3.095 (t, *J* = 6.9 Hz, 2H), 3.253 (t, *J* = 6.9 Hz, 2H), 4.046 (s, 2H), 4.180 (s, 2H), 5.058 (s, 2H), 7.308 (m, 5H).



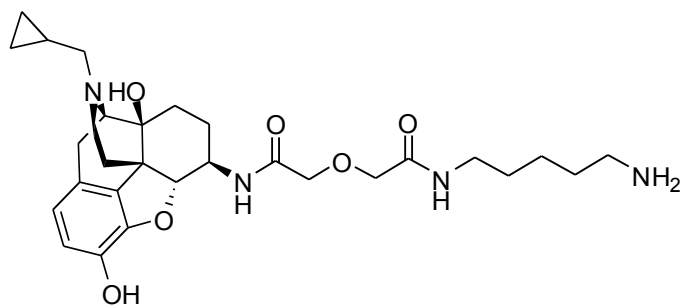
**32**

benzyl(5-(2-(2-(((4R, 4aS, 7R, 7aR, 12bS)-3-(cyclopropylmethyl)-4a,9-dihydroxy-2,3,4,4a,5,6,7,7a-octahydro-1H-4,12-methanobenzofuro[3,2-e]isoquinolin-7-yl)amino)-2-oxoethoxy)acetamido)pentyl)carbamate (**32**). **30** (1 eq, 0.145 g, 0.0004117 mol) was dissolved with 1 mL DMF in a 5 mL flask. To the solution, 1-hydroxybenzotriazole hydrate (1.5 eq, 0.083 g, 0.0006141 mol), triethylamine (6 eq, 0.166 g, 0.001644 mol) and molecular sieves were added and the reaction was placed under N<sub>2</sub> protection above an ice-water bath at 0 °C. N-(3-dimethylaminopropyl)-N'-ethylcarbodiimide hydrochloride (1.5 eq, 0.096 g, 0.0006194 mol) was added and the water bath was removed, thus allowing the reaction to return to RT. 6β-naltrexamine (**40**) (1 eq, 0.171 g, 0.0004120 mol) was dissolved in 1 mL DMF and added to the reaction dropwise. The reaction was monitored with TLC (10:1:0.01 DCM:MeOH:NH<sub>4</sub>OH) every 24 hours until completion and then filtered and evaporated to dryness. Column chromatography was conducted on the crude product (20:1:0.01 DCM:MeOH, NH<sub>4</sub>OH) to obtain 0.165 g of **32** at a yield of 60%. <sup>1</sup>H NMR (400 MHz, MeOD) δ .0414 (brs, 2H), 0.752 (d, *J* = 7.6 Hz, 2H), 1.041 (s, 1H), 1.306 (m, 4H), 1.530 (m, 6H), 1.712 (m, 2H), 1.986 (m, 1H), 2.529 (s, 2H), 2.744 (m, 2H), 2.989 (m, 2H), 3.118 (m, 2H), 3.204 (m, 2H), 3.725 (m, 2H), 4.073 (s, 4H), 4.653 (s, 1H), 5.060 (s, 2H), 6.715 (m, 2H), 7.277 (m, 5H), 7.698 (t, *J* = 5.5 Hz, 1H).



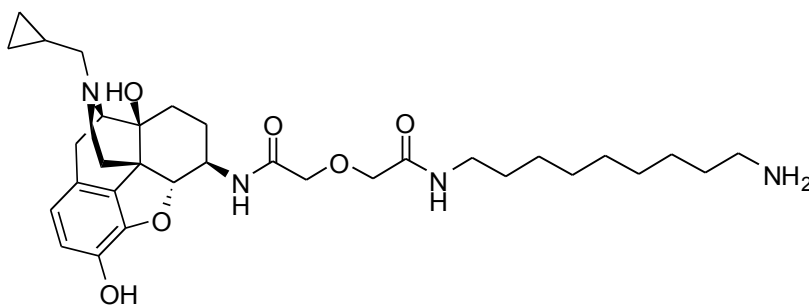
**33**

benzyl(9-(2-(2-(((4R, 4aS, 7R, 7aR, 12bS)-3-(cyclopropylmethyl)-4a,9-dihydroxy-2,3,4,4a,5,6,7,7a-octahydro-1H-4,12-methanobenzofuro[3,2-e]isoquinolin-7-yl)amino)-2-oxoethoxy)acetamido)nonyl)carbamate (**33**). **31** (1 eq, 0.220 g, 0.0005392 mol) was dissolved with 1 mL DMF in a 5 mL flask. To the solution, 1-hydroxybenzotriazole hydrate (1.5 eq, 0.109 g, 0.0008074 mol), triethylamine (6 eq, 0.220 g, 0.002178 mol) and molecular sieves were added and the reaction was placed under N<sub>2</sub> protection above an ice-water bath at 0 °C. N-(3-dimethylaminopropyl)-N'-ethylcarbodiimide hydrochloride (1.5 eq, 0.126 g, 0.0008129 mol) was added and the water bath was removed, thus allowing the reaction to return to RT. 6β-naltrexamine (**40**) (1 eq, 0.224 g, 0.0005398 mol) was dissolved in 1 mL DMF and added to the reaction dropwise. The reaction was monitored with TLC (10:1:0.01 DCM:MeOH:NH<sub>4</sub>OH) every 24 hours until completion and then filtered and evaporated to dryness. Column chromatography was conducted on the crude product (30:1:0.01 DCM:MeOH, NH<sub>4</sub>OH) to obtain 0.170 g of **33** at a yield of 43%. <sup>1</sup>H NMR (400 MHz, MeOD) δ 0.265 (m, 2H), 0.605 (m, 2H), 0.958 (m, 1H), 1.323 (brs, 12H), 1.477 (m, 6H), 1.616 (m, 2H), 1.952 (m, 1H), 2.246 (m, 2H), 2.701 (m, 2H), 3.092 (s, 2H), 3.261 (s, 3H), 3.480 (s, 2H), 3.748 (s, 1H), 4.080 (s, 4H), 4.561 (s, 1H), 5.057 (s, 2H), 6.665 (s, 2H), 7.332 (m, 5H), 7.753 (t, *J* = 5.5, 1H).



**34**

N-(5-aminopentyl)-2-(2-(((4R, 4aS, 7R, 7aR, 12bS)-3-(cyclopropylmethyl)-4a,9-dihydroxy-2,3,4,4a,5,6,7,7a-octahydro-1H-4,12-methanobenzofuro[3,2-e]isoquinolin-7-yl)amino)-2-oxoethoxy)acetamide (**34**). In a hydrogenation flask, **32** (1 eq, 0.165 g, 0.0002441 mol) was dissolved in 15 mL MeOH. To this solution, 10% Pd/C (0.0165 g, 10% w/w) was added. The flask was placed on a hydrogenator at 60 psi using H<sub>2</sub> gas for 24 hours and monitored by TLC (7:1:0.01 DCM:MeOH:NH<sub>4</sub>OH). Once completed, the reaction mixture was filtered and then evaporated to dryness to give 0.086 g **34** at 67% yield. <sup>1</sup>HNMR (400 MHz, MeOD) δ 0.153 (s, 2H), 0.526 (m, 2H), 0.547 (s, 1H), 1.387 (m, 4H), 1.616 (m, 6H), 1.923 (m, 1H), 2.161 (m, 1H), 2.219 (m, 1H), 2.396 (m, 2H), 2.624 (m, 2H), 2.736 (t, *J* = 6.4 Hz, 2H), 3.106 (m, 2H), 3.315 (s, 2H), 3.771 (m, 1H), 4.068 (s, 4H), 4.504 (d, *J* = 7.6 Hz, 1H), 6.560 (d, *J* = 7.6 Hz, 1H), 6.643 (d, *J* = 7.6 Hz, 1H).

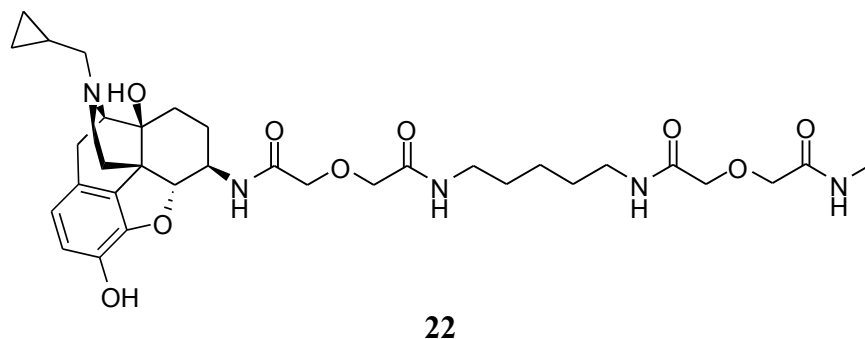


**35**

N-(9-aminononyl)-2-(2-(((4R, 4aS, 7R, 7aR, 12bS)-3-(cyclopropylmethyl)-4a,9-dihydroxy-2,3,4,4a,5,6,7,7a-octahydro-1H-4,12-methanobenzofuro[3,2-e]isoquinolin-7-yl)amino)-2-oxoethoxy)acetamide (**35**) In a hydrogenation flask, **33** (1 eq, 0.160 g, 0.0002186 mol) was dissolved in

15 mL MeOH. To this solution, 10% Pd/C (0.0160 g, 10% w/w) was added. The flask was placed on a hydrogenator at 60 psi using H<sub>2</sub> gas for 24 hours and monitored by TLC (7:1:0.01 DCM:MeOH:NH<sub>4</sub>OH). Once completed, the reaction mixture was filtered and then evaporated to dryness to give 0.091 g **35** at 72% yield. <sup>1</sup>H NMR (400 MHz, MeOD) δ 0.171 (m, 2H), 0.534 (d, *J* = 7.6 Hz, 2H), 0.879 (m, 1H), 0.896 (m, 12H), 1.357 (m, 6H), 1.576 (m, 1H), 2.436 (m, 2H), 2.676 (m, 2H), 2.839 (t, *J* = 3.5 Hz, 1H), 3.119 (m, 2H), 3.346 (s, 2H), 3.749 (m, 1H), 4.110 (s, 4H), 4.517 (d, *J* = 7.6 Hz, 1H), 5.481 (s, 4H), 6.628 (m, 2H), 7.352 (m, 1H).

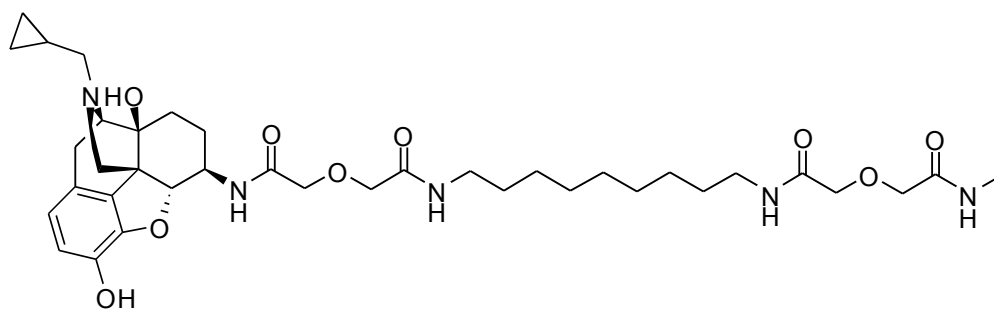
## Final Compounds



*5-carbon opioid monovalent compound (22)*. Methycarbamoylmethoxy acetic acid (1 eq, 0.024 g, 0.0001622 mol) was dissolved with 1 mL DMF in a 5 mL flask. To the solution, 1-hydroxybenzotriazole hydrate (1.5 eq, 0.031 g, 0.0002296 mol), triethylamine (6 eq, 0.061 g, 0.0006040 mol) and molecular sieves were added and the reaction was placed under N<sub>2</sub> protection above an ice-water bath at 0 °C. N-(3-dimethylaminopropyl)-N'-ethylcarbodiimide hydrochloride (1.5 eq, 0.035 g, 0.0002258 mol) was added and the water bath was removed, thus allowing the reaction to return to RT. **34** (1 eq, 0.086 g, 0.0001632 mol) was dissolved in 1 mL DMF and added to the reaction dropwise. The reaction was monitored with TLC (7:1:0.01 DCM:MeOH:NH<sub>4</sub>OH) every 24 hours until



completion and then filtered and evaporated to dryness. Column chromatography was conducted on the crude product (10:1:0.01 DCM:MeOH, NH<sub>4</sub>OH) to obtain 0.030 g of **22** at a yield of 30%. <sup>1</sup>H NMR (400 MHz, MeOD) δ 0.525 (s, 2H), 0.747 (m, 2H), 1.119 (s, 1H), 1.404 (brs, 2H), 1.670 (m, 8H), 2.019 (m, 1H), 2.549 (m, 2H), 2.716 (s, 4H), 2.882 (m, 2H), 3.117 (m, 2H), 3.269 (m, 4H), 3.721 (s, 1H), 4.042 (s, 4H), 4.080 (s, 4H), 4.715 (d, *J* = 7.6 Hz, 2H), 6.747 (s, 2H). <sup>13</sup>C NMR (400 MHz, MeOD) δ 3.48, 6.25, 6.90, 24.55, 24.67, 25.21, 25.95, 28.94, 30.05, 31.18, 39.92, 39.97, 47.62, 54.41, 58.87, 64.40, 71.39, 71.50, 71.64, 91.89, 119.72, 121.02, 121.85, 130.75, 143.15, 143.80, 171.75. IR (ATR, cm<sup>-1</sup>) ν<sub>max</sub>: 3274, 2933, 1644, 1549, 1530, 1455, 1373, 1323, 1185, 1124, 1034, 986, 917, 881, 856, 799. MS (ESI) *m/z* found, 672 (M + H)<sup>+</sup>, mp: 115 – 118 °C.



**23**

*9-carbon opioid monovalent compound (23)*. Methycarbamoylmethoxy acetic acid (1 eq, 0.023 g, 0.0001554 mol) was dissolved with 1 mL DMF in a 5 mL flask. To the solution, 1-hydroxybenzotriazole hydrate (1.5 eq, 0.032 g, 0.0002370 mol), triethylamine (6 eq, 0.065 g, 0.0006435 mol) and molecular sieves were added and the reaction was placed under N<sub>2</sub> protection above an ice-water bath at 0 °C. N-(3-dimethylaminopropyl)-N'-ethylcarbodiimide hydrochloride (1.5 eq, 0.037 g, 0.0002387 mol) was added and the water bath was removed, thus allowing the reaction to return to RT. **35** (1 eq, 0.091 g, 0.0001560 mol) was dissolved in 1 mL DMF and added to the reaction dropwise. The reaction was monitored with TLC (7:1:0.01 DCM:MeOH:NH<sub>4</sub>OH) every 24 hours until completion and then filtered and evaporated to dryness. Column chromatography was conducted on the

crude product (10:1:0.01 DCM:MeOH, NH<sub>4</sub>OH) to obtain 0.030 g **23** at a yield of 25%. <sup>1</sup>H NMR (400 MHz, MeOD)  $\delta$  0.227 (s, 2H), 0.600 (m, 2H), 0.927 (s, 1H), 1.339 (brs, 10H), 1.536 (m, 8H), 1.940 (m, 1H), 2.292 (s, 2H), 2.443 (s, 2H), 2.816 (m, 5H), 3.118 (m, 2H), 3.298 (m, 4H), 3.7501 (m, 1H), 4.027 (s, 4H), 4.071 (d,  $J = 4.4$  Hz, 4H), 4.801 (d,  $J = 7.6$  Hz, 1H), 6.610 (d,  $J = 7.6$  Hz, 1H), 6.665 (d,  $J = 7.6$  Hz, 1H). <sup>13</sup>C NMR (400 MHz, MeOD)  $\delta$  4.06, 4.80, 23.74, 25.30, 25.89, 27.90, 27.92, 27.96, 30.26, 30.42, 30.44, 30.48, 31.23, 40.08, 40.11, 52.49, 60.01, 60.04, 63.89, 71.40, 71.44, 71.50, 71.53, 71.56, 71.58, 71.66, 92.73, 118.78, 120.27, 124.89, 132.06, 142.15, 143.75, 171.49, 171.51, 171.57, 172.17. IR (ATR, cm<sup>-1</sup>)  $\nu_{\max}$ : 3273, 3078, 2926, 2853, 1651, 1548, 1503, 1454, 1374, 1322, 1258, 1185, 1126, 1035, 987, 916, 883, 857, 799, 747, 699. MS (ESI)  $m/z$  found, 728 (M + H)<sup>+</sup>, mp: 112 – 115 °C.

## 5.2 Biology Methods

### 5.2.1 hMOR Competitive Radioligand Binding Assay

The affinity and selectivity of the novel bivalent compounds and their controls were determined using a competitive radioligand binding assay. In this assay, the concentration of radioligand (i.e., tritiated naloxone) was fixed around its  $K_d$  value and its binding with respect to hMOR was tested by adding varying concentrations of drugs. The IC<sub>50</sub> values of the bivalents and controls were obtained from Hill plots and analyzed by linear regression. The  $K_i$  values were calculated from the IC<sub>50</sub> using the Cheng-Prusoff equation.

The assay was performed in triplicates with a fixed protein concentration of 30  $\mu$ g. The total assay volume was 500  $\mu$ L with TME buffer. Each assay rack included total binding, non-specific binding and drug-competition binding tubes. The total binding tubes contained the buffer, radioligand and protein. The non-specific binding tubes included all of the total binding components as well as excess unlabeled drug. A maximum of two drugs were tested at seven different concentrations per rack. These tubes contained the buffer, bivalents (or controls), radioligand and protein. Of note, the

drug concentration in each tube was multiplied by ten times in order to take the ten-fold dilution in each tube into account. After the first assay, the drug concentrations were optimized in order to get better  $IC_{50}$  values. It is also important to note that protein-bound tritiated radioligand was separated from unbound radioligand by a specialized type of fibrous filter paper, and the radioactive decay of the unbound radioligand was measured using a scintillation counter.

## 5.2.2 Calcium Mobilization Assays

### 5.2.2.1 hMOR-CHO Cells

hMOR-CHO cells were transfected with Gqi5 pcDNA1 and incubated for 6 hours at 37°C and 5%  $CO_2$ . After the 6-hour interval, the cells were detached from the plate with trypsin and transferred to a clear bottom, black 96-well plate at 20,000 cells per well. The cells were supplemented with DMEM/F-12 media containing 5% fetal bovine serum, 100  $\mu\text{g}/\text{mL}$  penicillin, 100  $\mu\text{g}/\text{mL}$  streptomycin and 0.25 mg/mL hygromycin B. 24 hours after the transfection the growth media was discarded and the wells were washed with 100  $\mu\text{L}/\text{well}$  of 50:1 HBSS:HEPES assay buffer. The cells were then incubated with 55  $\mu\text{L}/\text{well}$  of Fluo-4 loading buffer [30  $\mu\text{L}$  2  $\mu\text{M}$  Fluo4-AM and 84  $\mu\text{L}$  2.5 mM probenacid in 5.5 mL assay buffer] for 30 minutes. Varying concentration (in triplicate) of ligands and controls were added to the wells to bring the total volume to 80  $\mu\text{L}/\text{well}$ , and the well-plate was again incubated, this time for 15 minutes. The plate was then read on a FlexStation3 microplate reader (Molecular Devices) at 494/516 ex/em for a total of 2 minutes. After 15 second of reading, 20  $\mu\text{L}$  of 1.25  $\mu\text{M}$  DAMGO in assay buffer, or assay buffer alone for the control wells, was added to bring the total volume of each well up to 100  $\mu\text{L}$ . The changes in  $Ca^{2+}$  mobilization were monitored using SoftMaxPro software. Non-linear regression curves and  $IC_{50}$  values were generated using GraphPad Prism software. This experiment was performed three times to get an average of each  $IC_{50}$  value.

### 5.2.2.2 CCR5-MOLT-4 Cells

CCR5-MOLT-4 cells were transfected with Gqi5 pcDNA1 and maintained in RPMI 1640 media supplemented with 10% fetal bovine serum, 100 µg/mL penicillin, 100 µg/mL streptomycin and 1 mg/mL G418 before being incubated for 48 hours at 37°C and 5% CO<sub>2</sub>. 48 hours after the transfection, the 2.5 million cells were spun down and diluted in 8 mL of 50:1 HBSS:HEPES assay buffer. The cells were then plated at 25,000 cells per well (80 µL of diluted cell solution) into a clear bottom, black 96-well plate. Then, 50 µL/well of Fluo-4 loading buffer [40 µL 2 µM Fluo4-AM and 100 µL 2.5 mM probenacid in 5 mL assay buffer] was added to bring the volume of each well up to 130 µL. The plate was incubated for 45 minutes, after which varying concentrations (in triplicate) of ligands and controls were added to the wells to bring the total volume up to 180 µL. The plate was then incubated for an additional 15 minutes. The plate was then read on a FlexStation3 microplate reader (Molecular Devices) at 494/516 ex/em for a total of 1.5 minutes. After 15 second of reading, 20 µL of 200 nM RANTES in assay buffer, or assay buffer alone for the control wells, was added to bring the total volume of each well up to 200 µL. The changes in Ca<sup>2+</sup> mobilization were monitored using SoftMaxPro software. Non-linear regression curves and IC<sub>50</sub> values were generated using GraphPad Prism software. This experiment was performed three times to get an average of each IC<sub>50</sub> value.

## 5.3 Computational Methods

### 5.3.1 Small Molecule Construction

All ligands used in the conformational analysis studies were built with standard bonds and angles using the molecular modeling software SYBYL-X 2.0. The proper stereochemical arrangements were also assigned for each asymmetric carbon to ensure viability of results and uniform spatial

arrangements between each spacer molecule. For the process of energy minimization (to establish a local minimum conformation for each small molecule), each small molecule was assigned Gasteiger-Huckel charges and then minimized using the Tripos Force Field.

### 5.3.2 Global Minimization Conformational Analysis

The molecules were first drawn in the SYBYL-X 2.0 molecular modeling program and then, after assigning them Gasteiger-Huckel charges, minimized using the Tripos Force Field. The parameters for the global minimization conformational analysis studies were then set up using Confort conformational analysis modeling software, a program developed by Professor Robert Pearlman and Dr. Renzo Balducci.<sup>128</sup> For the global minimization of each small molecule, the search options were optimized to give accurate and viable results. First, the search was set to include the conformations of all rotatable bonds. Then, the maximum number of concurrently searched rotors was set to 100 for acyclic bonds, 20 for bonds included in ring systems and 10 for bonds in single rings (these parameters were required to ensure accuracy of results). Gasteiger-Huckel electrostatics were assigned to each molecule and the precision of results was set to .001 kcal/mol. The maximum output of low energy conformers was set to 10 in order to produce a global minimum and 9 low-energy conformers within approximately 10 kcal/mol of the global minimum. The program was then run and the results were put into a SYBYL spreadsheet, organizing each conformer by energy relative to the global minimum. After each of the conformers were analyzed, the global minimum conformer was placed into the SYBYL molecular area and a snapshot of it was taken.

### 5.3.3 Diverse Conformer Subset Conformational Analysis

The molecules were first drawn in the SYBYL-x 2.0 molecular modeling software and then minimized using the Tripos Force Field. Each molecule was assigned Gasteiger-Huckel charges before

energy minimization. The parameters for the diverse conformer subset conformational analysis studies were then set up using Confort conformational analysis software.<sup>128</sup> In developing a diverse conformer subset for each molecule, the search options were optimized to give repeatable, accurate and viable results. Like in the global minimization conformational analysis studies, the search was set to include all conformations of rotatable bonds. The maximum number of concurrently searched rotors was set to 100 for acyclic bonds, 20 for bonds included in ring systems and 10 for bonds in single rings. Again, these parameters were required to produce accurate results. Gasteiger-Huckel electrostatics were assigned to each molecule and the precision of results was set to .001 kcal/mol. Also included in the search options was a maximum conformer output of 500 low-energy conformations. The output settings were further modified to include a maximum of 500 diverse low-energy conformers (i.e., any conformer nearly identical in spatial arrangement and energy to another already-produced conformer would be rejected from the search results) within at least 100 kcal/mol of the lowest-energy conformer. The program was then run and the results were put into a SYBYL spreadsheet, organizing each conformer by energy relative to the lowest-energy conformer. A subset of 10 low-energy conformers within 20 – 30 conformers of the lowest-energy conformer were then extracted from the spreadsheet and placed into the SYBYL molecular area. These 10 conformers were aligned according to specific atoms within the molecule to give a comparative analysis. Once this was completed, a snapshot of the superimposed molecules was taken.

## List of References

1. Medzhitov, R. Origin and physiological roles of inflammation. *Nature* **2008**, *454*, 428–435.
2. Laskin, D. L.; Pendino, K. J. Macrophages and inflammatory mediators in tissue injury. *Annu. Rev. Pharmacol. Toxicol.* **1995**, *35*, 655–677.
3. Borish, L. C.; Steinke, J. W. Cytokines and chemokines. *K. Allergy Clin. Immunol.* **2003**, *111*, S460–S475.
4. Oppermann, M. Chemokine receptor CCR5: Insights into structure, function and regulation. *Cell Signaling* **2004**, *16*, 1201–1210.
5. Zlotnik, A; Yoshie, O. Chemokines: a new classification system and their role in immunity. *Immunity* **2000**, *12*, 121–127.
6. Horuk, R. Chemokine receptors. *Cytokine Growth Factor Rev.* **2001**, *88*, 263–273.
7. Gimpl, G.; Fahrenholz, F. The oxycotin receptor system: structure, function and regulation. *Physiol. Rev.* **2001**, *81*, 629–683.
8. Li, G; Haney, K. M.; Kellogg, G. E.; Zhang, Y. Comparative docking study of anibamine as the first natural product CCR5 antagonist in CCR5 homology models. *J. Chem. Inf. Model.* **2009**, *49*, 120–132.
9. Cherezov, V.; Rosenbaum, D. M.; Hanson, M. A.; Rasmussen, S. G.; Thian, F. S.; Kobilka, T. S.; Choi, H. J.; Kuhn, P.; Weis, W. I.; Kobilka, B. K.; Stevens, R. C. High resolution crystal structure of an engineered human  $\beta$ 2-adrenergic G protein-coupled receptor. *Science* **2007**, *318*, 1258–1265.
10. Rasmussen, S. G. F.; DeVree, B. T.; Zou, Y.; Kruse, A. C.; Chung, K. Y.; Kobilka, T. S.; Thian, F. S.; Chae, P. S.; Pardon, E.; Calinski, D.; Mathiesen, J. M.; Shah, S. T. A.; Lyons, J. A.; Caffrey, M.; Gellman, S. H.; Steyaert, J.; Skiniotis, G.; Weis, W. I.; Sunahara, R. K.; Kobilka, B. K. Crystal structure of the  $\beta$ 2 adrenergic receptor-Gs protein complex. *Nature* **2011**, *477*,

549–557.

11. Kontoyianni, M.; Liu, Z. Structure-based design in the GPCR target space. *Curr. Med. Chem.* **2012**, *19*, 544–556.
12. Ballesteros, J. A. Integrated methods for the construction of three dimensional models and computation probing of structure function relations in G protein-coupled receptors. *Methods Neurosci.* **1995**, *25*, 366–428.
13. Congreve, M.; Langmead, C. J.; Mason, J. S.; Marshall, F. H. Progress in structure based drug design for G protein-coupled receptors. *J. Med. Chem.* **2011**, *54*, 4283–4311.
14. Park, P. S. H. Ensemble of G protein-coupled receptor active states. *Curr. Med. Chem.* **2012**, *19*, 1146–1154.
15. Fanelli, F.; Benedetti, P. G. D. Update 1 of: Computational modeling approaches to structure – function analysis of G protein-coupled receptors. *Chem. Rev.* **2011**, *111*, PR438–PR535.
16. Lederman, M. M.; Penn-Nicholson, A.; Cho, M.; Mosier, D. Biology of CCR5 and its role in HIV infection and treatment. *J. Am. Med. Assoc.* **2006**, *296*, 815–826.
17. Lin, Y. L.; Mettling, C.; Portales, P.; Reant, B.; Robert-Hebmann, V.; Reynes, J.; Clot, J.; Corbeau, P. The efficacy of R5 HIV-1 infection is determined by CD4 T-cell surface CCR5 density through the G alpha i-protein signaling. *AIDS* **2006**, *20*, 1369–1377.
18. Mellado, M.; Rodriguez-Frade, J. M.; Manes, S.; Martinez, A. C. Chemokine signaling and functional responses: the role of receptor dimerization and TK pathway activation. *Annu. Rev. Immunol.* **2001**, *19*, 397–421.
19. Gainetdinov, R. R.; Premont, R. T.; Bohn, L. M.; Lefkowitz, R. J.; Caron, M. G. Desensitization of G protein-coupled receptor and neuronal functions. *Annu. Rev. Neurosci.* **2004**, *27*, 8875–8885.
20. Oppermann, M.; Mack, M.; Proudfoot, A. E. I.; Olbrich, H. Differential effects of CC



- chemokines of CC chemokine receptor 5 (CCR5) phosphorylation and identification of phosphorylation sites on the CCR5 carboxyl terminus. *J. Biol. Chem.* **2008**, *14*, 253–274.
21. Verkaar, F.; Van Rosmalen, J. W. G.; Blomenrohr, M.; Van Koppen, C. J.; Blankesteyn, W. M.; Smits, J. F. M.; Zaman, G. J. R. G protein-independent cell-based assays for drug discovery on seven-transmembrane receptors. *Biotech. Annu. Rev.* **2008**, *14*, 253–274.
22. Rask-Andersen, M.; Almen, M. S.; Schioth, H. B. Trends in the exploitation of novel drug targets. *Nat. Rev. Drug Disc.* **2011**, *10*, 47–60.
23. Chen, W.; Zhan, P.; DeClercq, E.; Liu, X. Recent progress in small molecule CCR5 antagonists as potential HIV-1 entry inhibitors. *Curr. Pharm. Des.* **2012**, *18*, 100–112.
24. Zhang, X.; Haney, K. M.; Richardson, A. C.; Wilson, E.; Gewirtz, D. A.; Ware, J. L.; Zehner, Z. E.; Zhang, Y. Anibamine, a natural product CCR5 antagonist, as a novel lead for the development of anti-prostate cancer agents. *Bioorg. Med. Chem. Lett.* **2010**, *20*, 4627–4630.
25. Zhang, Y.; Arnatt, C. K.; Zhang, F.; Wang, J.; Haney, K. M.; Fang, X.; The potential role of anibamine, a natural product CCR5 antagonist, and its analogues as leads toward development of anti-ovarian cancer agents. *Bioorg. Med. Chem. Lett.* **2012**, *22*, 5093–5097.
26. Opdenakker, G.; Van Damme, J. Cytokines and proteases in invasion processes: molecular similarities between inflammation and cancer. *Cytokine* **1992**, *4*, 251–258.
27. Mantovania, A.; Bottazi, B.; Colotta, F.; Sozzani, S.; Luigi, R. The origin and function of tumor-associated macrophages. *Immunol. Today* **1992**, *4*, 265–270.
28. Opdenakker, G.; Van Damme, J. Chemotactic factors, passive invasion and metastasis of cancer cells. *Immunol. Today* **1992**, *13*, 463–464.
29. Frederick, M. J.; Clayman, G. L.; Chemokines in cancer. *Expert Rev. Mol. Med.* **2001**, *3*, 1–18.
30. Kedzierska, K.; Corwe, S. M.; Turville, S.; Cunningham, A. L.; The influence of cytokines, chemokines and their receptor on HIV-1 replication in monocytes and macrophages. *Rev. Med.*

*Viol.* **2003**, *13*, 39–56.

31. Chinen, J.; Shearer, W. T. Molecular virology and immunology of HIV infection. *Allergy Clin. Immunol.* **2002**, *110*, 189–198.
32. Deng, H.; Liu, R.; Ellmeier, W.; Choe, S.; Unutmaz, D.; Burkhart, M.; Di Marzio, P.; Marmon, S.; Sutton, R. E.; Hill, C. M.; Davis, C. B.; Peiper, S. C.; Shall, T. J.; Littman, D. R.; Landau, N. R. Identification of a major co-receptor for primary isolates of HIV-1. *Nature* **1996**, *381*, 661–666.
33. Alkhatib, G.; Comadiere, C.; Broder, C. C.; Feng, Y.; Kennedy, P. E.; Murphy, P. M.; Berger, E. A. CC CKR5: a RANTES, MIP-1alpha, MIP-1beta receptor as a fusion cofactor for macrophage-tropic HIV-1. *Science* **1996**, *272*, 1955–1958.
34. Barre-Sinoussi, F.; Chermann, J. C.; Rey, F.; Nugeyre, M. T.; Chamaret, S.; Gruest, J.; Dauguet, C.; Axler-Blin, C.; Vezinet-Brun, F.; Rouzioux, C.; Rosenbaum, W.; Montagnier, L. Isolation of a T-lymphotropic retrovirus from a patient at risk for acquired immunodeficiency syndrome (AIDS). *Science* **1983**, *220*, 868–871.
35. Samson, M.; Libert, F.; Doranza, B. J.; Rucker, J.; Liesnard, C.; Farber, C. M.; Saragosti, S.; Lapoumeroulie, C.; Cognaux, J.; Forceille, C.; Muyltermans, G.; Verhofstede, C.; Burtonboy, G.; Georges, M.; Imai, T.; Rana, S.; Yi, Y.; Smyth, R. J.; Collman, R. J.; Doms, R. W.; Vassart, G.; Parmentier, M. Resistance to HIV-1 infection in caucasian individuals bearing mutant alleles of the CCR5 chemokine receptor gene. *Nature* **1996**, *382*, 722–725.
36. Liu, R.; Paxton, W. A.; Choe, S.; Ceradini, D.; Martin, S. R.; Horuk, R.; MacDonald, M E.; Stufmann, H.; Koup, R. A.; Landau, N. R. Homozygous defect in HIV-1 coreceptor accounts for resistance of some multiply-exposed individuals to HIV-1 infection. *Cell* **1996**, *86*, 367–377.
37. National Institute of Allergies and Infectious Diseases.

<http://www.niaid.nih.gov/daids/dtpdb/attach.asp> (accessed Apr 30, 2014).

38. Cocchi, F.; DeVico, A. L.; Garzino-Demo, A.; Arya, S. K.; Gallo, R. C.; Lusso, P. Identification of RANTES, MIP-1alpha, and MIP-1beta as major HIV-suppressive factors produced by CD8+ T cells. *Science* **1995**, *270*, 1811–1815.
39. Wilkin, T. J.; Gulick, R. M. CCR5 antagonism in HIV infection: current concepts and future opportunities. *Annu. Rev. Med.* **2012**, *63*, 81–93.
40. Lemoine, R. C.; Wanner, J. Small molecule antagonists of the chemokine receptor CCR5. *Curr. Top. Med. Chem.* **2010**, *10*, 1299–1338.
41. Allegretti, M.; Cesta, M. C.; Garin, A.; Proudfoot, A. E. I. Current status of chemokine receptor inhibitors in development. *Immunol. Lett.* **2012**, *145*, 68–78.
42. Palani, A.; Tagat, J. Discovery and development of small-molecule chemokine coreceptor CCR5 antagonists. *J. Med. Chem.* **2006**, *49*, 2851–2855.
43. Nichols, W. G.; Steel, H. M.; Bonny, T.; Adkison, K.; Curtis, L.; Millard, J.; Kabeya, K.; Clumeck, N. Hepatotoxicity observed in clinical trials of aplaviroc (GW873140). *Antimicrob. Agents Chemother.* **2008**, *52*, 858–865.
44. Gilliam, B. L.; Riedel, D. J.; Redfield, R. R. Clinical use of CCR5 inhibitors in HIV and beyond. *J. Transl. Med.* **2010**, *9*, S9–S23.
45. Bab, M.; Nishimura, O.; Kanzaki, N.; Okamoto, M.; Sawada, H.; Iizawa, Y.; Shirashi, M.; Aramaki, Y.; Okonogi, K.; Ogawa, Y.; Meguro, K.; Fujino, M. A small-molecule, nonpeptide CCR5 antagonist with highly potent and selective anti-HIV-1 activity. *Proc. Natl. Acad. Sci. USA* **1999**, *96*, 5698–5703.
46. Waldoer, M.; Bartlett, S. E.; Whistler, J. L.; Opioid receptors. *Annu. Rev. Biochem.* **2004**, *73*, 953–990.
47. Wu, H.; Wacker, D.; Mileni, M.; Katritch, V.; Han, G. W.; Vardy, E.; Liu, W.; Thompson, A. A.; Huang, X. H.; Carroll, F. I.; Mascarella, S. W.; Westkaemper, R. B.; Mosier, P. D.; Roth, B. L.;

- Cherezov, V.; Stevens, R. C. Structure of the human  $\kappa$ -opioid receptor in complex with JDTic. *Nature* **2012**, *485*, 327–332.
48. Thompson, A. A.; Liu, W.; Chun, E.; Katritch, V.; Wu, H.; Vardy, E.; Huang, X. P.; Trapella, C.; Guerrini, R.; Calo, G.; Roth, B. L.; Cherezov, V.; Stevens, R. C. Structure of the nociception/orphanin FQ receptor in complex with a peptide mimetic. *Nature* **2012**, *485*, 321–326.
49. Manglik, A.; Kruse, A. C.; Kobilka, T. S.; Thian, F. S.; Mathiesen, J. M.; Sunahara, R. K.; Pardo, L.; Weis, W. I.; Kobilka, B. K.; Granier, S. Crystal structure of the  $\mu$ -opioid receptor bound to a morphinan antagonist. *Nature* **2012**, *485*, 400–404.
50. Dhawan, B. N.; Cesselin, F.; Raghbir, R.; Reisine, T.; Bradley, P. B.; Portoghese, P. S.; Hamon, M. International union of pharmacology. XII. Classification of opioid receptors. *Pharmacol. Rev.* **1996**, *48*, 567–592.
51. Martin, W. R.; Eades, C. G.; Thompson, J. A.; Huppler, R. E.; Gilbert, P. E. The effects of morphine- and nalorphine-like drugs in the nondependent and morphine dependent chronic spinal dog. *J. Pharmacol. Exp. Ther.* **1976**, *197*, 517–532.
52. Pert, C. B.; Snyder, S. H. Opiate receptor: demonstration in nervous tissue. *Science* **1973**, *179*, 1011–1014.
53. Mannalack, D. T.; Beart, P. M.; Gundlach, A. L. Psychotomimetic sigma-opiates and PCP. *Trends Pharm. Sci.* **1986**, *7*, 448–451.
54. Lord, J. A. H.; Waterfield, A. A.; Hughes, J.; Kosterlitz, H. W. Endogenous opioid peptides: multiple agonists and receptors. *Nature* **1997**, *267*, 495–499.
55. Henderson, G. The orphan opioid receptor and its endogenous ligand – nociceptin/orphanin FQ. *Trends Pharm. Sci.* **1997**, *18*, 293–300.
56. Ballantyne, J. C.; LaForge, K. S. Opioid dependence and addiction during treatment of chronic

- pain. *Pain* **2007**, *129*, 235–255.
57. Stromer, W.; Michaeli K.; Sander-Kiesling, A. Perioperative pain therapy in opioid abuse. *Eur. J. Anaesthesiol.* **2013**, *30*, 55–64.
58. Matthes, H. W. D.; Maldonado, R.; Simonin, F.; Valverde, O.; Slowe, S.; Kitchen, I.; Befort, K.; Dierich, A.; LeMeur, M.; Dolle, P.; Tzavara, E.; Hanoune, J.; Rosques, B. P.; Kiefer, B. L. Loss of morphine-induced analgesia, reward effect and withdrawal symptoms in mice lacking the mu-opioid receptor gene. *Nature* **1996**, *383*, 819–823.
59. Kieffer, B. L.; Gaveriaux-Ruff, C.; Exploring the opioid system by gene knockout. *Prog. Neurobiol.* **2002**, *66*, 285–306.
60. Goodman, A. J.; Bourdonnec, B. L.; Dolle, R. E. Mu opioid receptor antagonists: recent development. *ChemMedChem* **2007**, *2*, 1552–1570.
61. Law, P. Y.; Wong, Y. H.; Loh, H. H. Molecular mechanisms and regulation of opioid receptor signaling. *Annu. Rev. Pharmacol. Toxicol.* **2000**, *40*, 389–430.
62. Hauser, K. F.; Fitting, S.; Dever, S. M.; Podhaizer, E. M.; Knapp, P. E.; Opiate drug use and the pathophysiology of neuroAIDS. *Curr. HIV Res.* **2012**, *10*, 435–452.
63. Turchan-Cholewo, J.; Liu, Y.; Gartner, S; Reid, R.; Jie, C.; Peng, X.; Chen, K. C.; Chauhan, A.; Haughey, N.; Cutler, R.; Mattson, M. P.; Pardo, C.; Conant, K.; Sacktor, N.; McArthur, J. C.; Hauser, K. F.; Gairola, C.; Nath, A. Increased vulnerability of ApoE4 neurons to HIV proteins and opiates: protection by diosgenin and L-deprenyl. *Neurobiol. Dis.* **2006**, *23*, 109–119.
64. Hauser, K. F.; El-Hage, N.; Buch, S.; Berger, J. R.; Tyor, W. R.; Nath, A.; Bruce-Keller, A. J.; Knapp, P. E. Molecular targets of opiate drug abuse in neuroAIDS. *Neurotoxic. Res.* **2005**, *8*, 63–80.
65. Nath, A.; Hauser, K. F.; Wojna, V.; Booze, R. M.; Maragos, W.; Prendergast, M.; Cass, W.; Turchan, J. T. Molecular basis for interactions of HIV and drugs of abuse. *JAIDS, J. Acquired*

- Immune Defic. Syndr.* **2002**, *31*, S62–S69.
66. Norman, K. F.; Basso, M.; Kurmar, A.; Malow, R.; Neuropsychological consequences of HIV and substance abuse: a literature review and implications for treatment and future research. *Curr. Drug Abuse Rev.* **2009**, *2*, 143–156.
67. Anthony, I. C.; Arango, J. C.; Stephens, B.; Simmonds, P.; Bell, J. E. The effects of illicit drugs on the HIV infected brain. *Front. Biosci.* **2008**, *13*, 1294–1307.
68. Noel, R. J. J.; Rivera-Amill, V; Buch, S.; Kurmar, A. Opiates, immune system, acquired immunodeficiency syndrome, and nonhuman primate model. *J. Neurovirol.* **2008**, *14*, 279–285.
69. Chen, C.; Li, J.; Bot, G.; Szabo, I.; Rogers, T. J.; Liu-Chen, L. Y. Heterodimerization and cross-desensitization between the mu-opioid receptor and chemokine CCR5 receptor. *Eur. J. Pharmacol.* **2004**, *483*, 175–186.
70. Rogers, T. J.; Peterson, P. K.; Opioid G protein-coupled receptors, signals at the crossroads of inflammation. *Trends Immunol.* **2003**, *24*, 116–121.
71. Rogers, T. J.; Steele, A. D.; Howard, O. M.; Oppenheim, J. J. Bidirectional heterologous desensitization of opioid and chemokine receptors. *Ann. NY Acad. Sci.* **2000**, *917*, 19–28.
72. Thompson, K. A.; Cherry, C. L.; Bell, J. E.; McLean, C. A. Brain cell reservoirs of latent virus in presymptomatic HIV-infected individuals. *Am. J. Pathol.* **2011**, *179*, 1623–1629.
73. Peridsky, Y.; Gendelman, H. E. Mononuclear phagocyte immunity and the neuropathogenesis of HIV-1 infection. *J. Leukoc. Biol.* **2003**, *74*, 691–701.
74. Chuang, T. K.; Killam, K. F. J.; Chuang, L. F.; Kung, H. F.; Sheng, W. S.; Chao, C. C.; Chuang, R. Y.; Mu opioid receptor gene expression in immune cells. *Biochem. Biophys. Res. Commun.* **1995**, *216*, 922–930.
75. Suzuki, S.; Chuang, L. F.; Yau, P.; Doi, R. H.; Chuang, R. Y. Interactions of opioid and chemokine receptors: oligomerization of mu, kappa, and delta with CCR5 on immune cells.

- Exp. Cell Res.* **2002**, *280*, 192–200.
76. Hauser, K. F.; El-Hage, N.; Steine-Martin, A.; Maragos, W. F.; Nath, A.; Peridsky, Y.; Volsky, D. J.; Knapp, P. E. HIV-1 neuropathogenesis: glial mechanisms revealed through substance abuse. *J. Neurochem.* **2007**, *100*, 567–586.
77. El-Hage, N.; Wu, G.; Wang, J.; Ambati, J.; Knapp, P. E.; Reed, J. L.; Bruce-Keller, A. J.; Hauser, K. F. HIV-1 Tat and opiate-induced changes in astrocytes promote chemotaxis of microglia through the expression of MCP-1 and alternative chemokines. *Glia.* **2006**, *53*, 132–146.
78. Janecka, A.; Fichna, T. Opioid receptors and their ligands. *Curr. Top. Med. Chem.* **2004**, *4*, 1–17.
79. Emmerson, P. J.; Liu, M. R.; Woods, J. H.; Medzihradsky, F. Binding affinity and selectivity of opioids at mu, delta, and kappa receptors in monkey brain membranes. *J. Pharmacol. Exp. Ther.* **1994**, *3*, 1630–1637.
80. Schmidhammer, H.; Burckard, W. P.; Eggstein-Aeppli, L.; Smith, C. F. Synthesis and biological evaluation of 14-alkoxymorphinans. 2. (-)-N-(cyclopropylmethyl)-4,14-dimethoxymorphinan-6-one, a selective mu opioid receptor antagonist. *J. Med. Chem.* **1989**, *32*, 418–421.
81. Broadbear, J. H.; Sumpter, T. L.; Burke, T. F.; Husbands, S. M.; Lewis, J. W.; Woods, J. H.; Traynor, J. R. Methocinnamox is a potent, long-lasting and selective antagonist of morphine-mediated antinociception in the mouse: comparison with clocinnamox, beta-unaltrexamine, and beta-chlornaltrexamine. *J. Pharmacol. Exp. Ther.* **2000**, *294*, 933–940.
82. Kazmierski, W.; Wire, W. S.; Liu, G. K.; Knapp, R. J.; Shook, J. E.; Burks, T. F.; Yamamura, H. I.; Hruby, V. J. Design and synthesis of somatostatin analogues with topographical properties that lead to highly potent and specific mu opioid receptor antagonists with greatly reduced binding at somatostatin receptors. *J. Med. Chem.* **1988**, *31*, 2170–2177.

83. Ward, S. J.; Portoghese, P. S.; Takemore, A. E. Pharmacological profiles of beta-funaltrexamine (beta-FNA) and beta-chlornaltrexamine (beta-CNA) on the mouse vas deferens preparation. *Eur. J. Pharmacol.* **1982**, *80*, 377–384.
84. Portoghese, P. S.; Sultana, M.; Takemori, A. Design of peptidomimetic delta opioid receptor antagonists using the message-address concept. *J. Med. Chem.* **1990**, *33*, 1714–1720.
85. Fuxe, K.; Borroto-Escuela, D. O.; Marcellino, D.; Romero-Fernandez, W.; Frankowska, M.; Guidolin, D.; Filip, M.; Ferraro, L.; Woods, A. S.; Tarakanov, A.; Ciruela, F.; Agnati, L. F.; Tanganelli, S. GPCR heteromers and their allosteric receptor-receptor interactions. *Curr. Med. Chem.* **2012**, *19*, 356–363.
86. George, S. R.; O'Dowd, B. F.; Lee, S. P. G protein-coupled receptor oligomerization and its potential for drug discovery. *Nat. Rev. Drug Disc.* **2002**, *1*, 808–820.
87. Pfeiffer, M.; Koch, T.; Schroder, H.; Laugsch, M.; Holtt, V.; Schulz, S. Heterodimerization of somatostatin and opioid receptor cross-modulates phosphorylation, internalization, and desensitization. *J. Biol. Chem.* **2002**, *277*, 19762–19772.
88. Bai, M. Desensitization of G protein-coupled receptors: roles in signal transduction. *Cell. Signal.* **2004**, *16*, 175–186.
89. Herbert, T. E.; Moffet, S.; Morello, J. P.; Losiel, T. P.; Bichet, D. G.; Barret, C.; Bouvier, M. A peptide derived from a beta(2)-adrenergic receptor transmembrane domain inhibits both receptor dimerization and activation. *J. Biol. Chem.* **1996**, *271*, 16384–16392.
90. Pfleger, K. D. G.; Eidne, K. A. Monitoring the formation of dynamic G protein-coupled receptor-protein complexes in living cells. *Biochem. J.* **2005**, *385*, 625–637.
91. Angers, S.; Salahpour, A.; Joly, E.; Hilairet, S.; Chelsky, D.; Dennis, M.; Bouvier, M. Detection of beta 2-adrenergic receptor dimerization in living cells using bioluminescence resonance energy transfer (BRET). *Proc. Natl. Acad. Sci. USA* **2000**, *97*, 3684–3689.



92. Fotiadis, D.; Liang, Y.; Filipek, S.; Saperstein, D. A.; Engel, A.; Palczewski, K. Atomic-force microscopy: rhodopsin dimers in native disc membranes. *Nature* **2003**, *421*, 127–128.
93. Gouldson, P. R.; Higgs, C.; Smith, R. E.; Dean, M. K.; Gkoutos, G. V.; Reynolds, C. A. Dimerization and domain swapping in G protein-coupled receptors: a computational study. *Neuropsychopharmacology* **2000**, *23*, S60–S77.
94. Park, J. H.; Scheerer, P.; Hofmann, K. P.; Choe, H. W.; Ernst, O. P. Crystal structure of the ligand-free G protein-coupled receptor opsin. *Nature* **2008**, *454*, 183–187.
95. Wang, D.; Sun, X.; Bohn, L. M.; Sadee, W. Opioid receptor homo- and heterodimerization in living cells by quantitative bioluminescence resonance energy transfer. *Mol. Pharmacol.* **2005**, *67*, 2173–2184.
96. Pfeiffer, M.; Kirscht, S.; Stumm, R.; Koch, T.; Wu, D.; Laugsch, M.; Schroder, H.; Hollt, V.; Schulz, S. Heterodimerization of substance P and mu-opioid receptors regulates receptor trafficking and resensitization. *J. Biol. Chem.* **2003**, *278*, 51630–51637.
97. Evans, R. M.; You, H.; Hameed, S.; Altier, C.; Mezghrani, A.; Bourinet, E.; Zamponi, G. W. Heterodimerization of ORL1 and opioid receptors and its consequences for N-type calcium channel regulation. *J. Biol. Chem.* **2010**, *285*, 1032–1040.
98. Jordan, B. A.; Devi, A. L. G protein-coupled receptor heterodimerization modulates receptor function. *Nature* **1999**, *399*, 697–700.
99. George, S. R.; Fan, T.; Xie, Z.; Tse, R.; Tam, V.; Varghese, G.; O'Dowd, B. F. Oligomerization of mu- and delta-opioid receptors. Generation of novel functional properties. *J. Biol. Chem.* **2000**, *275*, 26128–26135.
100. Rios, C.; Gomes, I.; Devi, L. A. Mu opioid and CB1 cannabinoid receptor interaction: reciprocal inhibition of receptor signaling and neurogenesis. *Br. J. Pharmacol.* **2006**, *148*, 387–395.

101. He, L.; Fong, J.; Von Zastrow, M.; Whistler, J. L. Regulation of opioid receptor trafficking and morphine tolerance by receptor oligomerization. *Cell* **2002**, *108*, 271–282.
102. Portoghese, P. S.; Bivalent ligands and message-address concept in the design of selective opioid antagonists. *Trends Pharmacol. Sci.* **1989**, *10*, 230–235.
103. Shonberg, J.; Scammells, P. J.; Capuano, B. Design strategies for bivalent ligands targeting GPCRs. *ChemMedChem* **2011**, *6*, 693–974.
104. Portoghese, P. S. From models to molecules: opioid receptor dimers, bivalent ligands, and selective opioid receptor probes. *J. Med. Chem.* **2001**, *44*, 2259–2269.
105. Zheng, Y.; Akgun, E.; Harikumar, K. G.; Hopson, J.; Powers, M. D.; Lunzer, M. M.; Miller, L. J.; Portoghese, P. S. Induced association of mu-opioid (MOP) and type 2 cholecystokinin (CCK2) receptors by novel bivalent ligands. *J. Med. Chem.* **2009**, *52*, 247–258.
106. Zhang, S.; Yekkirala, A.; Tang, Y.; Portoghese, P. S. A bivalent ligand (KMN-21) antagonist for mu/kappa heterodimeric opioid receptors. *Bioorg. Med. Chem. Lett.* **2009**, *19*, 6978–6980.
107. Daniels, D. J.; Lenard, N. R.; Etienne, C. L.; Law, P. Y.; Roerig, S. C.; Portoghese, P. S. Opioid-induced tolerance and dependence in mice is modulated by the distance between pharmacophores in bivalent ligand series. *Proc. Natl. Acad. Sci. USA* **2005**, *102*, 19208–19213.
108. Harvey, J. H.; Long, D. H.; England, P. M.; Whistler, J. L. Tuned-affinity bivalent ligands for the characterization of opioid receptor heteromers. *ACS Med. Chem. Lett.* **2012**, *3*, 640–644.
109. Mather, B. M.; Degenhardt, L.; Phillips, B.; Wiessing, L.; Hickman, M.; Strathdee, S. A.; Wodak, A.; Panda, S.; Tyndall, M.; Toufik, A.; Mattick, R. P. Global epidemiology of injecting drug use and HIV among people who inject drugs: a systematic review. *Lancet* **2008**, *372*, 1733–1745.

110. Schmidhammer, H.; Burkard, W. P.; Eggstein-Aeppli, L.; Smith, C. F. Synthesis and biological evaluation of 14-alkoxymorphinans. 2. (-)-N-(cyclopropylmethyl)-4,14-dimethoxymorphinan-6-one, a selective mu opioid receptor antagonist. *J. Med. Chem.* **1989**, *32*, 418–421.
111. Gabudza, D.; Wang, J. Chemokine receptors and virus entry in the central nervous system. *J. Neurovirol.* **1999**, *5*, 643–658.
112. Luster, A. D.; Chemokines – chemotactic cytokines that mediate inflammation. *N. Engl. J. Med.* **1998**, *338*, 436–445.
113. Dorr, P.; Westby, M.; Dobbs, S.; Griffin, P.; Irvine, B.; Macartney, M.; Mori, G.; Rickett, G.; Smith-Burchnell, C.; Napier, C.; Webster, R.; Armour, D.; Price, D.; Stammen, B.; Wood, A.; Perros, M. Maraviroc (UK-427,857), a potent, orally bioavailable, and selective small-molecule inhibitor of chemokine receptor CCR5 with broad-spectrum anti-human immunodeficiency virus type 1 activity. *Antimicrob. Agents Chemother.* **2005**, *49*, 4721–4732.
114. Lindl, K. A.; Marks, D. R.; Kolson, D. L.; Jordan-Sciutto, K. L.; HIV-Associated neurocognitive disorder: Pathogenesis and therapeutic opportunities. *J. Neuroimmune Pharmacol.* **2010**, *5*, 294–309.
115. Minagar, A.; Commins, D.; Alexander, J. S.; Hoque, R.; Chiappelli, F.; Singer, E. J.; Nikbin, B.; Spapshak, P. NeuroAIDS: Characteristics and diagnosis of the neurological complications of AIDS. *Mol. Diagn. Ther.* **2008**, *12*, 25–43.
116. Gurwell, J. A.; Nath, A.; Sun, Q.; Zhang, J.; Martin, K. M.; Chen, Y.; Hauser, K. F. Synergistic neurotoxicity of opioids and human immunodeficiency virus-1 Tat protein in striatal neurons in vitro. *Neuroscience* **2001**, *102*, 555–563.
117. Zou, S.; Fitting, S.; Hahn, Y. K.; Welch, S. P. El-Hage, N.; Hauser, K. F.; Knapp, P. E. Morphine potentiates neurodegenerative effects of HIV-1 Tat through action at m-opioid

- receptor-expressing glia. *Brain* **2011**, *134*, 3613–3628.
118. Mahajan, S. D.; Schwatz, S. A.; Shanahan, T. C.; Chawda, R. P.; Nair, M. P. N. Morphine regulates gene expression of  $\alpha$ - and  $\beta$ -chemokines and their receptors on astroglial cells via the opioid receptor. *J. Immunol.* **2002**, *169*, 3589–3599.
119. Szabo, I.; Chen, X. H.; Xin, L.; Adler, M. W.; Howard, O. M.; Oppenheim, J. J.; Rogers, T. J. Heterologous desensitization of opioid receptors by chemokines inhibits chemotaxis and enhances the perception of pain. *Proc. Natl. Acad. Sci. USA* **2002**, *99*, 10276–10281.
120. Yuan, Y.; Arnatt, C. K.; Li, G.; Haney, K. M.; Ding, D.; Jacob, J.; Selley, D. E.; Zhang, Y.; Design and synthesis of a bivalent ligand to explore the putative heterodimerization of the mu opioid receptor and the chemokine receptor CCR5. *Org. Biomol. Chem.* **2012**, *10*, 2633–2646.
121. Guo, L.; Haney, K. M.; Kellogg, G. E.; Zhang, Y. Comparative docking study of anibamine as the first natural product CCR5 antagonist in CCR5 homology models. *J. Chem. Inf. Model.* **2009**, *49*, 120–132.
122. Lee, D. W.; Ha, H. J. Selective mono-BOC protection of diamines. *Synth. Commun.* **2007**, *37*, 732–742.
123. Pittelkow, M.; Lewinsky, R.; Christensen, J. B. Mono carbamate protection of aliphatic diamines using alkyl phenyl carbonates. *Org. Synth.* **2007**, *84*, 209–211.
124. Sayre, L. M.; Portoghese, P. S.; Stereospecific synthesis of 6 alpha and 6 beta-amino derivatives of naltrexone and oxymorphone. *J. Org. Chem.* **1980**, *45*, 3366–3368.
125. Conklin, B. R.; Farfel, Z.; Lustig, K. D.; Julius, D.; Bourne, H. R. Substitution of three amino acids switches receptor specificity of Gq to that of Gi alpha. *Nature* **1993**, *363*, 274–276.
126. Tan, Q.; Zhu, Y.; Li, J.; Chen, Z.; Han, G. W.; Kufareva, I.; Li, T.; Ma, L.; Fenalti, G.; Li, J.; Zhang, W.; Xie, X.; Yang, H.; Jiang, H.; Cherezov, V.; Liu, H.; Stevens, R. C.; Zhao, Q.; Wu,

- B. Structure of the CCR5 chemokine receptor-HIV entry inhibitor maraviroc complex. *Science* **2013**, *341*, 1387–1390.
127. Good, A. C.; Cheney, D. L. Analysis and optimization of structure-based virtual screening protocols (1): exploration of ligand sampling conformational techniques. *J. Mol. Graph. Model.* **2003**, *22*, 23 – 30.
128. Chen, I. Conformational sampling and energetics of drug-like molecules. *Curr. Med. Chem.* **2009**, *16*, 3381–3414.

## VITA

Thomas John Raborg was born on April 29, 1988 in Red Bank, New Jersey to Marija and Joseph Raborg. Growing up he had two siblings, an older brother and a young sister. He graduated from Red Bank Catholic High School in 2006 and went on to the University of Florida, later transferring to the University of Kansas whereupon he finished his degree. He graduated in the top 10% of his class at Kansas, earning the honor of *Distinction* with a bachelor of science in Cellular Biology. In the fall of 2011 he joined the Department of Medicinal Chemistry at Virginia Commonwealth University and came under the tutelage of Dr. Yan Zhang. He is a Master's Degree student.